

---

---

# **APPLICATION OF POLYMERS IN SEPARATION SCIENCE**

---

thesis submitted to the  
COCHIN UNIVERSITY OF SCIENCE AND TECHNOLOGY  
in partial fulfilment of the requirements for the degree of  
**DOCTOR OF PHILOSOPHY**  
in Chemistry

G.5610

by

**USHA K.**

**DEPARTMENT OF APPLIED CHEMISTRY**  
COCHIN UNIVERSITY OF SCIENCE AND TECHNOLOGY  
Kochi - 682 022, Kerala

October 1995

## **CERTIFICATE**

This is to certify that the thesis entitled **APPLICATION OF POLYMERS IN SEPARATION SCIENCE** is an authentic record of the work done by Ms. Usha K. under my supervision, and further that no part thereof has been presented before for the award of any other degree.



Kochi - 16  
October 1995

**V. N. SIVASANKARA PILLAI**  
(Supervising Teacher)

# CONTENTS

	Page
<b>Preface</b>	
<b>PART I</b>	<b>STUDIES ON MALEIC ACID BASED ION-EXCHANGE MEMBRANES</b>
<b>CHAPTER 1</b>	<b>ION-EXCHANGE MEMBRANES: AN OVERVIEW</b> 1
1.1	Introduction 2
1.2	Classification of Membranes 2
1.2.1	Heterogeneous membranes 3
1.2.2	Homogeneous membranes 4
1.3	Ion-exchange Membranes 5
1.3.1	Ion-exchange resins 5
1.3.2	Types of ion-exchange membranes 8
1.4	Polyamides as Membrane Materials 14
1.5	Maleic Acid Polymers 16
	References 20
<b>CHAPTER 2</b>	<b>EXPERIMENTAL METHODS</b> 27
2.1	Membrane Preparation 28
2.1.1	Synthesis of polymaleic acid (PMA) 28
2.1.2	Synthesis of nylon 666-g-maleic acid (N-g-MA) 29
2.1.3	Synthesis of nylon 666-PMA interpolymer (N-PMA) and lysine crosslinked nylon 666-PMA (N-PMA-Ly) 29
2.2	Characterization 30
2.2.1	Polymer characterization 30
2.2.2	Membrane characterization 31
2.3	Results and Discussion 41
2.3.1	Infrared spectra 41

---

---

		Page
	2.3.2 Properties of nylon 666	42
	2.3.3 Viscosity measurements	42
	References	48
<b>CHAPTER</b>	<b>3 NYLON 666-g-MALEIC ACID MEMBRANES</b>	<b>50</b>
	3.1 Introduction	51
	3.2 Experimental	53
	3.2.1 Membrane preparation	53
	3.2.2 Membrane characterization	53
	3.3 Results and Discussion	54
	3.3.1 Membrane preparation	54
	3.3.2 Characterization	54
	References	78
<b>CHAPTER</b>	<b>4 NYLON 666-POLYMALEIC ACID MEMBRANES</b>	<b>79</b>
	4.1 Introduction	80
	4.2 Experimental	82
	4.2.1 Preparation of membranes	82
	4.2.2 Characterization	82
	4.3 Results and Discussion	82
	4.3.1 Membrane preparation	82
	4.3.2 Characterization	82
	References	102
<b>CHAPTER</b>	<b>5 AC CONDUCTIVITY AND DIELECTRIC RELAXATION IN NYLON 666-g-MALEIC ACID AND NYLON 666-POLYMALEIC ACID</b>	<b>103</b>
	5.1 Introduction	104
	5.2 Theory	104
	5.2.1 ac Conductivity	104

---

---

	Page
5.2.2 Dielectric relaxation	106
5.3 ac Conductivity and dielectric relaxation in nylon polymers and polycarboxylic acids	110
5.4 Experimental	111
5.5 Results and Discussion	112
5.5.1 DSC thermograms	112
5.5.2 ac Conductivity	115
5.5.3 Dielectric relaxation	123
References	133
CHAPTER 6 SUMMARY AND CONCLUSIONS	135
<b>PART II POLYMERS AS FLOCCULANTS AND CONTROLLED-RELEASE AGENTS</b>	
CHAPTER 7 CONTROLLED-RELEASE: AN OVERVIEW	138
7.1 Introduction	139
7.2 Classification of Controlled-Release Systems	139
7.2.1 Diffusion controlled systems	139
7.2.2 Erosion or chemical reaction controlled systems	140
7.2.3 Swelling controlled-release systems	141
7.2.4 Osmotic pumping systems	141
7.3 Advantages of Controlled-Release	141
7.4 Basic Components of Controlled-Release Devices	142
7.5 Controlled-Release Molluscicides	143
7.5.1 Snail control techniques	145
References	147

---

---

		Page	
<b>CHAPTER</b>	<b>8</b>	<b>SALICYLIC ACID-FORMALDEHYDE CONDENSATE</b>	<b>149</b>
	8.1	Introduction	150
	8.2	Experimental	151
	8.2.1	Synthesis of polycondensate	151
	8.2.2	Preparation of Copper-PMS complex for controlled-release formulation	152
	8.2.3	Leaching studies	152
	8.2.4	Instrument	152
	8.3	Results and Discussion	153
	8.3.1	Spectral studies	153
	8.3.2	Thermal studies	160
	8.3.3	Leaching behaviour of copper ions	164
	8.4	Conclusion	165
		References	166
<b>CHAPTER</b>	<b>9</b>	<b>SEPARATION OF EUROPIUM FROM RARE EARTH CHLORIDE</b>	<b>167</b>
	9.1	Introduction	168
	9.2	Experimental	171
	9.2.1	Materials	171
	9.2.2	Methods	171
	9.3	Results and Discussion	173
	9.3.1	Characterization of polyampholite	173
	9.3.2	Effect of pH on reduction medium	173
	9.3.3	Effect of sulphate concentration	174
	9.3.4	Flocculation studies	174
	9.3.5	Sedimentation experiments	175
	9.3.6	Particle size analysis	175
	9.4	Conclusion	180
		References	181

---

## PREFACE

This dissertation contains the research work done by me during my tenure as a University Research Fellow and UGC Junior Research Fellow in the Department of Applied Chemistry, Cochin University of Science and Technology. The work broadly relates to the application of polymers in separation science. The work presented in Part I of this dissertation deals with the synthesis, characterization and transport of ionic and nonionic species through membranes derived from maleic acid. Two types of materials were used: (i) Nylon 666 grafted with maleic acid by  $\gamma$ -irradiation, and (ii) Nylon 666- polymaleic acid interpolymer. The effects of synthesis variables and solution variables on transport related properties like membrane potential, transport fraction, permeability and permselectivity with regard to typical solutes like KCl, NaCl, NaOH, Na<sub>2</sub>SO<sub>4</sub>, urea and creatinine have been investigated. The role of active transport has been identified and discussed.

Apart from the structure related engineering properties like tensile strength, elongation and burst strength, the structure and conformation related properties like ac conductivity and dielectric loss have been measured as a function of frequency as well as temperature. This, in turn, helps to evaluate the molecular relaxation phenomena and related energetics in terms of activation energy. The observations on temperature dependent electrical properties have been complimented by thermal measurement using differential scanning calorimetry.

Part II is an off-shoot of the studies on some interesting applications of polyelectrolytes in controlled-release devices. Salicylic acid-formaldehyde condensate, which had already been reported by earlier workers, was reinvestigated for the nature

of oligomers formed. The studies have shown that there are three oligomers of which the tetramer is probably a symmetric calixarene type molecule. The application of salicylic acid-formaldehyde condensate complexed to Cu(II) as a source for the controlled-release of Cu(II) ions was investigated and the results are presented.

The presently practised process for the separation of Eu(II) from rare earth concentrate is a tedious one. The main hurdle is the extremely slow growth of europium(II) sulphate. This problem has been approached from the angle of particle growth kinetics under the influence of a suitable polyelectrolyte. An amphiphilic polyelectrolyte was synthesized from polyacrylamide. The flocculation of europium(II) sulphate in presence of excess sulphate in acid medium was investigated by sedimentation technique. The optimum conditions for the flocculation of europium(II) sulphate has been established. This lends the possibility to develop a continuous flow-through process for the separation of europium.



**PART I**

---

**STUDIES ON MALEIC ACID  
BASED ION-EXCHANGE MEMBRANES**

**CHAPTER 1**

**ION-EXCHANGE MEMBRANES:**

**AN OVERVIEW**

**Abstract**

This chapter gives a comprehensive review of the literature on membranes in general and ion-exchange membranes in particular. Structure-property relation in ion-exchange membranes, their salient features and major applications of carboxylic acid based ion-exchange membranes have been covered in more details.

## 1.1 Introduction

Polymeric films are generally employed as barriers to the free transmission of gases, vapors, liquids, and ionic and nonionic substances. The generalized membrane is an interface between two regions of fluids.<sup>1-2</sup> The crucial condition is that this interface must be a partial barrier to material transport between the two regions. Both organic and inorganic polymeric materials can be shaped into a wide variety of forms with tailored macromolecular morphology, good physical properties, a wide range of chemical properties and a fair degree of chemical and thermal stability.<sup>3</sup>

A complete survey of the field of membrane studies would cover membrane preparation, characterization, experimental methodology, mathematical and thermodynamical analysis, biological studies, separation processes and commercial equipment. However, this review is limited in scope to the extent it is relevant to ion-exchange membranes.

## 1.2 Classification of Membranes

There are two different classes of membranes, namely, biomembranes and synthetic membranes.<sup>4</sup> Biomembrane is simply the functional boundary between two different spaces within the organism. There are several types of

biomembranes which exist in other living organisms, such as epithelial tissues or cell membranes.

The second category, synthetic membranes, consists of a large variety of materials including synthetic polymers, metals and ceramics.<sup>5</sup> They may further be categorized by structure or by function. Structure related properties are their chemical functions, microcrystallinity and pore structure. Functional properties are permeability and permselectivity. According to their microlevel structures membranes are classified into heterogeneous and homogeneous membranes.

#### 1.2.1 Heterogeneous membranes

Heterogeneous membranes consist of a solid matrix with defined pores which have a diameter ranging from 5 to 50 nm. They can be asymmetric or symmetric in structure. Asymmetric ones may be integral or composite which refers to two different polymer layers composed in one membrane. Asymmetric membranes have a skin layer on one side, which plays a critical role in the permselectivity of these membranes.

There are different methods for the preparation of heterogeneous membranes such as solvent casting, sintering, stretching, track-etching and others.<sup>5-15</sup>

### 1.2.2 Homogeneous membranes

Homogeneous membranes may be solid or liquid. Usually a homogeneous membrane consists of a dense film with no pores in the structure and consequently the transport rate is low. These membranes have very high selectivity. Thus two species with different solubilities, but identical diffusivities can be separated.<sup>16</sup> Separation of the components of a mixture is directly related to their transport rates within the membrane phase which is determined by their diffusivities and concentrations in the membrane phase. Since mass transport in homogeneous membrane occurs by diffusion, their permeabilities are rather low.

Homogeneous membranes can be made from inorganic materials or from polymers.<sup>17</sup> These membranes are generally made by casting from a solution or from a polymer melt by extrusion, blow or press molding. Different methods are followed depending on the desired membrane configuration. Membranes with different mass transfer rates and mechanical properties for specific applications such as pervaporation and blood oxygenation can be prepared by controlling the different characteristics of the polymer employed. The most popular homogeneous membranes are ion-exchange membranes.

### 1.3 Ion-exchange Membranes

The term ion-exchange membrane is used in a very broad sense and comprises of solid films, foils and disks. The characteristic which distinguishes an ion-exchange membrane from others is the presence of ionic groups in its component polymer molecules.<sup>18-22</sup>

The major requirements of ion-exchange membranes are selectivity i.e., the sorption of one counter-ion in preference to another, low electrical resistance, good mechanical stability and high chemical stability. The properties of ion-exchange membranes are determined by the type of polymer matrix and concentration of the fixed ionic moiety.<sup>23</sup> Usually it consists of a hydrophobic polymer such as polystyrene, polyethylene or polysulfone. Even though these polymers are water insoluble and exhibit low degree of swelling, they swell in water after the introduction of ionogenic groups. The properties of ion-exchange membranes are closely related to those of ion-exchange resins.

#### 1.3.1 Ion-exchange resins

The resins for use as ion-exchange membranes must be permeable to counter-ions and impermeable to co-ions. These are met by resins having high capacity and low resistance. Among the many types of resins which have been

used for ion-exchange applications are cation exchange resins, anion exchange resins, polyampholytes and redox resins.

(a) Cation exchange resins

The first synthetic cation exchange resins were of phenol-formaldehyde type.<sup>24,25</sup> Due to low acidity of phenolic OH group, other phenols have been used.<sup>26-28</sup> Strong acid cation exchange resins were prepared by sulfonation of phenols prior to polymerization. Weak acid resins were obtained by using phenols such as salicylic acid.<sup>29</sup> Since aliphatic sulfonic acids are weaker than aromatic type, their incorporation results in weakly acidic resins.<sup>30</sup>

The advantage of addition polymers for use as ion-exchange resins is the presence of nonhydrolyzable carbon skeleton in the polymer backbone. The most widely used resin type is polystyrene crosslinked with DVB. The properties of the resin can be varied by varying the crosslinking content.

Weak acid cation exchange resins are prepared by the copolymerization of esters of acrylic or methacrylic acid with divinyl benzene or dimethylmethacrylate. Selective cation exchange resins are those which have preference to certain counter-ion species over others, and usually this

is achieved by incorporating a chelating functional group having good selectivity to metal ions.

**(b) Anion exchange resins**

Anion exchange resins contain weak base primary or secondary ammonium groups  $-\text{NH}_3^+$ ,  $>\text{NH}_2^+$  or strong base quaternary ammonium, phosphonium or sulfonium groups.<sup>31</sup> Anion exchange resins were prepared from aromatic amines such as *m*-phenylenediamine by condensation with formaldehyde. Base strength and degree of crosslinking vary with the concentration of aldehyde. Ammonia and ammonium salts, urea and urea derivatives have also been utilized for the preparation of anion exchange resins.<sup>32</sup>

Another method for their preparation involves chloromethylation of crosslinked polystyrene and subsequent reaction with ammonia or primary, secondary or tertiary amines.<sup>33</sup> The extent of chloromethylation and hence capacity can be controlled by varying the reaction time. Weak base resins can also be formed by the polymerization of acrylic and methacrylic acids in presence of polyamines.

**(c) Amphoteric ion-exchangers**

These contain both acidic and basic groups. Above their isoelectric point, they function as cation exchange



resins whereas below this point they act as anion exchange resins.<sup>32</sup> Resins having both strong acid and strong base groups can be prepared by the copolymerization of styrene, vinyl chloride and a crosslinking agent followed by quaternization and sulfonation.<sup>34</sup> Weak amphoteric character is exhibited by resins with iminodiacetate groups. The most recent and important amphoteric resins are the snake cage polyelectrolytes.<sup>2</sup>

#### **(d) Redox ion-exchangers**

Redox ion-exchangers contain reversible redox couples such as methylene blue-leuco methylene blue.<sup>35</sup> These couples are held in the resin either as counter-ions or as a result of sorption. They are characterized by their redox capacity, redox potential and rate of reaction.

### **1.3.2 Types of ion-exchange membranes**

#### **(a) Heterogeneous membranes**

Heterogeneous membranes consist of colloidal particles of ion-exchange material embedded in an inert polymeric substrate. They are prepared by different methods.<sup>35</sup> The ion-exchange material can be pressed into a plastic film under pressure. The preparation procedure depends on the nature of the binder. The commonly used binders are polyethylene, polystyrene, phthalic resins,

polymethacrylates and synthetic rubber.<sup>36</sup> The ion-exchange particle embedded must be in contact with one another. Therefore, the volume percentage of ion-exchange material should be made as high as possible maintaining the required mechanical strength. Most heterogeneous membranes contain 50-70% ion-exchange material.<sup>37</sup>

The properties of a heterogeneous membrane depends on the ratio of the ion-exchange material to the binder.<sup>38,39</sup> It can be made from almost any ion-exchanger. The heterogeneous membranes are being replaced by homogeneous membranes due to their low electrical conductivity and permeability for electrolytes. Other disadvantages are the loss of capacity owing to the presence of the inert binder and the intrinsic difficulty to reproduce the factors controlling their structural characteristics.

#### (b) Homogeneous membranes

The homogeneous ion-exchange membranes lack structure at the colloidal level but does exist at the microcrystalline and molecular levels. The membranes are translucent, an indication that inhomogeneities, if present are smaller than the wavelength of visible light.

Many difficulties are encountered in the preparation of homogeneous membranes mainly those related to the initiation of the polymerization process and the swelling

consequent due to the introduction of charged groups into the polymer film.

The preparation of ion-exchangers by polymerization can be accomplished in such a way that the product is obtained in the membrane form. This is possible in many cases.<sup>40,41</sup> The condensation products of phenol sulphonic acid or its derivative with formaldehyde, and of polyethyleneimine and epichlorohydrin could be obtained in this form. The precondensed viscous reaction mixture may be formed as membranes by placing it between two glass plates.

Anion-exchange membranes have been prepared by condensing melamine-guanidine carbonate and formaldehyde.<sup>42</sup> The ion-exchange membranes manufactured by the Asahi Chemical Company are homogeneous membranes formed from partially polymerized styrene-divinylbenzene mixtures. For industrial applications, reinforced membranes have been prepared by polymerization over a wide-mesh plastic tissue support.

### (c) Interpolymer membranes

Interpolymer membranes are formed by the evaporation of solutions containing two compatible polymers, an inert film former and a linear ion-exchange polymer.<sup>42</sup> The films are water insoluble and the hydrophilic polyelectrolyte

cannot be leached out. Interpolymer membranes exhibit homogeneity at the colloidal level.

The factors that are to be considered while preparing the interpolymer membranes are: (1) ion-exchange and electrochemical properties of the charged polymer, (2) stability of both polymeric components, and (3) mutual solubility of the components. The commonly used solvents are dimethylformamide and dimethylsulfoxide, solvents that produce highly viscous solutions in which polymer elongation and chances for interwining during desolvation are maximum. Dynel(polyacrylonitrile-vinylchloride) is used as a binder in most cases. Copolymer of poly(vinylmethylether) is one of the polymers widely used for the preparation of such membranes.<sup>43</sup>

#### (d) Impregnated membranes

These are prepared using a porous substance as a binder and impregnating the interstices between elements of the binder network with ion-exchange material.<sup>44</sup> Some of the earliest membranes of this type were prepared by impregnating filter paper and porous glass with ion-exchange resins. Juda and McRae impregnated clothes of Saran, Vinyon and glass with phenolsulfonic acid-formaldehyde prepolymers.<sup>45,46</sup> The weak ion-exchange properties, physical structure and pore characteristics

could be improved by this technique. The properties of impregnated membranes deviate at low concentrations of ion-exchange component. Capacity of these membranes decrease with time due to leaching.

**(e) Grafted membranes**

These are prepared by grafting ionogenic or potentially ionogenic materials onto neutral films. This technique yields ion-exchange membranes with outstanding mechanical and good electrochemical properties. Grafting of monomers onto the film substrate is accompanied by chemical means involving peroxides<sup>47</sup> or redox catalysts,<sup>48</sup> and by means of high energy radiation.<sup>49,50</sup> Styrene-DVB is grafted to polyethylene by exposing a mixture of these to radiation. Strong acid cation exchange membranes are obtained by the sulfonation of graft copolymer, and strong base and weak base anion exchange membranes by chloromethylation and subsequent quaternization or amination.<sup>51</sup> The properties of these membranes could be varied by varying the grafted chain length. Membrane homogeneity can be expected to increase with decreasing length of the grafted chain. The chain length decreases<sup>52</sup> with increasing dose rate in the mutual irradiation technique (monomer present during irradiation) and increases with increasing dose rate in the preirradiation technique (monomer added after irradiation).

**(f) Mosaic membranes**

Mosaic membranes consist of an inhomogeneous composite structure in which the various elements are placed in parallel. Separate domains of cation and anion exchangers are present in them. The mosaic membrane is considered to be a combination of two membrane concentration cells arranged in a short circuited state without the presence of electrodes.<sup>53-55</sup> Difference in the concentration of electrolyte that exists across a mosaic membrane degenerates spontaneously to a state of equal concentration at the two sides of the membrane. This type of membranes find use in piezodialysis.

**(g) Polyelectrolyte complexes**

Polyelectrolyte complexes are formed by the interaction of soluble polyanions and polycations. They are neutral, or possess an excess of cationic or anionic charge. Polyelectrolyte complexes are prepared by phase inversion process. Therefore, their porosity and asymmetry in depth can be controlled by varying parameters such as casting-solution composition and the nature of the desolvation environment.<sup>56,57</sup> A typical polyelectrolyte complex is the reaction product formed from sodium polystyrene sulfonate and poly(vinylbenzyl trimethylammonium chloride).<sup>58</sup> Polyelectrolyte complex

membranes are either dense or porous structures which are hard and brittle when dry and leathery when wet. The water uptake depends upon the polyanion composition. Charged polyelectrolyte complexes in solution behave in the same manner as conventional ion-exchange resins.<sup>54</sup> The high water permeability of this type of membranes has resulted in attempts to apply them for separation by dialysis, ultrafiltration and reverse osmosis.<sup>59,60</sup>

#### 1.4 Polyamides as Membrane Materials

Polyamides are condensation products that contain recurring amide groups as an integral part of the polymer chain. Linear polyamides are formed from the condensation of bifunctional monomers. Polyamides are AB type or AABB type depending on the monomer used for synthesis.<sup>61-64</sup> Polyamides are frequently referred to as nylons. They are formed by condensation as well as by ring opening addition polymerization.

Typical structural formulae of a linear polyamide may be represented as

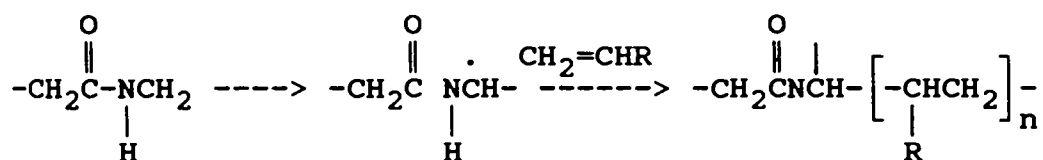


Most of the commercially available nylon fibers and plastics are unaffected by boiling water. Nylons are usually stable to aqueous alkali. However, aqueous acid

degrades nylon fiber rapidly, especially at elevated temperatures.<sup>65,66</sup>

#### 1.4.1 Grafting polyamides with unsaturated acids

Polyamides on exposure to high intensity radiation form free radicals which can be used as sites for polymerization with vinyl monomers on the polymer chain:



The predominant free radical in nylon irradiation is associated with the unpairing electron on the carbon adjacent to the amide nitrogen<sup>67</sup> ( $-\overset{\cdot}{\text{C}}\text{H}-\text{NH}-\text{CO}-$ ). Graft copolymers have been prepared from nylon 4,<sup>69</sup> nylon 6,6,<sup>70,71</sup> and nylon 6<sup>72,73</sup> with acrylonitrile, styrene or acrylamide.

Hydrophilic grafts have been prepared from nylon 6,6 with acrylic acid<sup>72</sup> or maleic acid.<sup>74</sup> These two acids form grafts distinguished by a wide range of properties. Acrylic acid polymerizes readily and forms graft of long polymeric chains. However, maleic acid does not homopolymerize and hence it give short grafts.<sup>75</sup> The acrylic acid and maleic acid grafts on nylon fibers



readily convert to the corresponding sodium or calcium salts by treatment with sodium carbonate or calcium acetate. The sodium salts of the grafts are highly hydrophilic. In these grafted polymers the crystalline portions of the nylon melt at the usual melting point of nylon, i.e., 260°C, but the inorganic-organic framework of the amorphous area remains infusible.

### 1.5 Maleic Acid Polymers

Maleic anhydride and maleic acid are interesting and versatile unsaturated vinylene compounds that are used commercially in the production of resins, coatings, rubbers, detergents, adhesives and additives.<sup>76</sup> They contain an ethylenic bond that is activated by the adjacent carboxyl groups, in addition they undergo reactions typical of the functional groups they hold. Of the two compounds, maleic anhydride is commercially more important and is produced in large quantity.

Homopolymerization of maleic anhydride was first demonstrated in 1961 by Lang, Pavelich and Clarey.<sup>77</sup> Due to its steric, resonance and polar characteristics, maleic anhydride appeared to be resistant to homopolymerization. However, the discovery of polyitaconic anhydride with similar characteristics lead to the preparation of polymaleic anhydride.<sup>78</sup> They demonstrated that solutions

of maleic anhydride exposed to radiation from a Cobalt-60 source produced poly(maleic anhydride) with a molecular weight of 19500. The molecular weight of the polymer depends on the monomer concentration and the dose rate. Attempts were also made using benzoyl peroxide as the initiator.<sup>79,80</sup> Polymerization was also effected by an ultraviolet light-diacetyl peroxide initiator system. Bryce-Smith, Gilbert and Vickery<sup>81</sup> have also demonstrated the homopolymerization of maleic anhydride using benzophenone-sensitized photo chemical technique.

Nakanishi and Hisayana<sup>82</sup> prepared ion-exchange resin by grafting maleic anhydride on a copolymer of styrene and divinylbenzene using aluminium chloride as catalyst. A mixture of acrylamide, maleic anhydride, urea and water (50:30:10:10) was melted to a uniform solution and on X-ray irradiation of this mixture lead to the formation of tan, opalescent resin. Heating at 170°C expanded the resin to a rigid crosslinked form which could be used as ion-exchange resin or filter.<sup>83</sup>

Maleic anhydride grafted on poly(butadiene) on amonolysis gives a water-soluble amide-ammonium salt which can be incorporated into water based coating baths.<sup>84</sup> It formed hard, flexible films on curing.

Uragami et al.<sup>85-91</sup> prepared ion-exchange membrane from poly(butadiene maleic anhydride) crosslinked with

poly(vinyl alcohol) and studied the mechanism of active transport of alkali metal ions, ammonium ion, aniline and amino acids. Fukuda et al.<sup>92</sup> studied the metal ion permeation using poly(maleic anhydride-2-methy-2-propen-1-ol) and poly(acrylonitrile) membranes. Selective transport of alkali metal ions was studied using poly(styrene-co-maleic acid) crosslinked with tetraethylene glycol.<sup>93</sup>

Maclaw and Alicja<sup>94,95</sup> reported water insoluble membranes produced from PVA crosslinked with maleic acid and fumaric acid. Ion-exchange membranes were prepared from a copolymer of maleic anhydride and vinyl acetate partially crosslinked with bifunctional crosslinking agents.<sup>96</sup> Eiichi and Junji<sup>97</sup> prepared amphoteric polyelectrolyte membranes from hydrolyzed N-vinyl-succinimide-maleic anhydride copolymer and studied the selective permeability of anions, cations and neutral species.

The kinetics of transport of alkali metal ions against their concentration gradient across poly(isobutylene-alt-maleic acid) and poly(styrene sulfonic acid) membranes has also been reported.<sup>98</sup> Elmidaoui et al.<sup>99</sup> prepared cation (or anion) exchange membrane and amphoteric ion-exchange membrane from grafted polymers of polyethylene with acrylic acid and

N,N-dimethylamino-2-ethyl acrylate. The separations of sodium chloride, urea and other compounds in the aqueous phase using nylon 4 membranes were investigated by Huang et al.<sup>100</sup> Radiation initiated process to graft vinyl monomers on to nylon 4 membranes for desalination purposes has been studied by Lai et al.<sup>101</sup>

This review on ion-exchangers in general and maleic acid based polymers in particular as ion-exchange membranes reveal that considerable lacuna exists in our information on the variety of polymers that can be synthesized using this monomer. A major portion of the work presented in this thesis relates to maleic grafted polymers—their synthesis, characterization and applications.

## References

1. Helfferich, F. "Ion-Exchange", McGraw-Hill: London, 1962.
2. Kesting, R. E. "Synthetic Polymeric Membranes", McGraw-Hill: New York, 1971.
3. Piskin, E. in "Synthetic Polymeric Membranes", Piskin, E., Hofmann, A. S., Eds.; "Polymeric Biomaterials", Martinus Nijhoff Publishers: The Netherlands, 1986.
4. Lakshminarayanaiah, N. "Transport Phenomena in Membranes", Academic Press: New York, 1969.
5. Keller, P. R. "Membrane Technology and Industrial Separation Techniques", Noyes Data Corporation: New Jersey, 1976.
6. Hwang, S.T.; Kammermeyer. "Membranes in Separations", John Wiley and Sons: New York, 1975.
7. Rogers, C. E. "Permselective Membranes", Marcel Decker: New York, 1971.
8. Sourirajan, S. "Reverse Osmosis and Synthetic Membranes", National Research Council: Canada, 1977.
9. Strathmann, H. *J. Memb. Sci.* 1982, 9, 121.
10. Strathmann, H.; Kock, K.; Amar, P.; Base, R. W. *Desalination* 1975, 16, 179.
11. Bierenbaum, H. S.; Isaacson, R. B.; Druin, M.; Plovan, S. G. *Ind. Eng. Chem. Prod. Res. Develop.* 1974, 13, 2. 12. Gore, R. W. *U. S. Pat.* 1976, 3953566.

13. Fleischer, R. L.; Brice, P. B.; Walker, R. M. *Science* 1965, 149, 383.
14. Price, P. B.; Malcker, R. M. *U. S. Pat.* 1967, 3303.
15. Thiele, H.; Hallick, K. *Kolloid Z.* 1959, 163, 15.
16. Wyllie, M. R.; Patnode, H. W. *J. Phys. Colloid. Chem.* 1950, 54, 204.
17. Jenckel, E.; von Lillin, H. *Kolloid Z.* 1956, 146, 159.
18. Cornaz, J.; Deuel, H. *Experientia* 1954, 10, 137.
19. Cornaz, J.; Hutschneker, K.; Deuel, H. *Helv. Chim. Acta.* 1957, 40, 2015.
20. Flett, D. S. "Ion Exchange Membranes", Ellis Horwood Chichester: UK, 1983.
21. Kunin, R. "Ion Exchange Resins", Wiley-Interscience: New York, 1958.
22. Kesting, R. E. "Synthetic Polymeric Membranes, A Structural Perspective", Wiley-Interscience: New York, 1985.
23. Strathmann, H. "Ullman's Encyclopedia of Industrial Chemistry", Elvers, B., Hawkins, S., Schalz, G. Eds.; VCH: FRG, 1990. Alb.
24. Adams, B.; Holmes, E. *J. Soc. Chem. Ind.* 1935, 54, IT.
25. Adams, B.; Holmes, E. *Brit. Pat.* 1936, 450308.
26. Evers, W. *U. S. Pat.* 1950, 2518420.
27. Kuwada, T. *Chem. Abstr.* 1954, 48, 6049.

28. Ohtuska, Y.; Umezawa, S. *Chem. Abstr.* 1953, 47, 10766.
29. Thomas, S.; Jones, J. *Brit. Pat.* 1956, 762085.
30. Abrams, I. *Ind. Eng. Chem.* 1956, 48, 1469.
31. Gregor, H.; Wetstone, D. *J. Phys. Chem.* 1957, 61, 147.
32. Bauman, W.; Heustead, G. *U. S. Pat.* 1952, 2601202.
33. Pepper, K.; Paisley, H.; Young, M. *J. Chem. Soc.* 1953, 4097.
34. Stach, H. *Angew. Chem.* 1951, 63, 263.
35. Bodamer, G. *U. S. Pat.* 1954, 2681319.
36. Patnode, H.; Wyllie, H. *U. S. Pat.* 1952, 2614976.
37. Wyllie, M. R. J.; Patnode, H. *J. Phys. Chem.* 1950, 54, 204.
38. Wyllie, M. R. J.; Kanaan, S. *J. Phys. Chem.* 1954, 58, 73.
39. Woermann, D.; Bonhoeffer, K.; Helfferich, F. *Z. Physik. Chem.* 1956, 8, 265.
40. Bayer, F.; Haagen, K.; Helfferich, F. *Ger. Pat.* 1959, 971729.
41. Kasper, A. *U. S. Pat.* 1955, 2702272.
42. Gregor, H.; Jacobson, H.; Shair, R.; Wetstone, D. *J. Phys. Chem.* 1957, 6, 141.
43. Wetstone, D.; Gregor, G.; *J. Phys. Chem.* 1957, 61, 151.
44. Kressman, T. *Nature* 1950, 165, 568.

45. Juda, W.; McRae, W. *U. S. Pat.* 1953, 2636851-52.
46. Neihof, R. *J. Phys. Chem.* 1954, 58, 916.
47. Smets, G.; Roovers, J.; van Humbeek, W. *J. Appl. Polym. Sci.* 1961, 5, 149.
48. Mino, G.; Kaizerman, S.; Rasmussen, E. *J. Polym. Sci.* 1959, 38, 393.
49. Myers, A. *J. Polym. Sci.* 1960, 4, 159.
50. Chen, W. K. W. *U. S. Pat.* 1966, 3247133.
51. Chen, W.; Mesrobian, R. *J. Polym. Sci.* 1957, 23, 903.
52. Kesting, R.; Stannett, V. *Makromol. Chem.* 1963, 65, 247.
53. Sollner, K. *Biochem. Z.* 1932, 244, 370.
54. Neihof, R.; Sollner, K. *J. Phys. Chem.* 1950, 54.
55. Gregor, H.; Sollner, K. *J. Phys. Chem.* 1946, 50, 88.
56. Michaels, A. *Ind. Eng. Chem.* 1965, 57(10), 32.
57. Michaels, A. Mieccka, R. *J. Phys. Chem.* 1961, 65, 1765.
58. Michaels, A.; Bixler, H.; Hausslein, R.; Fleming, S. *OSW Res. Develop. Rept.* 1965, 149.
59. Grot, W. *Chem. Ind. Tech.* 1975, 47, 617.
60. Eisenberg, A.; Yeager, H. L. *ACS Symp. Ser.* 1982, 180.
61. Mark, H.; Whitby, G. S. "High Polymers", Interscience Publishers: New York, 1940.
62. Starkweather, H. W. *J. Polym. Sci.* 1956, 21, 189.



63. Dismore, P. F.; Statton, W. O. *J. Polym. Sci.* 1966, 13C, 133.
64. Statton, W. O. *Ann. N. Y. Acad. Sci.* 1959, 83, 27.
65. Preston, T. *J. Polym. Sci.* 1966, 1A, 529.
66. Sweeny, W. *U. S. Pat.* 1966, 3287324.
67. Burrell, E. J. *J. Am. Chem. Soc.* 1961, 83, 574.
68. Bevington, J. C.; Eaves, D. E. *Nature* 1959, 178, 1112.
69. Korshak, V. V. *Vysokomol. Soedin.* 1959, 1, 1604.
70. Nayak, P. L. *Angew. Makromol. Chem.* 1979, 80, 95.
71. Huang, R. Y. M.; Kim, U. Y.; Dickson, J. M.; Lloyd D. R.; Peng, C. Y. *J. Appl. Polym. Sci.* 1981, 26, 1135.
72. Huang, R. Y. M.; Kim, U. Y.; Dickson, J. M.; Lloyd, D. R.; Peng, C. Y. *J. Appl. Polym. Sci.* 1981, 26, 1907.
73. Nayak, P. L. *Macromol. Sci. Rev. Macromol. Chem.* 1979, C17, 269.
74. Magat, E. E. *J. Polym. Sci.* 1963, 4C, 615.
75. Othmer, K. "Encyclopaedia of Chemical Technology", 1981, 18, 337.
76. Yocum, R. H.; Nyquist, E. B. "Functional Monomers", Marcel Dekker: New York, 1974, II.
77. Lang, J. L.; Pavelich, A. W.; Clarey, H. O. *J. Polym. Sci.* 1961, 55, 531.

78. Lancelot, C. J.; Blumberg, J. H.; Mackeller, D. G. *Brit. Pat.* 1974, 1349769.
79. Cochrane, C. C. *U. S. Pat.* 1969, 3427233.
80. Lang, J. L.; Pavelich, W. A. *U.S. Pat.* 1965, 3186972.
81. Smith, B. D.; Gilbert, A.; Vickery, B. *Chem. Ind.* London, 1962, 2060.
82. Nakanishi, S.; Hisayana, H. *Jpn. Pat.* 1961, 17839.
83. Sekismi Kogaku Kagyo Kabushiki Kerisha. *Brit. Pat.* 1965, 994725.
84. Dickakian, G. B. M. *U. S. Pat.* 1970, 3511816.
85. Uragami, T.; Watanabe, S.; Nakamura, R.; Yoshida, F.; Sugihara, M. *J. Appl. Polym. Sci.* 1983, 28, 1613.
86. Uragami, T.; Watanabe, S.; Nakamura, R.; Sugihara, M. *Polym. Bull.* 1982, 7, 71.
87. Wada, T.; Uragami, T.; Sugihara, M. *Polym. Bull.* 1985, 14.
88. Uragami, T.; Watanabe, S.; Sugihara. *Angew. Macromol. Chem.* 1982, 107, 20985. Uragami, T.; Watanabe, S.; Sugihara, M. *J. Polym. Sci. Polym. Chem. Ed.* 1982, 20, 1193.
89. Uragami, T.; Watanabe, S.; Sugihara, M. *Macromol. Chem.* 1982, 3, 141.
90. Uragami, T.; Moriyama, K.; Yamamoto, M.; Suguihara, M. *Macromol. Chem.* 1987, 187, 583.
91. Uragami, T. "Membrane Science and Technology", Marcel Dekker Inc.: New York, 1982, 377.

92. Fukuda, K.; Suzuc. S. *Chem. Soc. Jpn.* 1983, 880.
93. Iwabuchi, S.; Nakahira, T.; Ando, H.; Kawaguchi, H.; Murukoshi, M.; Kojima, K. *Polym. Commun.* 1989, 30, 58.
94. Maclaw, W.; Alicja, V. *Polimery* 1983, 28, 153.
95. Maclaw, W.; Alicja, V. *Polimery* 1983, 29, 14.
96. Agony of Industrial Science and Technology, *Jpn. Pat.* 1982, 57192463.
97. Eiichi, K.; Junji, P. *Kocoshu Kyete Daigaku Nippon Kogaku Senii Kenkyusho.* 1981, 38, 103.
98. Uragami, T.; Tamura, T. *Macromol. Chem. and Phys.* 1993, 194, 1027.
99. Elmidaoui, A.; Saraff, T.; Gavach, C.; Bonefevin, B. *J. Appl. Polym. Sci.* 1991, 42, 2551.
100. Huang, R. Y. M.; Kim, U. Y.; Dickson, J. M.; Lloyd, D. R.; Peng, C. Y. *J. Appl. Polym. Sci.* 1981, 26, 1907.
101. Lai, J. Y.; Chang, T. C.; Wu, Z. J.; Hsich, T. S. *J. Appl. Polym. Sci.* 1986, 32, 4709.

## CHAPTER 2

### EXPERIMENTAL METHODS

#### Abstract

Polymaleic acid was synthesized via polymaleic anhydride route. The polymer was characterized by infrared spectroscopy, dilute solution viscosity measurements and functional group determination. Membranes were prepared by varying monomer concentration and preparation conditions. The membranes were characterized by measuring thickness, water content, mechanical strength, electrical resistance, membrane potential and permeability coefficients of different solutes.

## 2.1 Membrane Preparation

### 2.1.1 Synthesis of polymaleic acid (PMA)

PMA was prepared by a modification of the procedure reported by Lang et al.<sup>1</sup> Maleic anhydride was purified by sublimation under reduced pressure. Acetic anhydride was purified by Dippy and Evans method.<sup>2</sup> Acetic anhydride (1 l) was allowed to stand with  $P_2O_5$  (100 g) for 3 h. It was then decanted and allowed to stand with ignited  $K_2CO_3$  for a further period of 3 h. The supernatant liquid was distilled and the fraction boiling at 137-138°C was collected.

The maleic anhydride solution 50% (w/v) in acetic anhydride was sealed in an ampoule under vacuum and was polymerized at room temperature by irradiation from a  $^{60}Co$ - $\Gamma$ -ray source (Rubber Research Institute of India, Kottayam). The dose rate was  $1.5 \times 10^4$  rad/h. The total dose given for polymerization was 43 Mrads. The reaction mixture was taken out and distilled under vacuum to remove acetic anhydride.

Polymaleic anhydride thus prepared was dissolved in acetone and precipitated using chloroform. The precipitate was washed repeatedly with chloroform. The polymaleic anhydride obtained was refluxed with excess of sodium hydroxide solution. PMA was precipitated by

neutralizing with hydrochloric acid. The PMA so obtained was washed with water and dried in vacuum at 80°C.

### **2.1.2 Synthesis of nylon 666-g-maleic acid (N-g-MA)**

Membranes were cast from a formic acid solution containing different ratios of nylon 666 (TUFNYL F 120 SRF, Madras, relative viscosity 2.6) and maleic acid. The membranes were cured at 80 to 90°C for 4 h and then cooled. These membranes were washed with distilled water several times to take out any leachable acid, dried in vacuum for 1 h at room temperature and stored in a glass container. Grafting was carried out by exposing the membranes to different doses of radiation from a  $^{60}\text{Co}$  source (0.18 Mrad/h, Department of Chemistry, University of Poona). The grafted membranes were washed to remove any homopolymer and then dried in vacuum. The grafted film was kept in water for 72 h and the absence of any leachable maleic acid was confirmed by titrating the leachate with NaOH solution.

### **2.1.3 Synthesis of nylon 666-PMA interpolymer (N-PMA) and lysine crosslinked nylon 666-PMA (N-PMA-Ly)**

N-PMA membranes were cast from a formic acid solution containing different ratios of nylon 666 and PMA. In the case of crosslinked membrane the solution also contained different ratios of lysine. Membranes were cured at 80 to

90°C for 4 h and then cooled. N-PMA-Ly membranes were dried at 140°C for 2 h in dynamic vacuum to effect the condensation of lysine with PMA. The membranes were stored in distilled water.

## 2.2 Characterization

### 2.2.1 Polymer characterization

The polymer was characterized by IR spectroscopy, carboxylic acid content and dilute solution viscosity.

#### (a) Determination of carboxylic acid content

An accurately weighed dry sample of PMA was dissolved in water. To this solution a standardized NaOH solution was added dropwise from a burette until it gave turbidity, indicating half neutralization.<sup>3</sup>

#### (b) Viscosity measurement

Intrinsic viscosity was determined by the solution viscosity method using Ubbelohde viscometer.<sup>4</sup> The intrinsic viscosity ( $\eta$ ) was obtained by a graphical procedure using flow times with solution in relation to flow time with the solvent.  $\eta_k = t/t_0$ , where  $\eta_k$  is relative viscosity,  $t$  is the flow time of the solution and  $t_0$  that of the solvent.  $\eta_k$  leads to  $\eta_{sp}$  as  $\eta_{sp} = \eta_k^{-1}$ .

$\eta_{sp}/c$  is plotted as a function of  $C_p$  and the intercept of the linear plots gives  $(\eta)$ , where  $C_p$  is the concentration of polymer in solution. The intrinsic viscosity of PMA was measured in 0.05 N NaCl solution. The intercept of the plot of  $\eta_{sp}/C_p$  Vs  $C_p$  extrapolated to  $C_p = 0$  gives the intrinsic viscosity.

### 2.2.2 Membrane characterization

#### (a) Pretreatment and equilibration

The counter-ions associated with the fixed ions in an ion-exchange membrane are changed to selected species by allowing it to equilibrate in a solution containing a high concentration of the desired ion. The reference ionic form of the membrane is designated by this counter ion. Before measuring the membrane properties the membrane samples were subjected to a pretreatment. The carboxylic acid functions were converted to the  $Na^+$  form by equilibrating with excess of 0.1 M NaOH solution for 72 h. Membranes in the acid form were prepared by dipping the  $Na^+$  form in excess of dilute HCl for 24 h and removing the excess HCl by washing with distilled water.

#### (b) Thickness

Thickness of the membrane was measured with a micrometer after claspig the membrane between two glass



plates. The thickness of the two glass plates were separately determined in the same way.

**(c) Determination of pinholes**

The method permits detection of small apertures by forcing a solution of food grade dye through the membrane under firm hand wiping pressure into an absorbent paper.<sup>5</sup> The membrane samples were placed on Whatman No.1 filter paper. Erythrosin B solution (2.0 g/l) was applied on the sample with a polyurethane sponge. The absence of pinholes was confirmed by the non-appearance of dye spots on the paper observed with a magnifying glass.

**(d) Ion-exchange capacity**

The membrane sample in COOH form was immersed in a known volume of 0.05 M NaOH solution at room temperature for 72 h. The amount of COOH groups was determined by back titrating the solution with 0.05 M HCl. Then the sample was washed with distilled water, dried in vacuum and weighed. Ion-exchange capacity was calculated as the number of milliequivalents of COOH groups per gram of the dry membrane sample using the equation (2.1).

$$\text{Ion exchange capacity (meq/g)} = \frac{(C_0 - C)V}{W} \dots (2.1)$$

Where  $C_0$  and  $C$  are the NaOH concentration in moles/litre in the blank and in the membranes equilibrated solution, respectively,  $V$  (ml) is the volume of 1 M NaOH solution consumed by the membranes and  $W$  (g) is the weight of dry membrane sample.

**(e) Water retention capacity**

The wet membranes were placed in distilled water for 24 h to reach equilibrium swelling. Then the membranes were gently pressed between sheets of filter paper. The water content was determined by drying the weighed samples of the wet membranes in vacuum at 70°C for 8 h. The dry membrane was then weighed and the water content ( $W$ ) was calculated using the following equation.<sup>5</sup>

$$W \% = \frac{W_{\text{wet}} - W_{\text{dry}}}{W_{\text{wet}}} \times 100 \quad . . . . (2.2)$$

**(f) Tensile strength**

The tensile strength of the non-grafted and maleic acid grafted nylon 666 membranes were measured using a Zwick UTM Model 1445. Samples for measurements were prepared according to ASTM D412-80 procedures.<sup>5</sup> The dumbbell shaped samples were placed in the grips of the testing machine, taking care to adjust the specimen symmetrically to distribute the tension uniformly over the

cross-section. The force at elongation and at the time of rupture were recorded to the nearest 10%.

#### (g) Burst strength

Burst strength is expressed as the hydrostatic pressure required to produce rupture of a membrane that has an exposed circular test area 30.5 mm in diameter. Burst strength is the ability of the membrane to resist the pressure difference which may occur in applications such as dialysis and electro dialysis. The apparatus used to measure burst strength is a clamp cell of special design.

Figure 2.1 shows the schematic diagram of the clamp cell.<sup>5,6</sup> The upper clamping surface consists of a stainless steel ring having a circular opening  $30.48 \pm 0.02$  mm in diameter. The surface that is in contact with the membrane during testing has a continuous spiral  $60^\circ$  V-groove, 2.5 mm deep and 0.8 mm pitch. The lower clamping surface has a thickness of 3.25 mm and an opening  $33.07 \pm 0.08$  mm in diameter. The surface has a series of concentric  $60^\circ$  V-grooves, 0.3 mm deep, 0.8 mm apart, the centre of the first groove being 3.2 mm from the edge of the opening. The thickness of the plate at the opening is 0.64 mm. The lower edge which is in contact with a rubber diaphragm has 6.4 mm radius.

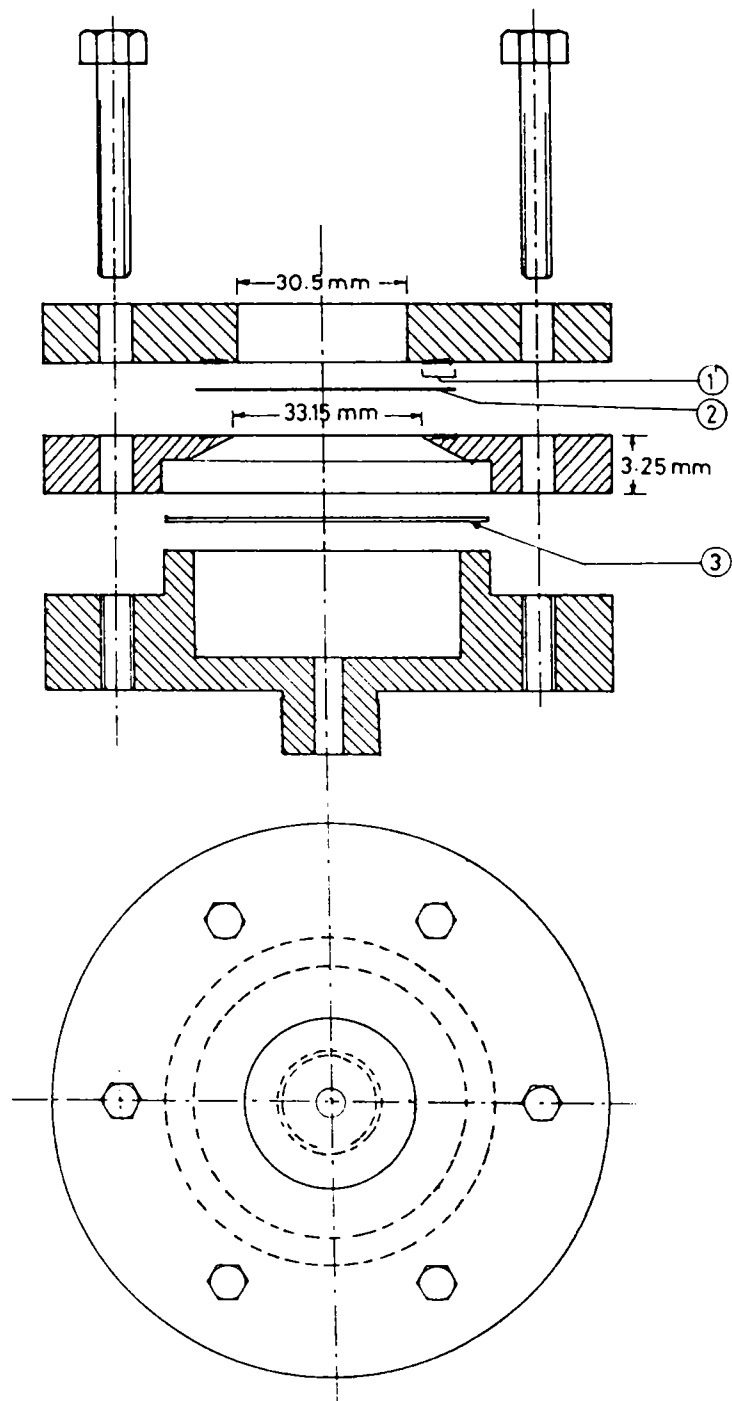


Figure 2.1 Burst strength apparatus

- |    |                        |    |          |    |        |
|----|------------------------|----|----------|----|--------|
| 1. | V-grooves<br>diaphragm | 2. | Membrane | 3. | Rubber |
|----|------------------------|----|----------|----|--------|

The membrane sample was firmly clamped around the periphery over a gum rubber diaphragm. Hydrostatic pressure on the diaphragm was increased at a uniform rate until the membrane material ruptured. The maximum pressure indicated by a pressure gauge is reported as the burst strength of the sample.

**(h) Membrane resistance**

Electrical resistance is inversely related to the ability of membranes to carry electric current when put to applications such as electrodialysis and electrolysis. Electrical resistance per unit area is an important engineering property of a membrane and is used as a quality control parameter. It is expressed in ohm cm<sup>2</sup>, which is the electrical resistance of one square centimeter of membrane material.<sup>5,6</sup> Membrane sample was clamped in a cell of the configuration shown in Figure 2.2.

The cell was filled with 0.1 N KCl whose pH was adjusted using HCl/KOH. After, equilibration the combined resistance of the membrane and electrolyte solution was measured using two gold electrodes. The resistance of the cell containing only electrolyte was measured separately.

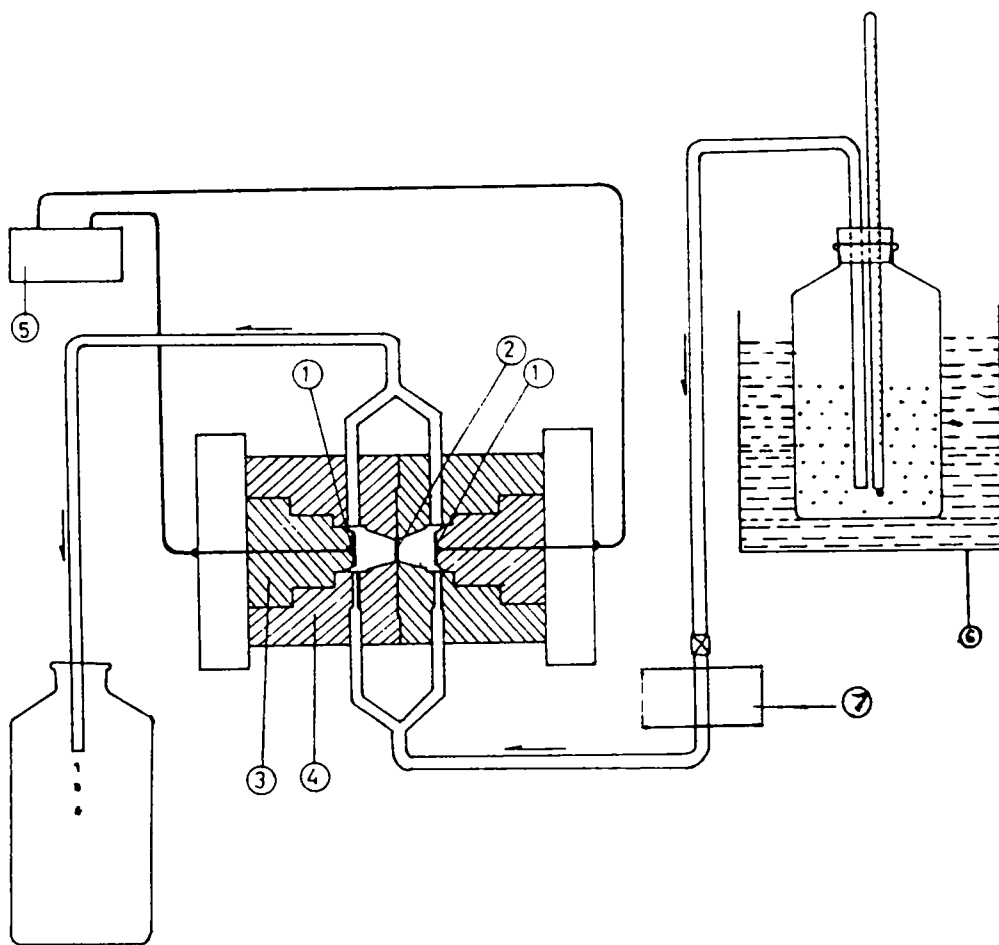


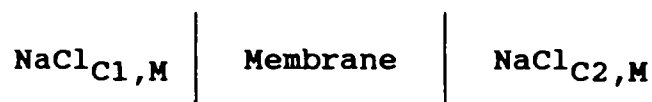
Figure 2.2 Membrane resistance cell

- |    |                  |    |                    |
|----|------------------|----|--------------------|
| 1. | Gold electrode   | 5. | Conductivity meter |
| 2. | Membrane         | 6. | Thermostat         |
| 3. | Electrode holder | 7. | Peristaltic pump   |
| 4. | Cell body        |    |                    |

The difference between the two values multiplied by the area of one principal face of the electrode exposed to the electrolyte solution gave the resistance of the sample. The temperature was maintained at  $30 \pm 1^\circ\text{C}$  and measurements were made using a conductivity meter operating at 1 kHz. The measurements were replicated and average values are reported.

(i) Membrane potential

Potentials were measured using two calomel reference electrodes in an electrochemical cell of the following configuration.<sup>7</sup>



The solutions on the two sides were renewed until further renewal did not cause any change in potential (+0.02 mV) over a period of 1 h. All the measurements were made with the solutions at rest. In order to eliminate any potential arising out of the asymmetry of membranes or electrodes, all potentials are reported as the average of four measurements.<sup>8</sup>

## (j) Dialysis experiments

Permeability measurements were performed in a two compartment glass cell (Figure 2.3) thermostated at  $30 \pm 1^\circ\text{C}$ . The compartments were separated by the membrane. One of the compartments contained the solution of the target species and other with distilled water. The contents of the compartments were stirred magnetically using identical stirrers driven by the same motor. At specified intervals of time, samples were withdrawn from both the compartments and concentration of metal ion was determined by atomic absorption or inductively coupled plasma spectrometry. The concentration of chloride ion was determined by volumetric titration with  $\text{AgNO}_3$ . Urea and creatinine concentrations were measured by spectrophotometry.<sup>9</sup>

### (i) Creatinine permeability

At predetermined times 0.2 ml samples were withdrawn; 5.8 ml water, 2 ml saturated picric acid and 2 ml of 0.75 N NaOH were added to the aliquot. The absorbance of the coloured complex at 550 nm was measured after 20 min.<sup>9</sup>



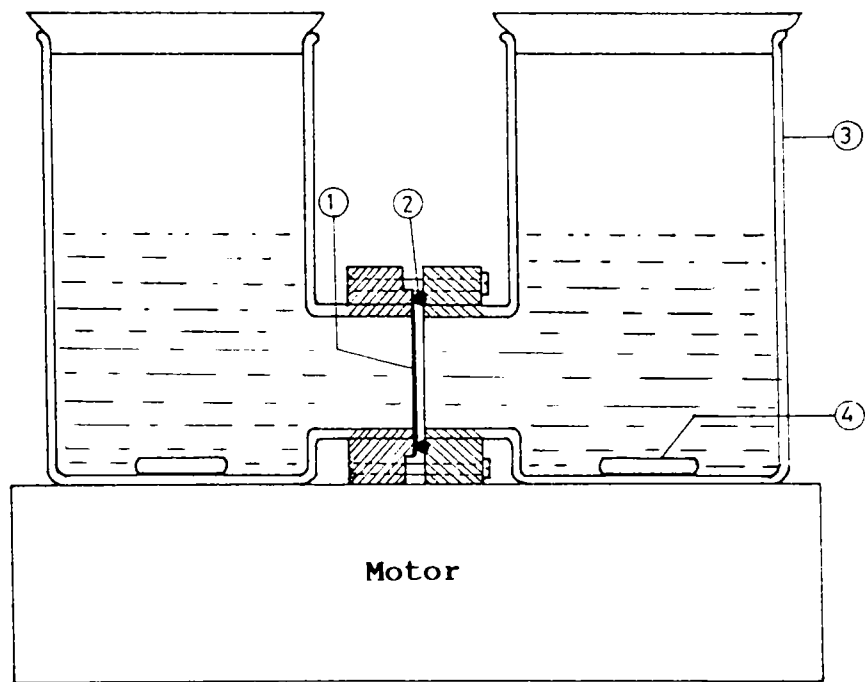


Figure 2.3 Transport cell

- |    |                 |    |                  |
|----|-----------------|----|------------------|
| 1. | Membrane        | 3. | Glass cell       |
| 2. | Neoprene O'ring | 4. | Magnetic stirrer |

## (ii) Urea permeability

To 1 ml of the sample taken from the solute compartment, 10 ml p-dimethylaminobenzaldehyde solution (2 g p-dimethylaminobenzaldehyde in 100 ml of 95% alcohol) were added. After dilution to 25 ml, absorbance values were measured at 420 nm.

## (k) Active and selective transport of $\text{Na}^+$ and $\text{K}^+$

For active transport studies of cations KCl ( $1.0 \times 10^{-2}$  M) was placed in the right side compartment and an equal volume of KOH ( $1.0 \times 10^{-2}$  M) in the left side compartment. For selective transport  $5.0 \times 10^{-2}$  M solutions of NaOH and KOH were placed in the left side compartment and the right side compartment contained  $5.0 \times 10^{-2}$  M solutions of KCl and NaCl. pH of the right side solution was adjusted using HCl.

## 2.3 Results and Discussion

### 2.3.1 Infrared spectra

The acid content of PMA is 6.2 meq/g. The IR spectra of N-g-MA shows new bands at 1720 to 1700  $\text{cm}^{-1}$  and at 1430 to 1400  $\text{cm}^{-1}$  characteristic of carboxyl functional group. The complete conversion of polymaleic anhydride to polymaleic acid was confirmed by the disappearance of

peaks at 1850 and 1780  $\text{cm}^{-1}$  characteristic of cyclic anhydrides. The absorption bands at 1000  $\text{cm}^{-1}$  due to N-H stretching and at 850  $\text{cm}^{-1}$  due to N-H bending disappeared as a result of crosslinking.

### 2.3.2 Properties of nylon 666

Property	Test method	Unit	Value
Appearance	-	-	Clear uniform 2 mm chips
Density	ASTM D 792	$\text{g/cm}^3$	1.11
Melting range	ASTM 2117	$^{\circ}\text{C}$	160-170
Water absorption (Max 23 $^{\circ}\text{C}$ )	ASTM D 570	%	10-12
Moisture regain (after 24 h)	ASTM D 570	%	2.5-3.5
Relative viscosity (in 95% sulphuric acid, 0.5 g/100 ml)	-	-	2.5-2.7
Tensile strength	ASTM D 630	MPa	49.7
Elongation	ASTM D 630	%	300
Impact strength	ASTM D 256 A	$\text{kg/cm}^2$	4.9

### 2.3.3 Viscosity measurements

Polyelectrolyte solutions are known to have a number of properties different from those of both non-polymeric electrolytes and non-ionic polymers. The properties

characteristic of polyelectrolyte solutions have been accounted for by the strong electrostatic potential produced by a large number of charges on a polymer chain.<sup>10,11</sup> PMA which has charge density twice as high as polyacrylic acid (PAA), dissociates in two steps.<sup>12,13</sup> This dissociation suggests that there are two kinds of ionisable carboxyl groups though they are essentially indistinguishable from each other when polyelectrolyte chain has no charge.<sup>13</sup> Half of the carboxyl groups may first dissociate in the same way as the usual polyacids, while the dissociation of the other half ( $\alpha > 0.5$ ) is suppressed by the strong electrostatic interaction from the neighbouring ionized groups.

Lang et al.<sup>1</sup> reported that titration curves of PMA with several kinds of bases always have clear inflection points near the middle of neutralization as if it had two kinds of carboxyl groups with different dissociation constants in an equal amount.

Polymaleic anhydride is a white solid, melting about 300°C (with decomposition). It dissolves in water, alcohols, ketones, ethers and nitroparaffins, but is insoluble in aromatic and aliphatic hydrocarbons and chlorinated solvents. The monosodium salt is soluble in water, but disodium salt is insoluble in water.

Figure 2.4 shows plots of  $\eta_{sp}/C_p$  Vs  $C_p$ , where  $\eta_{sp}$  is the specific viscosity, at different degree of dissociation. The intrinsic viscosities at  $\alpha = 0.3$  is 0.10 and at  $\alpha = 0.5$  is 0.11.

Figure 2.5 shows the plot of  $(\alpha)$  Vs  $\eta$  at  $C_s = 0.050$  N NaCl.  $(\eta)$  of PMA increases with  $\alpha$ , till  $\alpha = 0.5$ , and the solution becomes turbid beyond this.

For a polyelectrolyte solution there are three types of pairwise electrostatic interactions: (1) between small ions from both polyelectrolytes and added salts, (2) between a small ion and a charge on a polyion, and (3) between charges on the same polyion or on different polyions. This repulsive force between the charges on the same polyion through the ionic atmosphere of added salts, causes the expansion of a polyelectrolyte chain. Such an interaction affects little the local conformation of a polyelectrolyte chain whose apparent stiffness has proved to be kept almost constant during the course of the dissociation from a small angle X-ray scattering measurement by Muroga et al.<sup>14</sup> Thus it should be considered as a long range interaction in a similar way as the so called excluded volume effect of a non-ionic polymeric chain.<sup>15,16</sup> The intrinsic viscosity of the polyelectrolyte chain can also be related to the mean

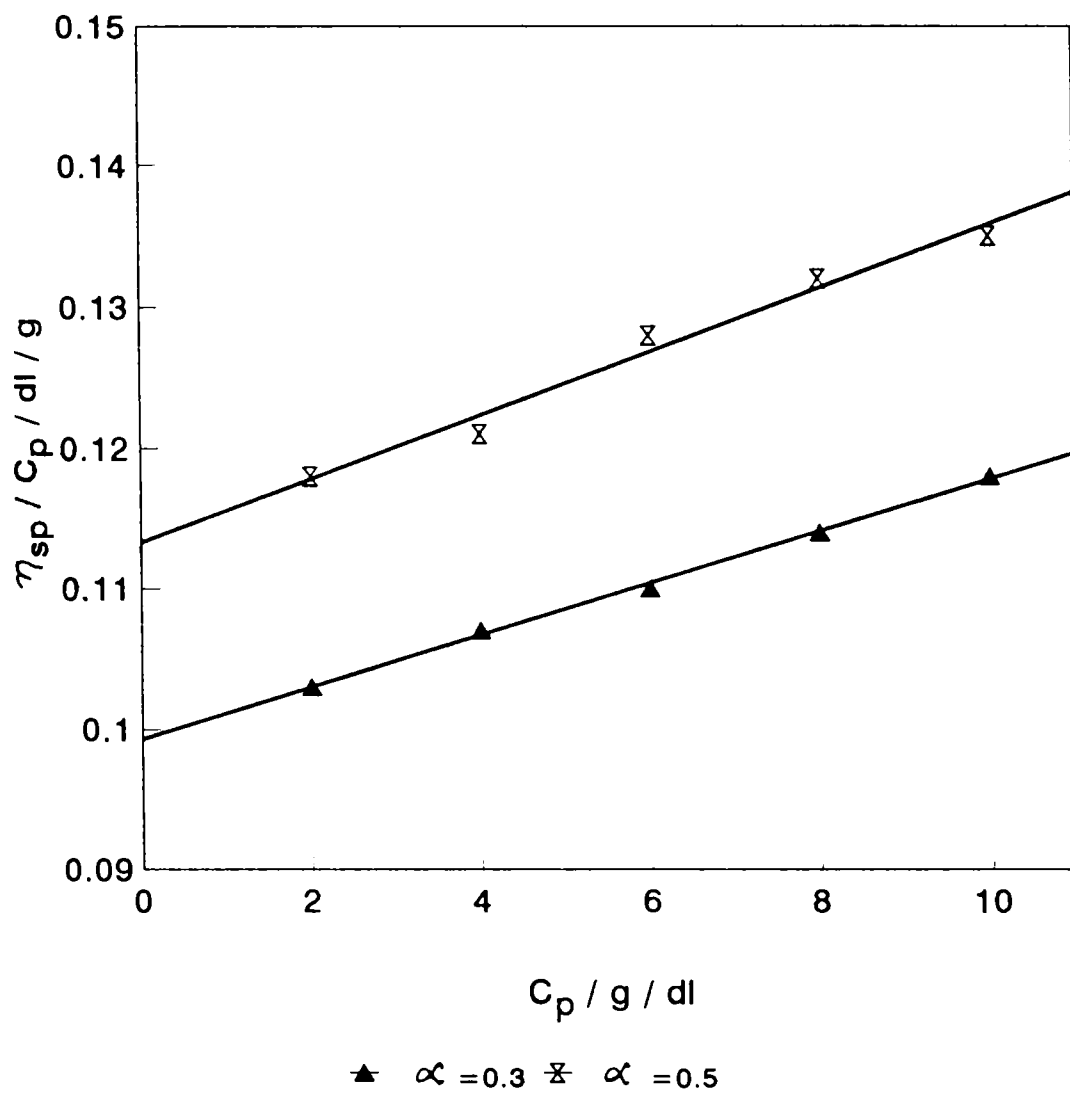


Figure 2.4 Intrinsic viscosity of PMA in 0.05 N NaCl at 30°C.

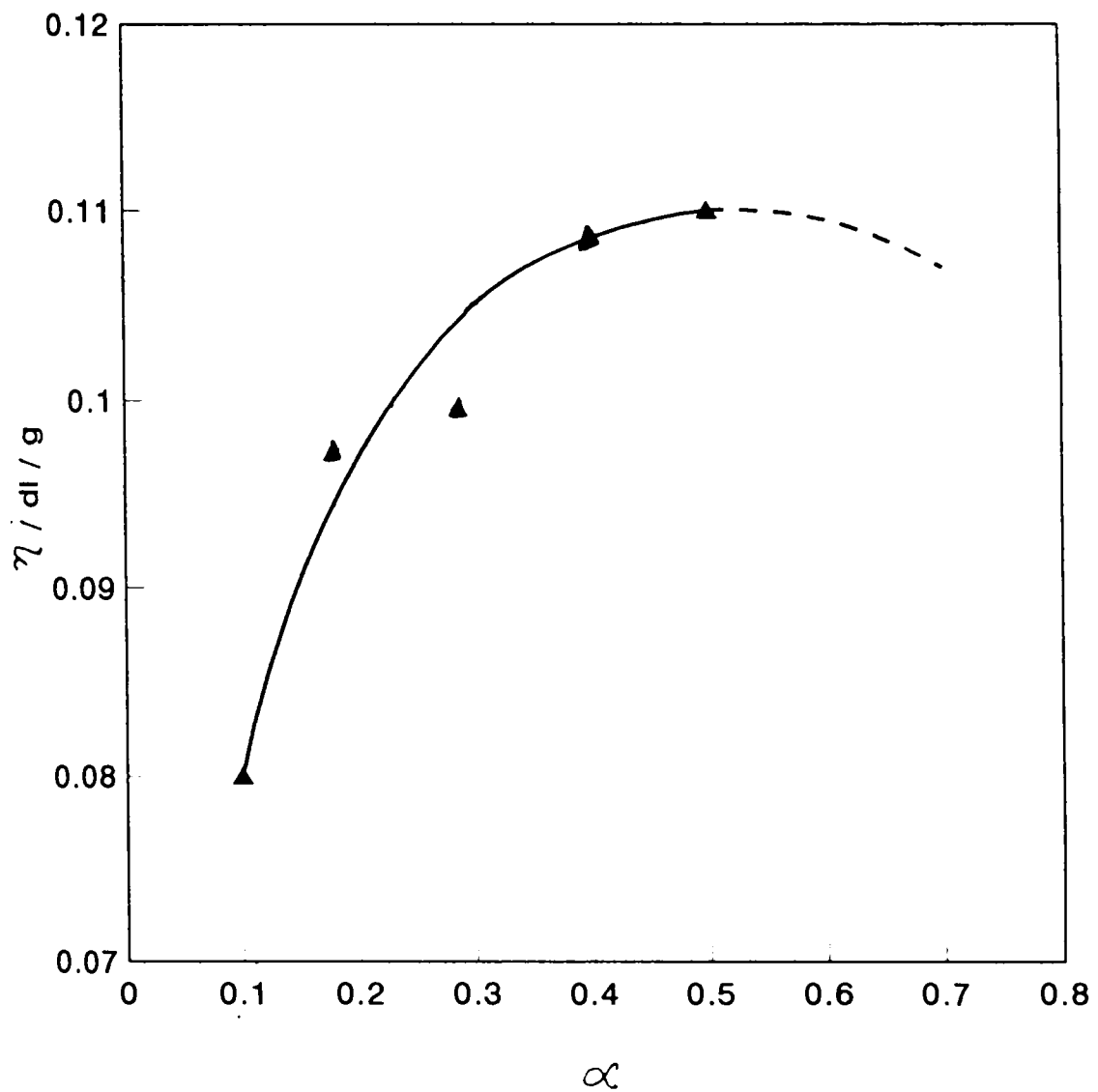


Figure 2.5 Dependence of  $[\eta]$  of PMA on  $\alpha$  in 0.05 N NaCl at 30°C.

square end to end distance  $R^2$ , by the well-known Flory-Fox equation.<sup>17-19</sup>

$$[\eta] = \phi \langle R^2 \rangle^{3/2} / M$$

Where  $\phi$  is the Flory constant, slightly dependent on the excluded volume effect and  $M$  is the molecular weight of the polymer.  $\phi$  being a constant the change in  $[\eta]$  must be directly related to the dimensional change of the polymer chain.  $[\eta]$  of polyacrylic acid increases monotonously with  $\alpha$  due to the electrostatic long range interaction, that is, the coulombic repulsion between the ionic group within a chain.<sup>18</sup> The increase in the  $[\eta]$  value of polymaleic acid at  $\alpha < 0.5$  is attributable to the electrostatic repulsion in the same way as that of PAA, while at  $\alpha > 0.5$  any effect reduces  $[\eta]$  and their chain dimensions until PMA is precipitated out of the solutions.



## References

1. Lang, L. L.; Pavelich, W. A.; Clarey, H. D. *J. Polym. Sci. Part A*, 1963, **A1**, 1123.
2. Dippy; Evans. *J. Org. Chem.* 1950, **15**, 451.
3. Kawaguchi, S.; Toui, S.; Onodera, M.; Ito, K. *Macromolecules* 1993, **26**, 3081.
4. Rabek, J. F. "Experimental Methods in Polymer Chemistry", John Wiley & Sons: New York, 1980.
5. Annual Book of ASTM Standards, 1977, **31**, D 374, D 774, D 2096, D 2187, E 380, D 412-80.
6. Philip, K. C. "Studies on Ion-exchange Membranes and Flocculants Based on Poly(styrene-co-maleic acid)", (Ph.D Thesis); CUSAT, India, 1993.
7. Bockris, J. O'M.; Diniz, F. B. *Electrochim. Acta.* 1989, **34**, 567.
8. Grydon, W. F.; Stewart, R. J. *J. Phys. Chem.*, 1955, **59**, 86.
9. Williams, S. "Official Methods of Analysis", 4th ed.; AOAC Inc.: Virginia, 1984.
10. Rice, S.A.; Nagasawa, M. "Polyelectrolyte Solutions", Academic Press: New York, 1961.
11. Selegny, E. "Polyelectrolytes", D. Reidel Publ. Co.: Amsterdam, 1972.
12. Kitano, T.; Kawaguchi, S.; Minekata, A. *Macromolecules* 1987, **20**, 1598.

13. Kawaguchi, S.; Nishikawa, Y.; Kitano, T.; Ito, K.; Minekata, A. *Macromolecules* 1990, 23, 2710.
14. Muroga, Y.; Noda, L.; Nagasawa, M. *Macromolecules* 1985, 18, 1576.
15. Kitano, T.; Taguchi, A.; Noda, L.; Nagasawa, M. *Macromolecules* 1980, 13, 537.
16. Nagasawa, M.; Kitano, T.; Noda, I. *Biophys. Chem.* 1980, 11, 435.
17. Flory, P. J. "Principles of Polymer Chemistry", Cornell University Press: New York, 1955.
18. Takahashi, A.; Nagasawa, M. *J. Am. Chem. Soc.* 1964, 86, 543.
19. Noda, I.; Tsuge, T.; Nagasawa, M. *J. Phy. Chem.* 1970, 74, 710.

### CHAPTER 3

#### NYLON-666-g-MALEIC ACID MEMBRANES

##### Abstract

Ion-exchange membranes were prepared by grafting maleic acid on nylon 666. The ion-exchange capacity varied from 1.8 to 4.1 meq/g for different membranes. Membrane resistance decreases with increasing pH due to the dissociation of COOH groups. Burst strength was measured as a function of exchange capacity. The permselectivity value decreases with increasing solute concentration. All the membranes show good permeability to urea and creatinine. Due to the difference in anion mobility and size, the permeability coefficients of alkali metal salts are higher than that of neutral solutes. Mean transport rate, transport fraction and selectivity were obtained from active transport of  $\text{Na}^+$  and  $\text{K}^+$  through the membranes. The membranes show good selectivity to  $\text{K}^+$  over  $\text{Na}^+$ .

### 3.1 Introduction

Efficient separation processes are needed to obtain high grade products in the food and pharmaceutical industries, to produce high quality water and to recover or remove valuable or toxic metal components from industrial effluents. The conventional separation methods such as distillation, crystallization, precipitation, extraction, adsorption and ion-exchange have recently been supplemented by processes that utilize semipermeable membranes as separation barriers. In the beginning membranes were used only on a laboratory scale to produce potable water from the sea, to clean industrial effluents, to remove urea and other toxic constituents from the blood stream and for the controlled-release of drugs and biocides.<sup>1,2</sup>

Membrane processes have several features that make them particularly attractive tools for the separation of molecular mixtures. They are modest in energy requirements, in most cases simpler, faster, more efficient and more economical. They can be used for large-scale continuous operations (e.g., desalination of sea water) and for batch-wise treatment of lean process liquors (e.g., antibiotics).

Membrane structure can be tailored to suit to specific tasks. Selection of the proper membrane or

membrane process depends on several factors such as nature of the constituents in a mixture, the volume of solution to be handled and the degree of separation desired. In many cases, membrane processes compare favourably with conventional separation techniques.

Ion-exchange constitutes an important class of membrane separation process. Polymeric ion-exchange membranes find numerous applications in industrial electrochemistry as for instance, diaphragms in chloralkali cells and storage batteries and as solid electrolytes in new generation batteries and fuel cells. Other areas where ion-exchange membranes find applications are production of ultra pure water, controlled-release devices, artificial kidneys and sensors.<sup>3</sup>

Preparation of ion-exchange membranes with adequate operational characteristics like exchange capacity, ion selectivity, electrical conductivity and mechanical strength is a difficult task. Ion-exchange membranes prepared by grafting ionogenic moiety onto a neutral film substrate give more stable structure than those produced by other techniques.<sup>4</sup> Grafting can be accomplished for the purpose of decreasing as well as increasing permeability. Not only permeability but also permselectivity can be improved by grafting suitable monomers.<sup>4</sup> Attachment of acrylic monomers to cellulose films followed by hydrolysis of the graft chains to

polyacrylic acid results in a substantial increase in the permeability of composite membranes over that of cellulose membranes.<sup>5</sup> Nylon grafted with acrylic, and methacrylic acids has been reported to improve the water absorbency and heat resistance of membranes.<sup>6</sup> The radiation initiated grafting of vinyl monomers to nylon 4 membranes, and their use in desalination have been reported by Lai et al.<sup>7</sup>

The following sections describe the preparation and characterization of ion-exchange membranes based on nylon 666-g-maleic acid. The membranes were characterized by their physicochemical properties, mechanical strength and permeability to KCl, NaCl, Na<sub>2</sub>SO<sub>4</sub>, urea and creatinine.

## **3.2 Experimental**

### **3.2.1 Membrane preparation**

The preparation of N-g-MA membranes are described in Section 2.1.2.

### **3.2.2 Membrane characterization**

The membranes were characterized according to the ASTM standards as reported in Section 2.2.2.

### **3.3 Results and Discussion**

#### **3.3.1 Membrane preparation**

Membranes with different ratios of maleic acid content were prepared by varying the radiation dose and amount of maleic acid.

#### **3.3.2 Characterization**

The membranes were characterized by determining some typical physicochemical parameters which reveal the fitness of the membranes for applications. The following parameters were evaluated in the present case: thickness, ion-exchange capacity, water content, tensile strength, membrane potential and transport number.

##### **(a) Ion-exchange capacity and water content**

The characteristics of the membranes used in this study are summarized in Table 3.1. Water content increases with increasing maleic acid content. Higher dose for irradiation enhances the degree of grafting. It is also reported<sup>7</sup> that nylon 6 is grafted only with difficulty by irradiation. Hence larger doses (200 to 400 rads) have been used for grafting 10% maleic acid and the dosage exposed is proportionate to the content of maleic acid so as to effect a higher degree of grafting.

However, it is found that ion-exchange capacity is neither proportional to the amount of maleic acid nor to the dosage given as is evident from Table 3.1.

**(b) Tensile strength**

The tensile strength and elongation of nylon 666-g-maleic acid and nongrafted membranes are given in Table 3.2. It is seen that both tensile strength and elongation of grafted membranes decrease with increasing degree of grafting. The decrease in the tensile strength of the grafted membranes could be attributed to the decrease in the crystallinity of grafted membranes.<sup>8</sup>

**(c) Electrical resistance**

The values of electrical resistance are plotted in Figure 3.1 as a function of external pH. When the external solution is acid, the carboxylic acid groups are not dissociated and the resistance is high as is clear from the resistance data. In basic solutions the acid groups are dissociated and the membrane shows low resistance. In general, it may be concluded that the electrical resistance of the membrane is influenced by the degree of ionisation of -COOH groups which in turn depends on the pKa of the acid and the pH of the medium.



**Table 3.1 Preparation conditions and properties of N-g-MA membranes**

Membrane	Maleic acid content (wt%)	Dose (rads)	Exchange capacity (meq/g)	Water content (wt%)
M1	60	2400	4.1	50.0
M2	50	2000	3.8	46.0
M3	40	1600	2.2	41.0
M4	30	1800	1.8	40.0

**Table 3.2 The tensile properties of N-g-MA membranes**

Membrane	Non grafted		Grafted	
	Tensile strength (kg/cm <sup>2</sup> )	Elongation (%)	Tensile strength (kg/cm <sup>2</sup> )	Elongation (%)
M1	143.1	62.3	47.5	40.7
M2	159.5	69.4	62.6	55.3
M3	169.2	92.2	93.3	84.7
M4	178.5	147.1	121.9	135.3

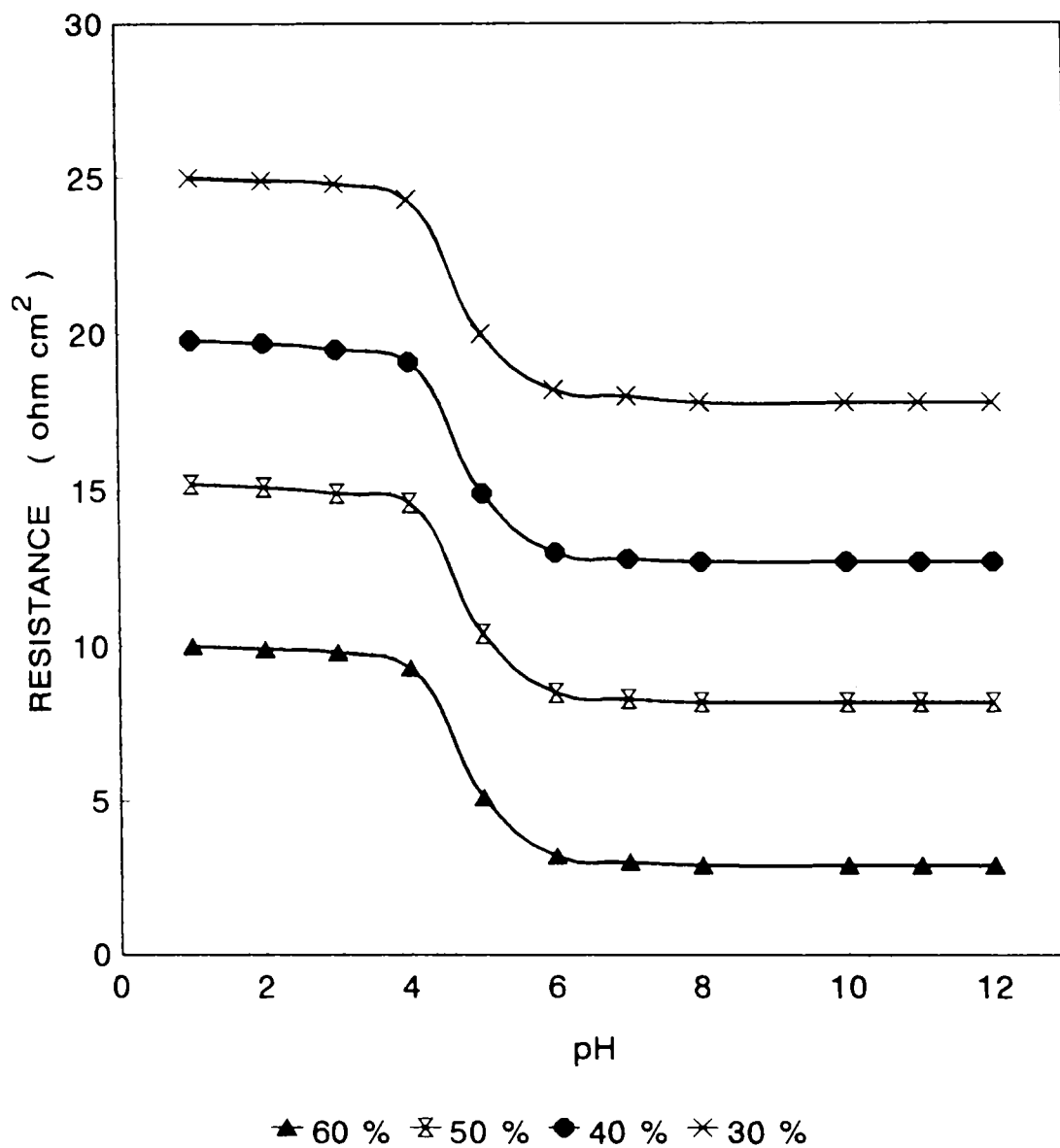
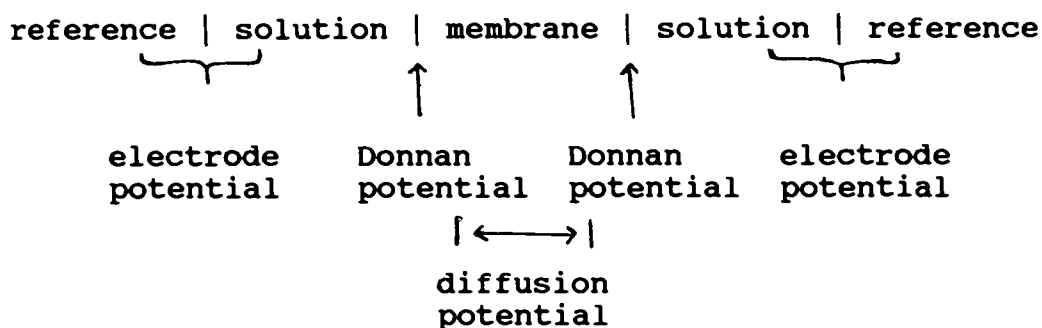


Figure 3.1 Variation of electrical resistance of N-g-MA membranes with different degree of grafting as a function of external pH.

Table 3.3 illustrates the relation between membrane resistance and ion-exchange capacity. Ion-exchange capacity and membrane resistance are compared at pH 6 where the membrane resistance Vs pH plot show a plateau indicating complete neutralization of COOH groups. A decrease in membrane resistance with exchange capacity is observed since the ionizable groups are responsible for both the properties. In the case of membrane resistance, it depends not only on the concentration of the ionogenic groups but also on the polymeric backbone.

**(d) Membrane potential and permselectivity**

When a membrane separates two electrolyte solutions, an electric field (diffusion potential) arises. The magnitude and sign of the potential depend on the nature of the membrane and the permeating species. If the membrane carries no fixed charge, the potential is the same as the liquid junction potential. Membranes can be made cation selective or anion selective by making them absorb large anions or cations which may be held loosely or firmly. This property is very typical of many uncharged membranes. The electrical potential arising across an ionic membrane separating different salt solutions is usually measured by constructing a cell of the type



The magnitude of this membrane potential depends on the electrical characteristics of the membrane. Torell, Meyer and Siever theory gives a reasonable explanation for membrane potential across the ion-exchange membrane.<sup>9</sup> In the case of a cation exchange membrane, the membrane potential  $E$  is given by the following equation.

$$E = (1 - 2\bar{t}_+) \frac{RT}{F} \ln \frac{a_1}{a_2} \quad \dots \quad (3.1)$$

where  $\bar{t}_+$  denotes the transport number of cation in the membrane phase and  $a_1$  and  $a_2$  are the activities of the electrolyte solutions separated by the membrane. In an ideal ion-exchange membrane co-ion transfer does not take place at all and the maximum value of the membrane potential is given by equation (3.2).

$$E_{\max} = \frac{RT}{F} \ln \frac{a_1}{a_2} \quad \dots \quad (3.2)$$

From equations (3.1) and (3.2) it follows that

$$\bar{t}_+ = 0.5 \left( \frac{E}{E_{\max}} + 1 \right) \quad . . . . (3.3)$$

Membrane potentials measured for nylon 666-g-maleic acid membranes are given in Table 3.4. Concentration is used instead of "a" since the accuracy of the potential measurement does not match with the accuracy with which "a" has been measured. Moreover, in the computation of  $t_+$  values the ratio of activities is taken. Hence the influence of activity coefficient on the accuracy of computed values becomes diminished. In order to bring out the dependence of membrane potential on mean concentration  $C_1/C_2$  was kept fixed in all cases. The relative ease with which counterions migrate through a charged membrane is expressed in terms of permselectivity, defined as

$$P_s = \frac{\bar{t}_+ - \bar{t}_-}{t_+ - (2\bar{t}_+ - 1)t_+} \quad . . . . (3.4)$$

$E_{\max}$ , calculated using equation (1), and  $t_+$  values used for calculations are shown in Table 3.5.

**Table 3.3 Variation of membrane resistance with exchange capacity at pH 6**

Membrane	Exchange capacity (meq/g)	Resistance (ohm cm <sup>2</sup> )
M1	4.1	7.1
M2	3.8	10.0
M3	2.2	13.9
M4	1.8	17.6

**Table 3.4 Membrane potential of N-g-MA membranes at different mean concentrations of NaCl**

C <sub>1</sub>	C <sub>2</sub>	Mean concentration	Membrane potential (mV)			
			1	2	3	4
0.025	0.075	0.050	24.50	23.96	24.50	25.05
0.050	0.150	0.100	22.13	22.13	21.59	21.05
0.100	0.300	0.200	18.71	18.70	19.25	18.18
0.200	0.600	0.400	16.09	15.56	13.95	14.48

It is clear from the measurements that the membrane potential can be determined with reasonable accuracy and that for a dilute external solution, the membrane potential is close to the maximum value. As the concentration increases the membrane potential progressively decreases.

This can be readily explained by a decrease in the selectivity of the membrane as a result of which counter-ion transport is affected. In an ideal ion-exchange membrane, ion transfer does not take place at all. The higher values of transport number ( $>0.96$ ) at lower concentration of sodium chloride indicate that nylon 666-g-maleic acid membranes are nearly ideal. The permselectivity values at different mean concentrations are given in Table 3.6. Permselectivity values also show the same trend with an increase in the mean concentration indicating that the membrane deviates from ideal behaviour at high electrolyte concentrations. The increasing concentrations of co-ions, and diffusion of electrolyte through the membrane are responsible for the observed deviation in membrane potential characteristics.

Table 3.5  $E_{\max}$  and  $t_+$  values for NaCl at different mean concentrations

M	$E_{\max}$	$t_+$
0.010	27.68	0.342
0.050	27.23	0.388
0.100	26.99	0.385
0.200	26.74	0.382
0.400	26.83	0.365

Table 3.6 Permselectivity values of  $\text{Na}^+$  at different mean concentrations of NaCl for the membranes studied

Mean concentration (mol l <sup>-1</sup> )	Permselectivity			
	M1	M2	M3	M4
0.05	0.95	0.94	0.95	0.96
0.10	0.91	0.91	0.90	0.89
0.20	0.85	0.85	0.86	0.84
0.40	0.80	0.79	0.76	0.77



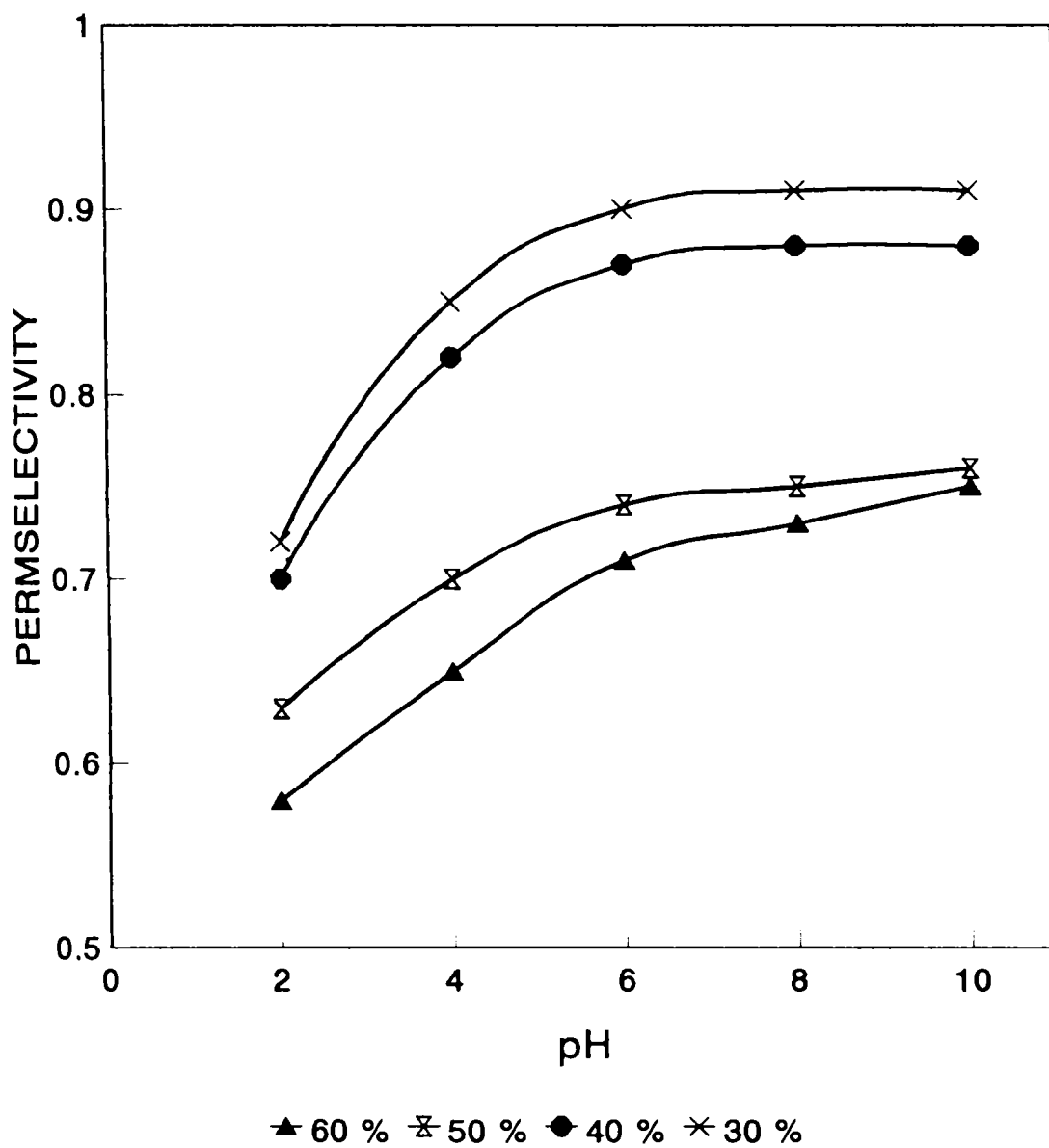


Figure 3.2 Variation of permselectivity of N-g-MA membranes with different degree of grafting as a function of external pH.

Figure 3.2 shows the effect of pH on permselectivity. When concentration ratio and mean concentration are kept fixed, the permselectivity depends on the pH of the solution. As the pH increases the membrane potential increases due to the dissociation of COOH groups.

**(e) Burst strength**

Table 3.7 illustrates the relationship between exchange capacity and burst strength. It is clear from the values that the yield strength decreases rapidly with increasing ion-exchange capacity.

**(f) Permeability studies**

In dialysis experiments the target solutes are transferred from one solution to another through a membrane down the concentration gradient. Separation of different solutes is achieved by the difference in the diffusion rates of solutes within the membrane phase which in turn is a function of the hydrodynamic condition of the dialyzer.<sup>4</sup> The diffusion of any single solute in a dialyzer may be considered in two rate controlling steps: (a) diffusion of the solute through the adjacent fluid films on both faces of the membrane and (b) diffusion of the solute into the pores of the membrane. Thus, the

diffusion rate in a dialyzer may be expressed using the following equation.

$$J = \frac{P \Delta C}{b} \quad . . . . (3.5)$$

where J is the solute flux, P is the permeability coefficient, C is the driving force for mass transfer, and b is the thickness of the membrane in wet form. Assuming that the volumes of the solutions in both compartments are equal and do not change,<sup>11</sup> and on simplification the following equation is obtained.

$$p = \frac{tg\beta vb}{2q} \quad (\text{cm}^2/\text{sec}) \quad . . . . (3.6)$$

Permeability coefficient (P,  $\text{cm}^2\text{s}^{-1}$ ) is calculated using the above equation (3.6), where tgβ is the slope of the  $\ln C_0/(C_0-C_t)$  Vs time plot,  $C_0$  is the initial concentration in the left side compartment ( $\text{mol l}^{-1}$ ),  $C_t$  is the concentration in the right side compartment ( $\text{mol l}^{-1}$ ), b is the thickness of the wet membrane (cm), v is the volume of solution in a compartment ( $\text{cm}^3$ ) and q is the active area of the membrane samples ( $\text{cm}^2$ ). For all the membranes the exposed area was  $3.14 \text{ cm}^2$  and the thickness in the wet form varied from 170 to 240  $\mu\text{m}$ .

Table 3.7 Variation of burst strength with exchange capacity for N-g-MA membranes

Membrane	Exchange capacity (meq/g)	Burst strength (N/mm <sup>2</sup> )
M1	4.1	4.4
M2	3.8	7.1
M3	2.2	8.5
M4	1.8	10.1

Table 3.8 Permeability coefficients for NaCl, KCl, Na<sub>2</sub>SO<sub>4</sub>, NaOH, urea and creatinine (s<sup>-1</sup>cm<sup>2</sup>)

Membrane	KCl (x10 <sup>-5</sup> )	NaOH (x10 <sup>-4</sup> )	NaCl (x10 <sup>-6</sup> )	Na <sub>2</sub> SO <sub>4</sub> (x10 <sup>-6</sup> )	Urea (x10 <sup>-7</sup> )	Creatinine (x10 <sup>-7</sup> )
M1	2.00	1.00	8.40	3.21	2.10	2.30
M2	2.15	2.00	8.30	3.15	2.50	2.00
M3	2.20	1.70	8.25	3.10	2.10	2.10
M4	2.10	1.30	8.20	3.00	2.20	2.40

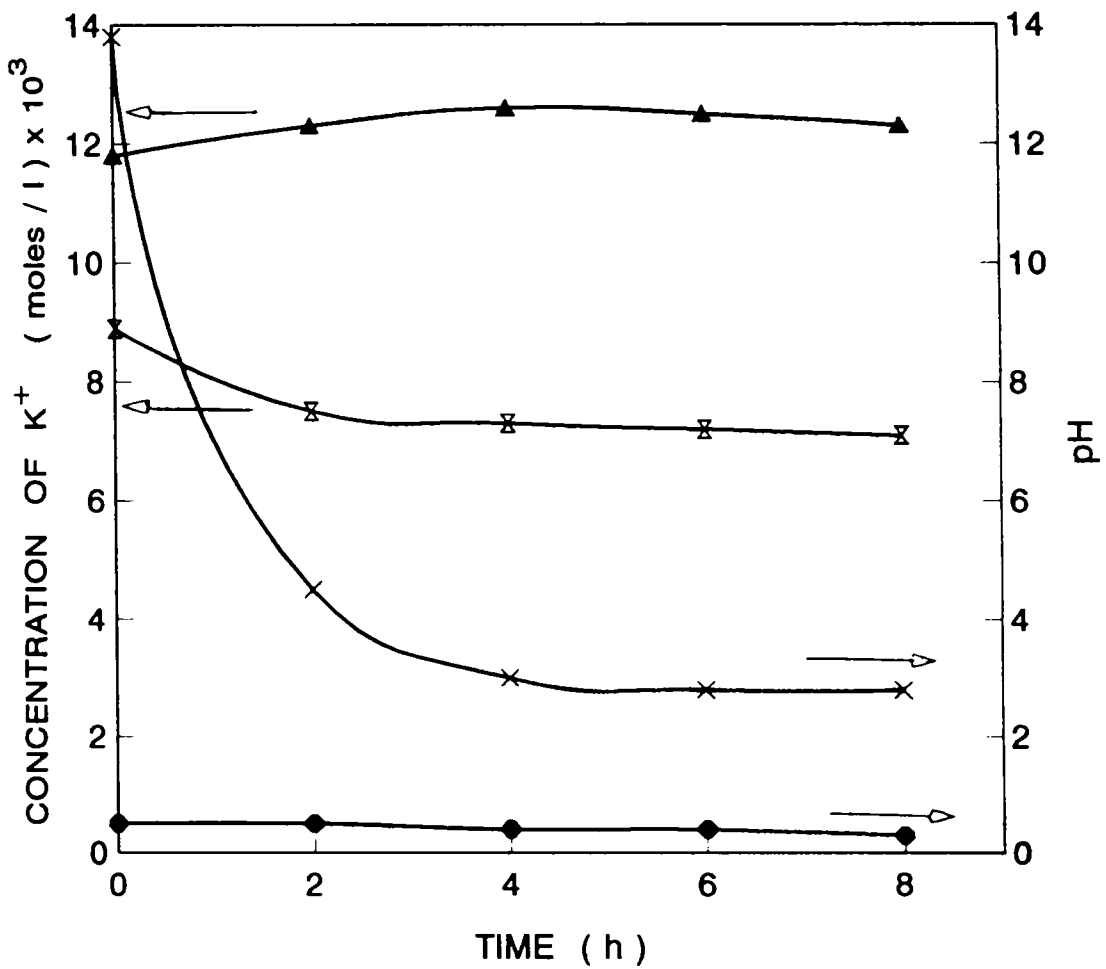
The permeability values obtained for different membranes are given in Table 3.8. It is observed that for all membranes there is significant difference in the permeability coefficient values for a salt and a base, and a salt and undissociated species. The difference in permeability coefficient values of the base and salt may be due to both electrostatic and geometrical effects of the membrane. The permeability of an electrolyte through a charged membrane is controlled by the mobility of both the ions. Due to the high mobility of  $\text{OH}^-$  ions compared to other ions, the permeability coefficient of a hydroxide base is expected to be higher than that of the salts. The large ionic radius of the sulfate ion permits only a low permeability for  $\text{Na}_2\text{SO}_4$ . The permeability coefficient decreases in the order  $\text{NaOH} > \text{KCl} > \text{NaCl} > \text{Na}_2\text{SO}_4$ . Urea and creatinine show lower values, as expected for the passive transport of neutral solutes through a charged membrane.

**(g) Active and selective transport of alkali metal ions**

The mechanism of active transport in carboxylic acid membranes has been discussed by Uragami *et al.*<sup>12</sup> Mass transfer through polymeric membranes is induced by the difference of pressure, concentration and/or electrical potential across the membrane. However, many complex phenomena which cannot be understood by simple

physicochemical mechanisms are found in biomembranes.<sup>13</sup> They include the selective transport of  $K^+$  and  $Na^+$  ions through the cell membrane against the potential gradient. This transport plays an important role for sustaining the function of life. Active transport in biomembranes has not yet been applied to practical fields, but possesses the capability to separate and concentrate materials that cannot be separated or concentrated by conventional techniques. To a limited extent analogous processes with synthetic membranes can be put to practical use.

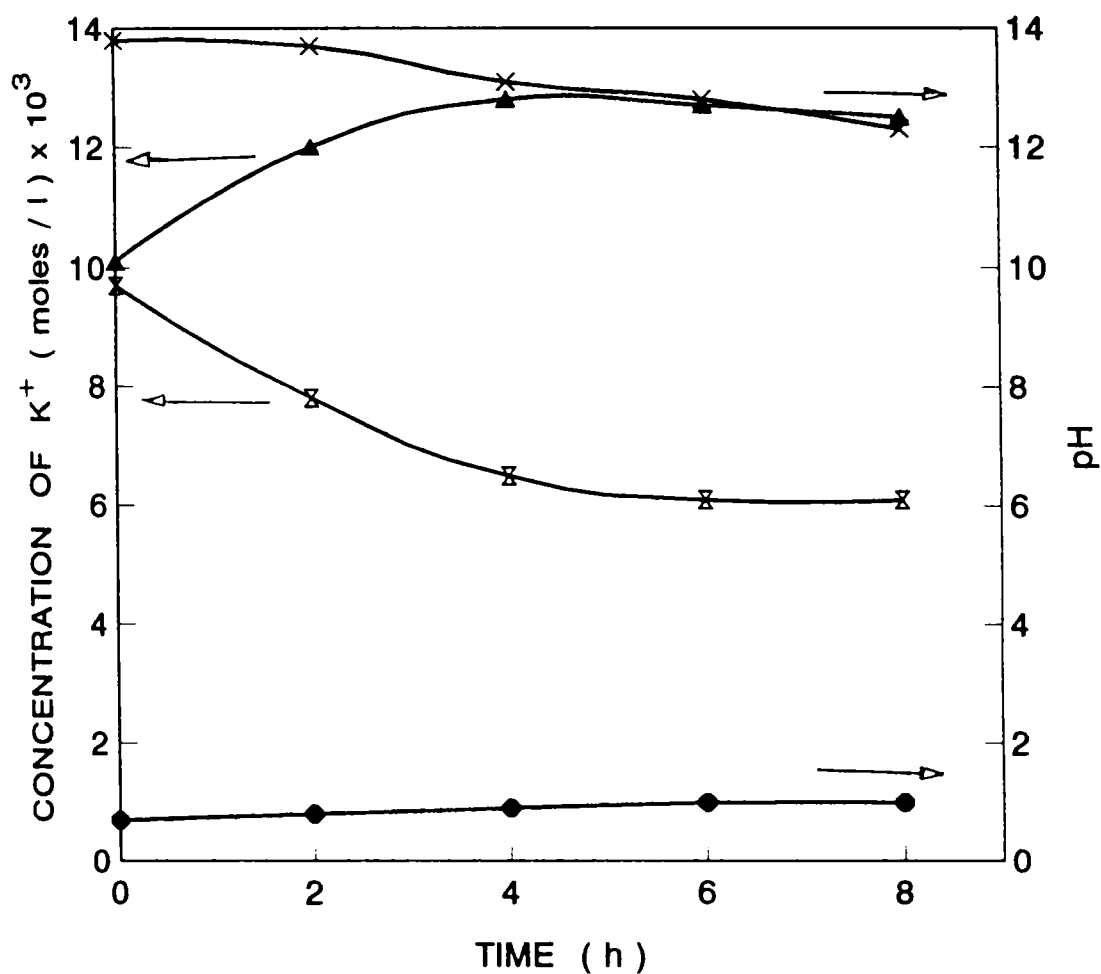
The variation in concentration of  $K^+$  and the changes in pH on both sides with time are shown in Figure 3.3. In all the cases the concentration of  $K^+$  ion on the right side increases for a certain period, while on the left side it decreases. These results suggest that  $K^+$  ions are transported against the concentration gradient existing between the two sides. This may also be related to the swelling of the membrane in alkaline medium and its contraction in acidic medium. During a long transport period,  $K^+$  concentration remains constant and then decreases after about 4 h as shown in Figure 3.3. This is due to the fact that the pH difference between the two solutions becomes small after some time. A moderate  $K^+$  concentration allows the metal ion to diffuse back to the membrane and to be transported back to the L side.



Initial pH in R side: 0.5

▲ K<sup>+</sup> in R side    ✕ K<sup>+</sup> in L side    ◆ pH in R side    \* pH in L side

Figure 3.3a Changes of the K<sup>+</sup> ion concentration and pH in both sides with time through membrane M1.

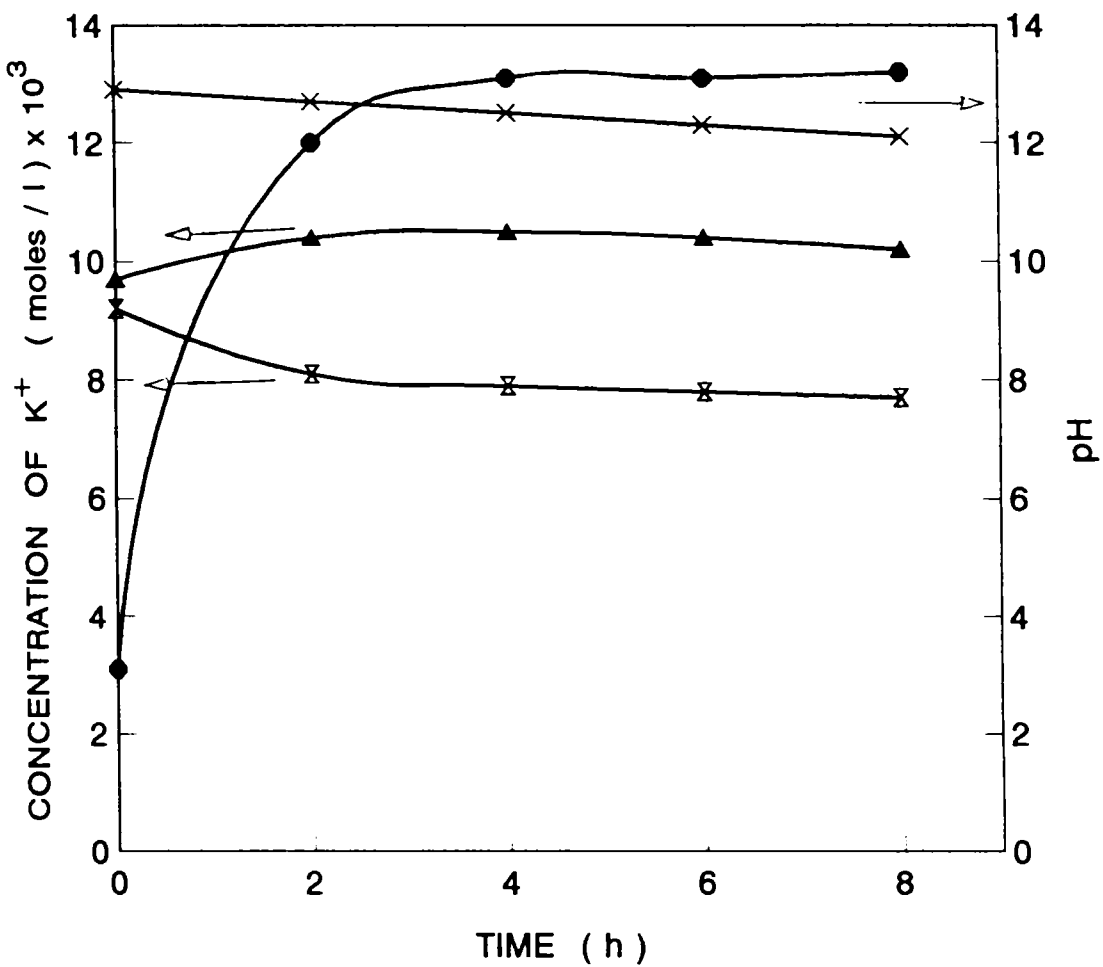


Initial pH in R side: 1.0

▲  $K^+$  in R side    ✕  $K^+$  in L side    ◆ pH in R side    \* pH in L side

Figure 3.3b Changes of the  $K^+$  ion concentration and pH in both sides with time through membrane M1.





Initial pH in R side: 3.0

▲ K<sup>+</sup> in R side    ✕ K<sup>+</sup> in L side    ● pH in R side    ✕ pH in L side

Figure 3.3c Changes of the K<sup>+</sup> ion concentration and pH in both sides with time through membrane M1.

The effect of initial pH in the right side compartment on the mean transport rate and transport fraction of  $K^+$  ions are presented in Table 3.9. These values are calculated using equations (3.7) and (3.8) given below.

$$\text{Mean transport rate} = \frac{[K^+]_{\max} - [K^+]_0}{t_{\max}} \quad \dots \quad (3.7)$$

$$\text{Transport fraction} = \frac{[K^+]_{\max} - [K^+]_0}{[K^+]_0} \quad \dots \quad (3.8)$$

where  $[K^+]_0$  and  $[K^+]_{\max}$  are the initial and maximum concentration of  $K^+$  on the R side and  $t_{\max}$  is the transport time for  $[K^+]_{\max}$ .

**Table 3.9 Effect of initial pH of solution in the right side on the mean transport rate and transport fraction for the membrane M1**

pH	Mean transport rate (mol/l.h) $10^{-4}$	Transport fraction (%)
0.5	2.00	6.70
1.0	6.75	26.70
3.0	2.00	8.20

L-side (High pH)

R-side (Low pH)

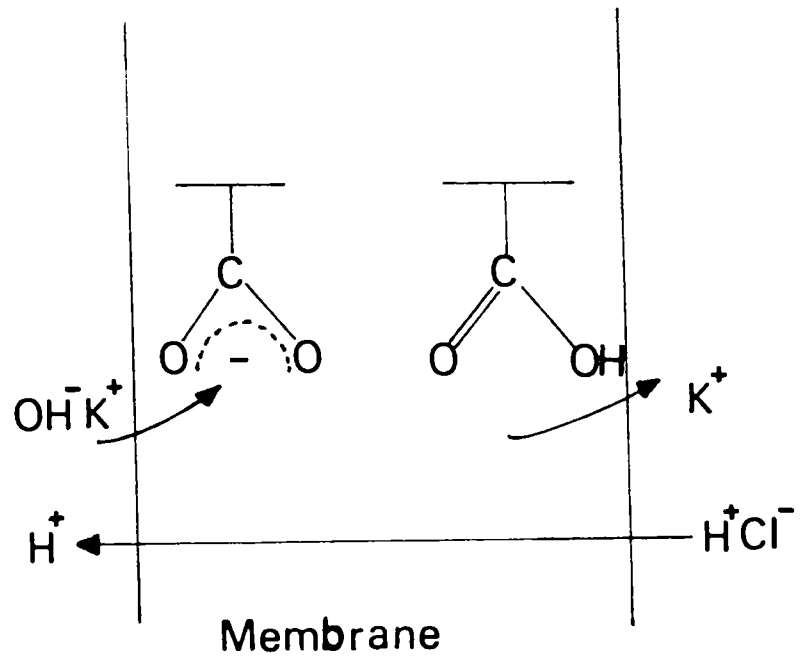


Figure 3.4 Mechanism of active transport of alkali metal ions through the cation exchange membrane having carboxyl group.

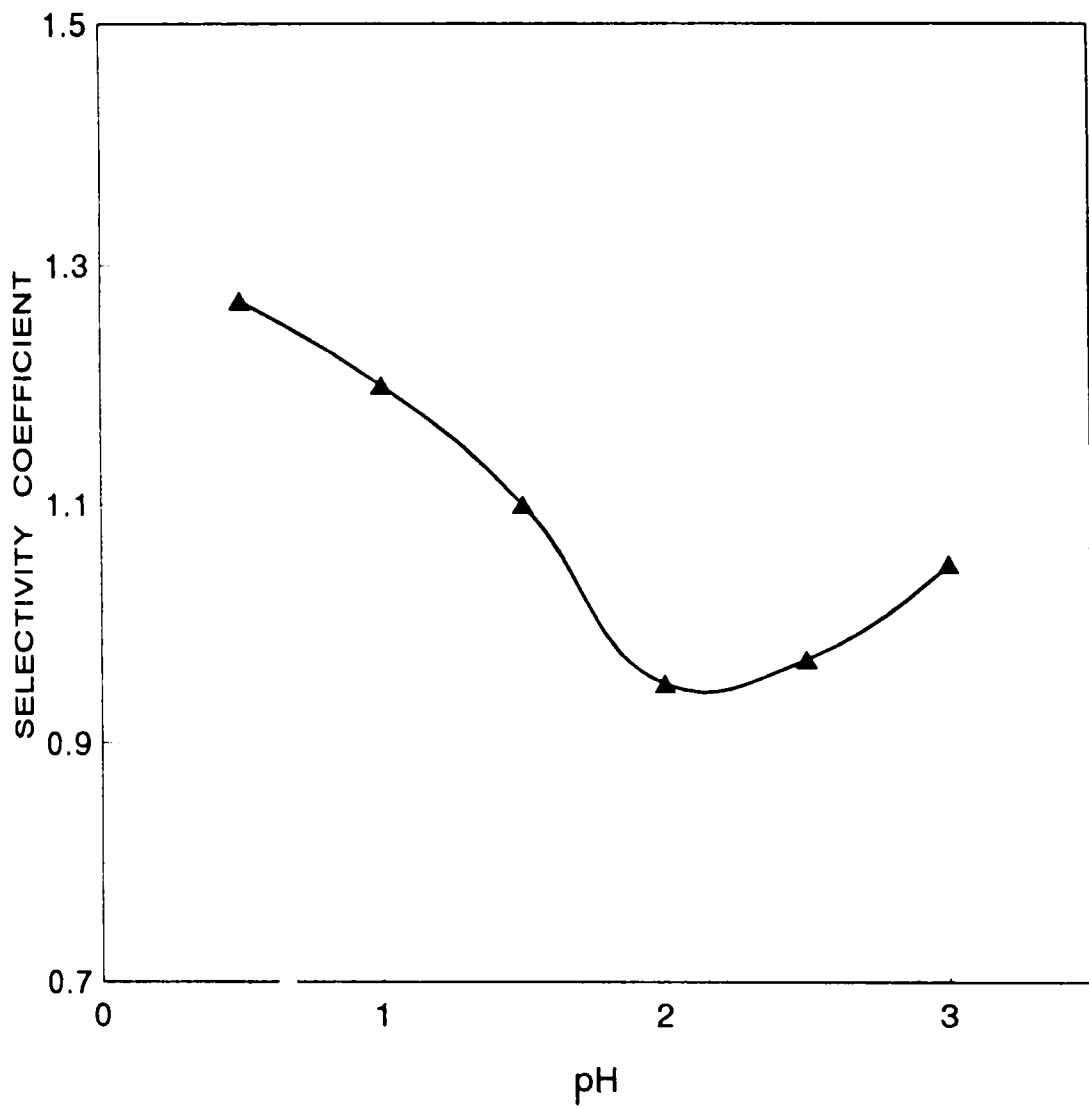


Figure 3.5 Effect of the initial pH in the R side on selectivities in the transport of alkali metal ions.  $K^+$ - $Na^+$  binary system:  
 $[KOH]_0 = [NaOH]_0 = 5.0 \times 10^{-2}$  M.

The mean transport rate and transport fraction show maximum values at pH 1.0 in the right side compartment. Figure 3.4 shows the scheme of a tentative transport mechanism operating during the active transport of cations through the membrane.<sup>12</sup> When one side of the membrane is alkaline and the other side acidic the carboxyl group in the membrane dissociate in the alkaline side ( $\text{OH}^-$ ), and the cations are incorporated into the membrane by the ion-exchange between  $\text{H}^+$  ions in the carboxyl group and the cations on the alkaline side, whereas the dissociation in the carboxyl group on the acidic side ( $\text{H}^+$ ) is very low. Therefore the membrane surface in the acidic side is very dense and consequently permeation of  $\text{Cl}^-$  ions into the membrane becomes very difficult. However,  $\text{H}^+$  ions can be transferred from the acidic side to the alkaline side through the membrane by a proton jump mechanism. When such  $\text{H}^+$  ions reach the region where cation carboxylate exists, cations are released by ion-exchange. The released cations are transferred to the acidic side by an electrical potential gradient.

### Selective transport

The ratio of the amount of metal ion transported from the left side to the right side through the membrane is calculated from equation (3.7).<sup>12</sup>

$$\text{Selectivity} = \frac{([K^+]_{R,t}/[K^+]_{L,0})}{([Na^+]_{R,t}/[Na^+]_{L,0})} \quad . . . . (3.7)$$

where R,t is the concentration of alkali metal ion on the right side at time t and L,0 is the initial concentration on the left side. Effect of initial pH in the right side on selectivity is shown in Figure 3.5. The permeation ratio of K<sup>+</sup> ion to Na<sup>+</sup> ion changes with the initial pH on the right side. The permeation ratio is higher than unity at lower pH and close to unity at higher pH. The high selectivity at low pH may be attributed to the difference in size of the hydrated ions.

## References

1. Lordsak, H. K. *J. Membr. Sci.* 1982, 10, 81.
2. Strathmann, H. "Ullman's Encyclopedia of Industrial Chemistry", Elvers, B., Hawkins, S., Schulz, G. Eds.; VCH: FRG, 1990, A16.
3. Piskin, E.; Hoffmann, A. S. "Polymeric Biomaterials", Martimuz Nijhoff Publishers: The Netherlands, 1986.
4. Kesting, R. E. "Synthetic Polymeric Membranes", McGraw-Hill Book Company: New York, 1971.
5. Baldwin, W.; Holcomb, D.; Johnson, J. *J. Polym. Sci.* 1965, A3, 833.
6. E. I. Du Pont de Nemours & Co., *Jpn. Pat.* 34-7248.
7. Lai, J. Y.; Chang, T. C.; Wu, Z. J.; Hsieh, T. S. *J. Appl. Polym. Sci.* 1986, 32, 1236.
8. Jong, A. Y.; Chung Li, Vn-Yih Lai. *J. Appl. Polym. Sci.* 1988, 36, 87.
9. Lakshminarayanaiah, N. "Transport Phenomena in Membranes", Academic Press: New York, 1962, p. 197.
10. Helfferich, F. "Ion Exchange", McGraw-Hill Book Company: New York, 1962, p. 332.
11. Wysick, R.; Trochimczuk, W. M. *J. Membr. Sci.* 1992, 65, 141.
12. Uragami, T.; Watanabe, S.; Nakamura, R.; Yoshida, F.; Sugihara, M. *J. Appl. Polym. Sci.* 1983, 28, 1613.
13. Katchalsky, A.; Spangler, R. *Rev. Biophys.* 1986, 1, 127.

## CHAPTER 4

### NYLON 666-POLYMALEIC ACID MEMBRANES

#### Abstract

Interpolymer ion-exchange membranes were prepared from nylon 666-polymaleic acid (N-PMA), and from nylon 666-polymaleic acid (N-PMA-Ly) crosslinked with lysine. The ion-exchange capacity of N-PMA membrane is proportional to the amount of PMA present. Membrane resistance and membrane potential studies reveal that N-PMA membranes are highly cation selective. N-PMA membranes show good permeability to NaOH, KCl and Na<sub>2</sub>SO<sub>4</sub> and low permeability to urea and creatinine. Mean transport rate, transport fraction and selectivity were obtained from active and selective transport of Na<sup>+</sup> and K<sup>+</sup> through the membrane. The ion-exchange capacity, membrane resistance and membrane potential data show that N-PMA-Ly membrane is amphoteric in character.



#### 4.1 Introduction

Compared to tailoring the molecular structure of a polymer, it is easier to blend two readily available polymers to combine their desirable properties in a single material.<sup>1</sup> Most of the interpolymer membranes are prepared from a solution in a strong solvent like dimethylformamide or dimethylsulfoxide. The solvents usually employed are those which produce highly viscous solutions, in which polymer elongation and the chances for interwining during dissolution are maximum. The major applications of interpolymer membranes include ion-exchange, reverse osmosis, desalination and ultrafiltration.<sup>2</sup> Interpolymer blends of primary and secondary cellulose acetate are used in the preparation of high salt retention membranes. Cellulose acetate and cellulose nitrate blends are used in the preparation of ultrafiltration membranes.<sup>3</sup>

Diffusion dialysis using carboxylic ion-exchange interpolymer membrane is shown to be effective for the separation of an acid and a salt.<sup>4-5</sup> A weak base ion-exchange membrane separates the aqueous solution of a mixture of a salt and a mineral acid from water. The mobility of hydronium cation is several times greater than that of other cations. Thus the permeation rate of acid

is much greater than that of a salt. The difference in permeation rates makes it possible to separate an acid and a salt. A similar mechanism operates in the case of a mixture of a base and a salt which can be separated by a weak acid ion-exchange membrane. Wycisk et al.<sup>6</sup> has reported such a salt-base separation with interpolymers type carboxylic ion-exchange membrane.

Amphoteric ion-exchange membrane can exchange anions and cations. The composite structure of the amphoteric ion-exchange membrane exhibits a number of interesting properties. It has a higher permeability for electrolytes. This property permits the separation of electrolytes from an aqueous solutions of electrolytes and non-electrolytes using such composite membranes by dialysis, electrodialysis or piezodialysis. Elmidaoui et al.<sup>7</sup> reported the physicochemical characteristics of the amphoteric ion-exchange membrane prepared from polyethylene by grafting with acrylic acid and N,N-dimethylamine-2-ethylacrylate. The introduction of  $\alpha$ -amino acid such as lysine into a nylon film is expected to confer properties such as bio-compatibility and biodegradability.<sup>8</sup> The physicochemical characterization of N-PMA and N-PMA crosslinked with lysine (N-PMA-Ly) are reported here.

## 4.2 Experimental

### 4.2.1 Preparation of membranes

The preparations of N-PMA and N-PMA-Ly membranes are described in Section 2.1.3.

### 4.2.2 Characterization

The membranes were characterized according to the ASTM procedures as reported in Section 2.2.2.

## 4.3 Results and Discussion

### 4.3.1 Membrane preparation

The preparation conditions and properties of N-PMA are summarized in Table 4.1. The membrane containing lysine became brittle with increasing lysine content and films could not be obtained when the lysine ratio exceeded 30%. The membranes containing 10-30% (w/w) of lysine were used in this investigation. The tensile properties are given in Tables 4.2 and 4.3.

### 4.3.2 Characterization

#### (a) Water content

The water content of N-PMA membranes increases with increasing PMA content due to their increased

hydrophilicity. Water content depends on many parameters: external pH, electrolyte concentration and chemical nature of the electrolyte in the solution in contact.

**Table 4.1 Preparation conditions and properties of N-PMA membranes**

Membrane	PMA content (wt%)	Exchange capacity (meq/g)	Water content (wt%)
I1	60	4.3	55.0
I2	50	3.5	49.0
I3	40	2.3	46.0
I4	30	2.0	43.0

**Table 4.2 Tensile properties of N-PMA membranes**

Membrane	Tensile strength (Kg cm <sup>-2</sup> )	Elongation (%)
I1	58.7	157
I2	73.2	134
I3	80.6	125
I4	92.3	112

Table 4.3 Tensile properties of N-PMA-Ly membranes

Membrane	Lysine content (wt%)	Tensile strength (Kg cm <sup>-2</sup> )	Elongation (%)
A1	10	3.0	54
A2	20	2.7	56
A3	30	2.5	59

Table 4.4 Water content (in percentage) in N-PMA-Ly membrane

NaCl (mol l <sup>-1</sup> ) in the external solution	Water content at different pH		
	2	6	10
0.01	57.6	54.3	54.8
0.10	56.2	53.1	53.3
0.50	55.1	52.5	52.6
1.00	53.2	51.0	51.5

The swelling of N-PMA-Ly membranes were carried out by varying both NaCl concentration and pH of the external solution. The water content decreases when NaCl concentration increases (Table 4.4). This decrease in water content is attributed to the osmotic pressure difference between the interior of the membrane and the external solution.<sup>7</sup>

**(b) Ion-exchange capacity**

The exchange capacity is the number of milliequivalents of ion that one gram of the membrane can exchange. The ion-exchange capacity of N-PMA membranes increases with increasing PMA content. In the case of N-PMA-Ly membranes, the ionogenic groups being weakly acidic or basic, their ionization depends on the pH in the external solution. The ion-exchange capacity was thus determined at different pH's (pH 2, 6 and 12) and are reported in Table 4.5. The difference of the exchange capacity between N-PMA-Ly and N-PMA membrane is due to the decrease in the concentration of carboxylic acid groups during its conversion to amphoteric membrane.<sup>7</sup>

**(c) Electrical resistance**

The electrical resistance of N-PMA and N-PMA-Ly membranes as a function of external pH is plotted in

Figures 4.1 and 4.2. The concentration of NaCl was fixed at 0.1 M for all the pH values. The membrane resistance is influenced by the degree of dissociation of the exchanger group, which in turn depends on the pKa of the ionizable groups and pH of the medium. When the external solution is acidic the acid groups are not dissociated. The observation is similar to that of grafted membranes. The COOH groups dissociate progressively as the pH is increased and this results in decreased electrical resistance. At basic pH the amphoteric membrane behaves like cation-exchange membrane and the electrical resistance is low. At neutral pH both acidic and basic groups are dissociated through zwitter ion formation. The zwitter ion being immobile the membrane has a high electrical resistance in the neutral pH range.

Table 4.6 illustrates the relation between membrane resistance and exchange capacity for N-PMA membranes. Ion-exchange capacity and membrane resistance are compared at pH 6 where the membrane resistance Vs pH plot shows a plateau indicating complete ionization of -COOH groups. The decrease in membrane resistance with exchange capacity is quite reasonable since the ionizable groups are responsible for both the properties. These observations are similar to that observed for N-g-MA membranes.

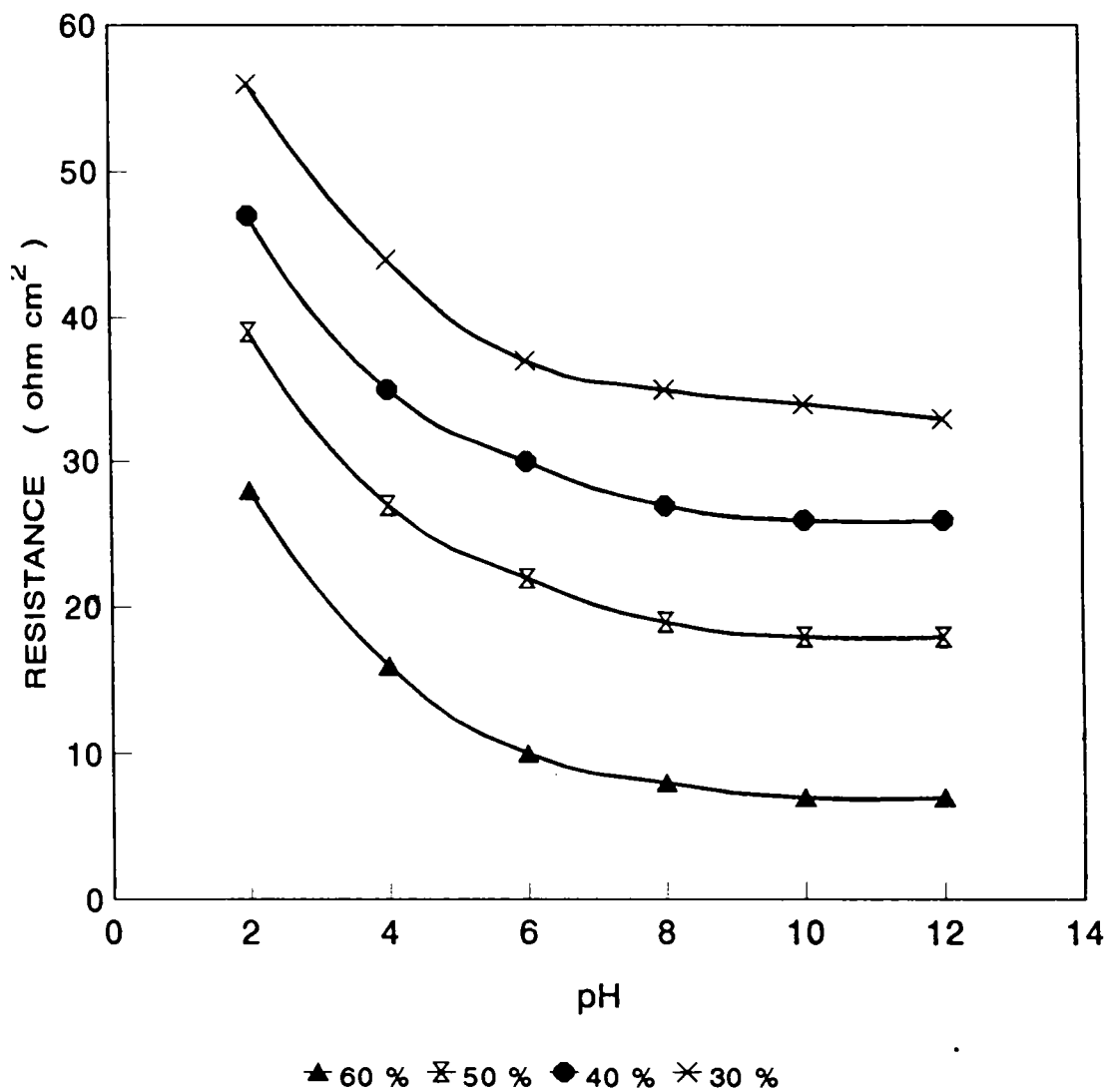


Figure 4.1 Variation of electrical resistance of N-PMA membranes with different composition as a function of external pH.



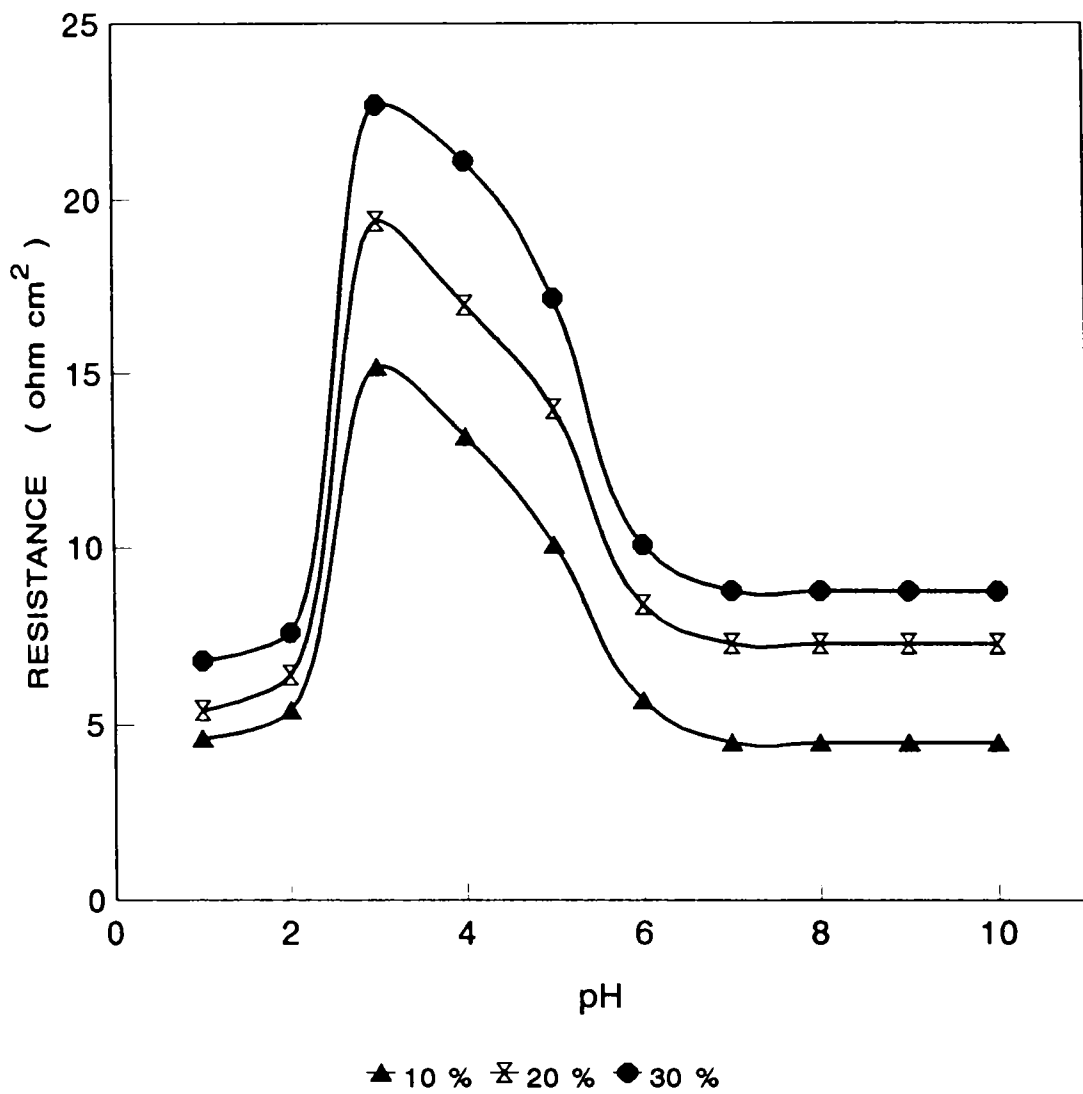


Figure 4.2 Variation of electrical resistance of N-PMA-Ly membranes with different composition as a function of external pH.

**Table 4.5 Exchange capacity of N-PMA-Ly membranes**

External pH	Exchange capacity (meq/g)		
	A1	A2	A3
2	0.24	0.20	0.28
6	0.36	0.35	0.30
12	0.70	0.67	0.65

**Table 4.6 Membranes resistance of N-PMA membranes at pH 6**

Membrane	Exchange capacity (meq/g)	Membrane resistance (ohm cm <sup>2</sup> )
I1	4.3	10
I2	3.5	22
I3	2.3	30
I4	2.0	37

#### **d) Burst strength**

Table 4.7 illustrates the relationship between exchange capacity and burst strength for N-PMA membranes. It is clear from the values that burst strength decreases rapidly with increasing capacity.

#### **e) Membrane potential and permselectivity**

The membrane potential is found to decrease with increasing concentration. This decrease is attributed to a decrease in the selectivity of the membrane as a result of which counter-ion transport is affected. The higher value of transport number (0.97) at lower concentration of NaCl indicate that N-PMA membranes are nearly ideal. Permselectivity values are found to decrease with increase in concentration of electrolyte, which may be due to increased concentrations of co-ions and diffusion of electrolyte through the membrane. The values of membrane potential and permselectivity are reported in Tables 4.8 and 4.9.

Figure 4.3 shows the effect of pH on permselectivity. When concentration ratio and mean concentration ratio are kept constant, the permselectivity depends on pH of the solution. Permselectivity reaches a maximum at higher pH for N-PMA membranes.

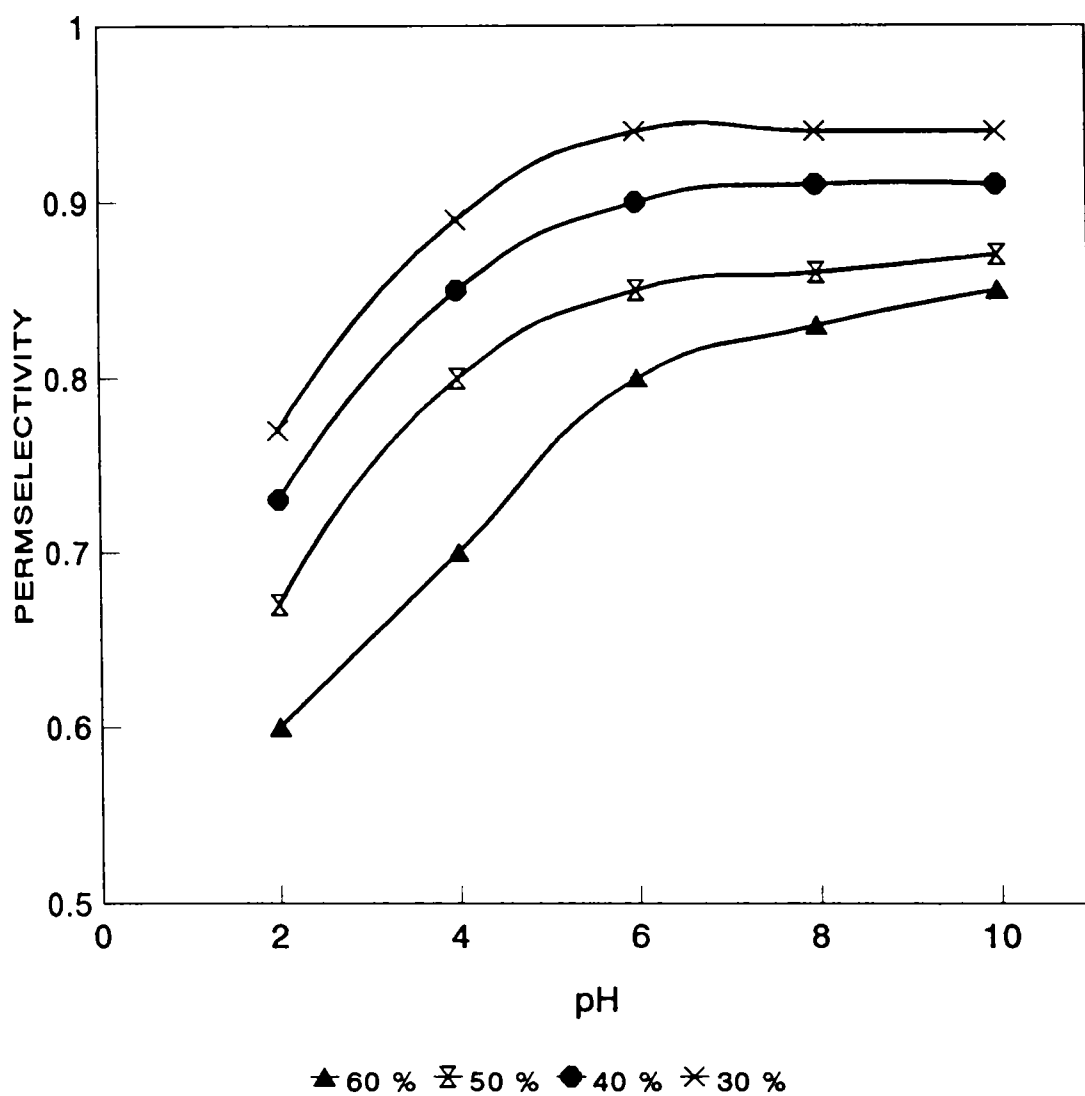


Figure 4.3 Variation of permselectivity of N-PMA membranes with different composition as a function of external pH.

Table 4.7 Burst strength of N-PMA membranes

Membrane	Exchange capacity (meq/g)	Burst strength (N/mm <sup>2</sup> )
I1	4.3	4.75
I2	3.5	6.26
I3	2.3	7.50
I4	2.0	9.26

Table 4.8 Membrane potential of N-PMA membranes at different mean concentrations of NaCl

C <sub>1</sub>	C <sub>2</sub>	Mean concentration	Membrane potential (mV)			
			I1	I2	I3	I4
0.025	0.075	0.050	26.5	26.3	26.4	26.5
0.050	0.150	0.100	24.1	23.5	24.1	24.5
0.100	0.300	0.200	21.4	20.7	21.1	20.9
0.200	0.600	0.400	18.7	18.4	18.9	18.8

**Table 4.9 Permselectivity values of Na<sup>+</sup> at different mean concentrations of NaCl for N-PMA membranes**

Mean concentration (mol l <sup>-1</sup> )	Permselectivity			
	I1	I2	I3	I4
0.05	0.97	0.97	0.95	0.96
0.10	0.94	0.93	0.94	0.95
0.20	0.89	0.88	0.89	0.84
0.40	0.84	0.84	0.82	0.80

**Table 4.10 Permselectivity values for Na<sup>+</sup> ions through N-PMA-Ly membranes at different pHs**

pH	Permselectivity		
	A1	A2	A3
2	0.02	0.01	0.01
6	0.44	0.49	0.43
10	0.79	0.82	0.76

Permselectivity values of crosslinked membranes at different pH are reported in Table 4.10. This membrane behaves like an anion exchange membrane at pH 2 and as a cation exchange membrane at pH 12. At intermediate pH's the membrane is not permselective, it can exchange cations as well as anions.

**(f) Permeability studies**

Dialysis experiments were carried out using N-PMA membrane (I1) which had the highest ion-exchange capacity. Here the solutes are transferred from one side of the membrane to the other down the concentration gradient. Permeability coefficients were calculated using the equation given in Section 3.3. Higher fluxes were obtained for N-PMA membranes compared to N-g-MA membranes.

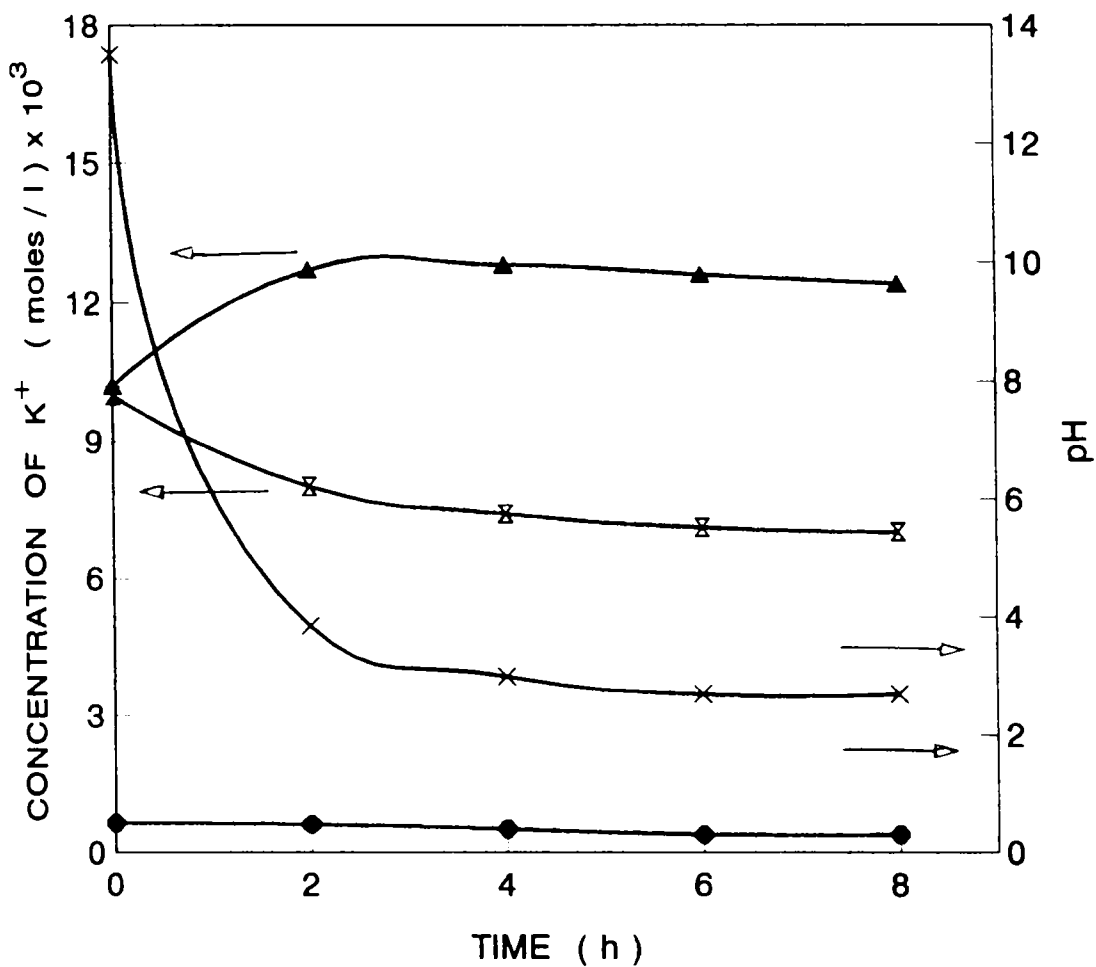
Permeability coefficients obtained are summarized in Table 4.11. It is observed that for all the membranes there is significant difference in the permeability coefficient values for the base and salt. This may be due to the combined effect of the electrostatic forces and geometrical nature of the membranes. The permeability of an electrolyte through a charged membrane is controlled by the mobility of both the ions. The permeability coefficient of the hydroxide base is higher due to the

higher mobility of the hydroxide ions compared to other anions. The permeability coefficient values for the solutes studied decrease in the order  $\text{NaOH} > \text{KCl} > \text{NaCl} > \text{Na}_2\text{SO}_4$ . The values obtained for neutral solutes are much lower as is expected for their passive transport.

**(g) Active and selective transport of alkali metal ions**

N-PMA membrane which had highest ion-exchange capacity (I1) was taken for these studies. The mechanism of active transport in carboxylic acid membranes has already been discussed in Section 3.3.2. The concomitant changes in the concentration of  $\text{K}^+$  and pH on both sides of the membrane with time are shown in Figure 4.4. In all the cases the concentration of  $\text{K}^+$  ion on the right side increases for a certain period, while on the left side it decreases. These results suggest that  $\text{K}^+$  ions are transported against the concentration gradient existing between the two sides. This may also be attributed to the swelling of the membrane in alkaline medium and its contraction in acidic medium. The effect of initial pH in the right side compartment on the mean transport rate and transport fraction of  $\text{K}^+$  ions are presented in Table 4.12. These values were calculated using equations (3.7 and 3.8) described in Section 3.3.2.

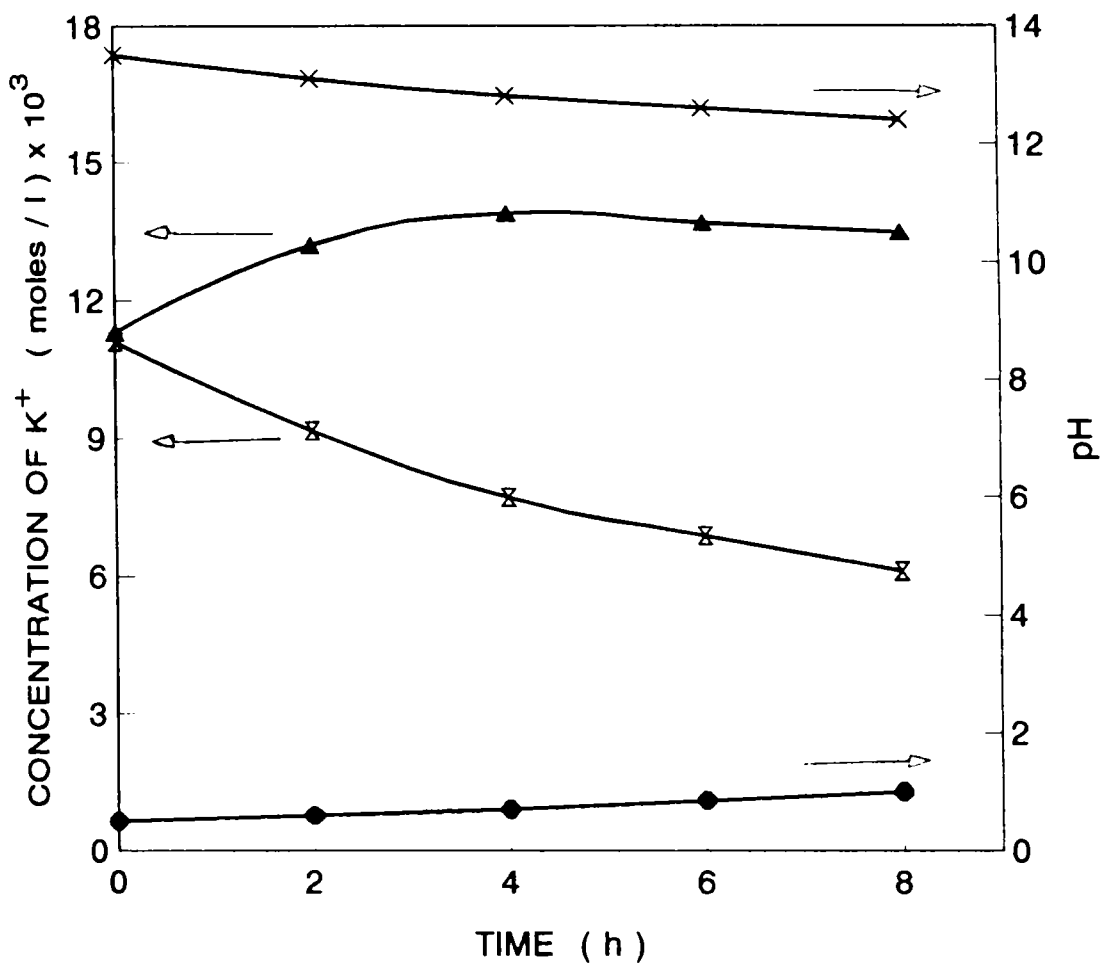




Initial pH in R side: 0.5

▲ K<sup>+</sup> in R side    ✕ K<sup>+</sup> in L side    ◆ pH in R side    \* pH in L side

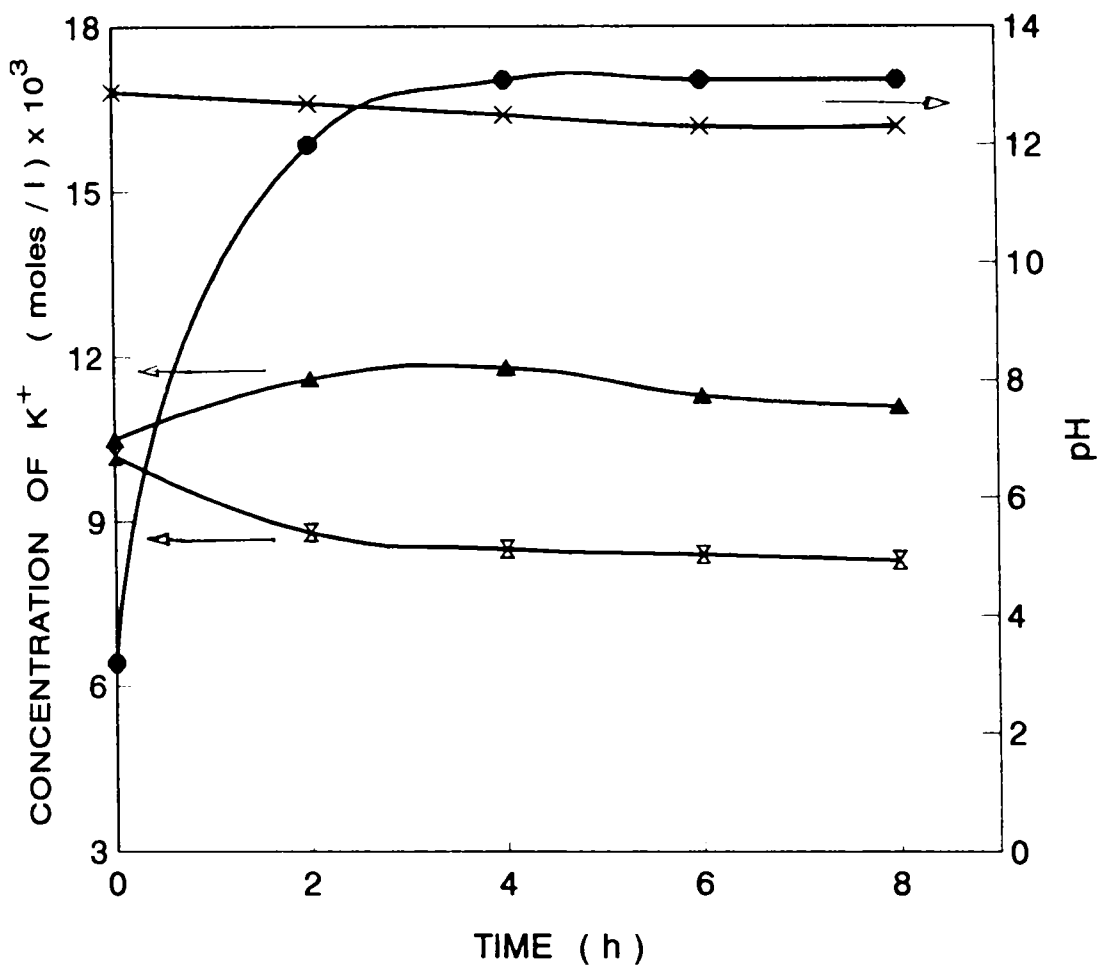
Figure 4.4a Changes of the K<sup>+</sup> ion concentration and pH in both sides with time through membrane I1.



Initial pH in R side: 1.0

▲  $K^+$  in R side    ✕  $K^+$  in L side    ● pH in R side    ✕ pH in L side

Figure 4.4b Changes of the  $K^+$  ion concentration and pH in both sides with time through membrane I1.



Initial pH in R side: 3.0

▲  $K^+$  in R side    ✕  $K^+$  in L side    ● pH in R side    ✕ pH in L side

Figure 4.4c Changes of the  $K^+$  ion concentration and pH in both sides with time through membrane I1.

Table 4.11 Permeability coefficients for KCl, NaOH, NaCl, Na<sub>2</sub>SO<sub>4</sub>, urea and creatinine (S<sup>-1</sup>cm<sup>2</sup>) for transmission through N-PMA membranes

Membrane	KCl (x10 <sup>-5</sup> )	NaOH (x10 <sup>-4</sup> )	NaCl (x10 <sup>-6</sup> )	Na <sub>2</sub> SO <sub>4</sub> (x10 <sup>-6</sup> )	Urea (x10 <sup>-7</sup> )	Creatinine (x10 <sup>-7</sup> )
I1	3.50	2.00	9.60	4.30	3.00	2.70
I2	3.25	2.50	9.50	4.16	2.70	2.40
I3	3.20	1.90	8.80	3.90	3.00	2.60
I4	3.00	1.80	9.00	4.15	2.90	2.20

Table 4.12 Effect of initial pH in the right side compartment on the mean transport rate and transport fraction for K<sup>+</sup> ions through N-PMA membrane

pH	Mean transport rate (mol/lh) x 10 <sup>-4</sup>	Transport fraction (%)
0.5	4.75	17.4
1.0	6.50	23.0
3.0	3.25	12.3

The mean transport rate and transport fraction show maximum values at pH 1.0 in the right side compartment. Effect of initial pH in the right side on selectivities is given Table 4.13. The selectivities are higher than unity at low pH and close to unity at higher pH. This may be due to the difference in size of the hydrated ions.



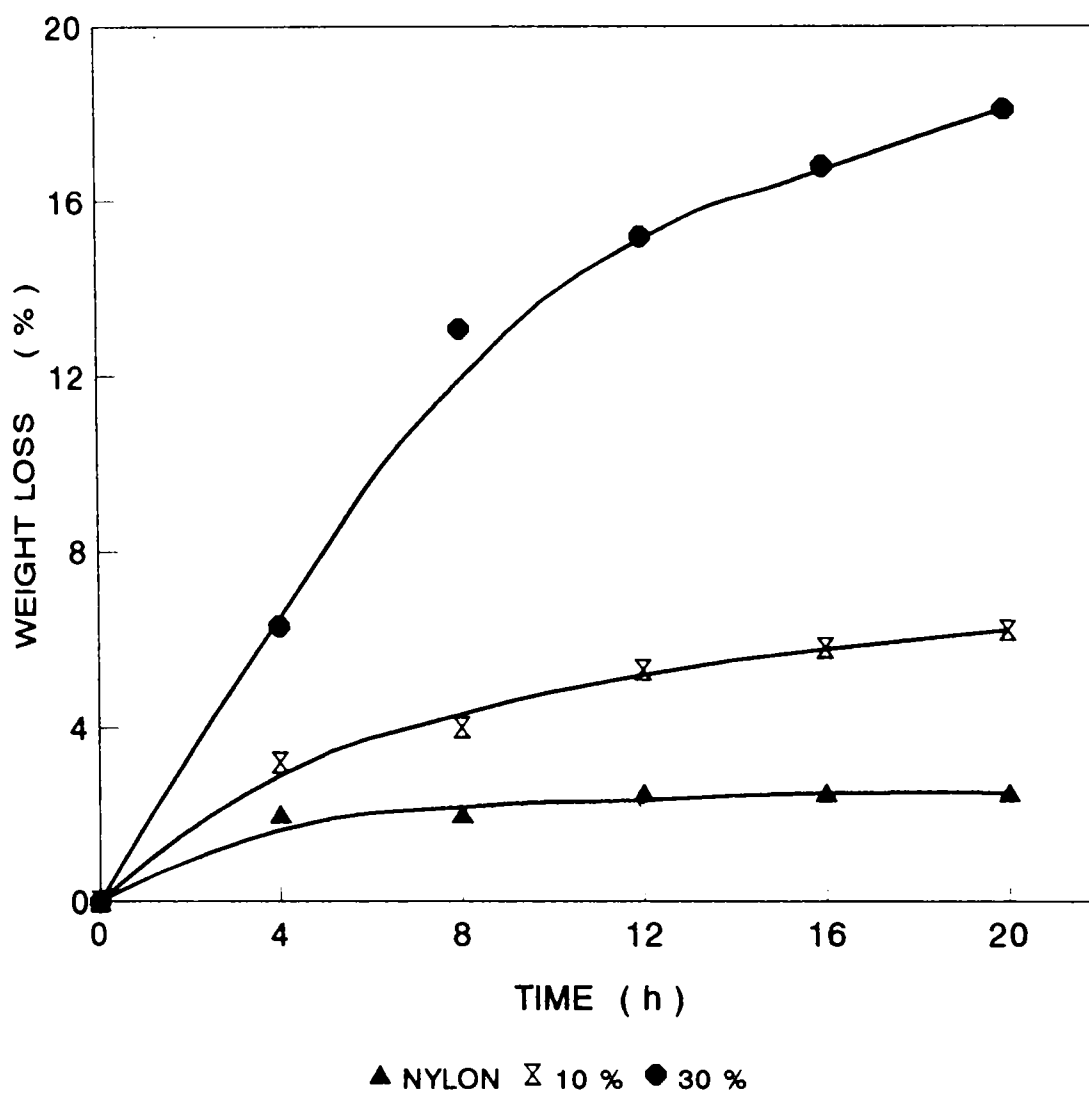


Figure 4.5 Alkaline degradation of N-PMA-Ly membranes in 10% NaOH aqueous solution at 80° containing different weight percentage of lysine.

Table 4.13 Effect of the initial pH in right side on the selectivities in the transport of alkali metal ions through membrane I1.  
 $[\text{KOH}]_0 = [\text{NaOH}]_0 = 5.0 \times 10^{-2} \text{ M}$

pH	Selectivity $\text{K}^+/\text{Na}^+$
1.0	1.10
1.5	1.10
2.0	1.13
2.5	1.15
3.0	1.20

**(h) Degradability of N-PMA-Ly membranes**

Degradation in alkaline medium is considered as an indication for the biodegradability of membranes.<sup>8</sup> Figure 4.5 shows weight loss of film in 10% NaOH aqueous solution at 80°C. The weight loss increases with increase in the gain in film weight. Membrane with 30% lysine content showed about 7 times weight loss after 18 h than for nylon 666. This suggests that the membrane is promising for biodegradation.

## References

1. Kesting, R. E. "Synthetic Polymeric Membranes", McGraw-Hill Book Company: New York, 1971.
2. Helfferich, F. "Ion Exchange", McGraw-Hill Book Company: New York, 1962, p. 332.
3. Gregor, H.; Jacobsen, H.; Shahir, R.; Wetstone, D. *J. Phys. Chem.* 1957, 6, 141.
4. Oda, Y.; Nishihara, A.; Hani, H.; Yawataya, T. *Ind. Eng. Chem., Prod. Res. Dev.* 1964, 3, 244.
5. Kobuchi, Y.; Motomura, H.; Noma, Y.; Hanada, F. *J. Membr. Sci.* 1986, 27, 173.
6. Wycisk, R.; Trochimczuk, W. M. *J. Membr. Sci.* 1992, 65, 141.
7. Elamidaoui, A.; Sarraf, T.; Gavach, C.; Boutevin, B. *J. Polym. Sci.* 1991, 42, 2551.
8. Nagata, M.; Kiyotsukuri, T.; Kohmoto, D.; Tsutsumi, N. *J. Euro. Polym.* 1994, 30, 135.

## CHAPTER 5

### AC CONDUCTIVITY AND DIELECTRIC RELAXATION IN NYLON 666-g-MALEIC ACID AND NYLON 666-POLYMALEIC ACID

#### Abstract

The ac conductivity ( $\sigma_{ac}$ ) and dielectric loss factor ( $\tan \delta$ ) were measured on membranes of nylon 666-g-maleic acid with different degree of grafting and on membranes of nylon 666-PMA with different composition from 100 kHz to 1 MHz in the temperature range 300 to 480 K in dynamic vacuum. The well-resolved  $\alpha$ -relaxation peak in the parent polymer broadens in the grafted polyelectrolyte. The activation energy evaluated from the Arrhenius plot for ac conduction in N-g-MA depends on the degree of grafting and in N-PMA on polymaleic acid content. The activation energy in the rubbery state is greater than that in the glassy state.



## 5.1 Introduction

Viscoelastic relaxations in macromolecules correspond to the onset of various types of internal motion with increasing temperature. They occur more rapidly as the temperature is increased and can be detected through their interactions with mechanical, electrical or magnetic fields. The techniques have been reviewed by McCrum *et al.*<sup>1</sup>

## 5.2 Theory

### 5.2.1 ac conductivity

The ionic conductivity in a polymer is a thermally activated process showing a discontinuity at the glass transition temperature  $T_g$ . The plot of  $\log \sigma_{ac}$  against  $1/T$  for different frequencies gives a series of parallel lines. In the rubber like state these curves converge to a point when  $1/T \rightarrow 0$ . Assuming a pure exponential dependence of conductivity on temperature in the glassy and rubber-like states the observed curves can be described by the following equations.<sup>2</sup>

$$\sigma_{ac} = \sigma_{or} e^{-E_r/kT} \quad \text{at } T \geq T_g \quad . . . . (5.1)$$

$$\sigma_{ac} = \sigma_{og} e^{-E_g/kT} \quad \text{at } T < T_g \quad . . . . (5.2)$$

For  $T = T_g$  it follows that

$$\frac{E_g - E_r}{kT_g} - \ln \sigma_{og} = -\ln \sigma_{or} \quad . . . . (5.3)$$

where  $\sigma_{og}$  = extrapolated value for conductivity for  $T \rightarrow \infty$  in the glassy state and  $\sigma_{or}$  = extrapolated value for conductivity for  $T \rightarrow \infty$  in the rubber like state.  $E_g$  and  $E_r$  are activation energies in the glassy and rubbery states respectively.

The  $\sigma_{ac}$  Vs  $1/T$  plots are concave down, therefore these curves can be represented by a sum of exponentially temperature dependent conductivities over the entire experimental temperature range.

$$\text{If } \sigma_{ac} = \sum_i \sigma_{oi} e^{-E_i/kT}$$

$$\frac{d^2\sigma}{d(1/T)^2} = 1/k^2 \sum_i E_i^2 \sigma_{oi} e^{-E_i/kT} > 0 \quad . . . . (5.4)$$

This means that  $\sigma_{ac}$  Vs  $1/T$  curves are concave down. The observed conductivity-temperature dependence is subject to a freezing in mechanism at the glass transition temperature. Such a mechanism is possible, if the ionic conductivity followed the free volume variation with temperature or if the dielectric permeability changes abruptly at the glass transition temperature. The first

case is considered within the framework of hole creation mechanism above the glass transition and affects the conductivity product  $\sigma = nq\mu$  through the change in mobility ( $\mu$ ). In the second case the number of free carriers ( $n$ ) is affected by the change in ionic dissociation energy with the change in the value of the dielectric constant. Both these mechanism may work side by side and has been reported for the ionic conductivity of polymers  $E_r > E_g$ .<sup>3-5</sup>

### 5.2.2 Dielectric relaxation in polymers

Dielectric measurements are closely related to dynamic mechanical techniques. It is easier to vary the measurement frequency, but the response depends on the presence of electrical dipoles in the sample. When the material is subjected to a relaxation process by increasing the temperature or decreasing the frequency, the modulus decreases, the dielectric constant increases, and the electrical loss has a peak value.<sup>6</sup>

The dielectric properties of a material depends on its interaction with an applied electric field at the electronic, atomic and molecular level. Polarization and dielectric loss are the phenomena of interest in macromolecular chemistry and are usually studied as a function of frequency.

When an electric field is applied to a dielectric material, the dipole moments of separate kinetic elements or atomic groups will tend to orient in the field direction. If the field is removed after a certain time, induced polarization of the sample will diminish to zero as a result of thermal agitation of separate kinetic elements, and the system will return to its equilibrium state. Such a process of reverting to equilibrium is called dielectric relaxation. It is characterized by the relaxation time  $\tau$ .<sup>7</sup>

If an alternating electric field is applied to the material, the dielectric properties will depend on the frequency of the applied potential and the dielectric relaxation time  $\tau$ .

The dielectric properties of a material can be expressed by its complex dielectric constant (relative permittivity).

$$\epsilon^* = \epsilon' - i\epsilon'' \quad . . . . (5.5)$$

where  $\epsilon'$  and  $\epsilon''$  are the real and imaginary parts of the complex dielectric constant.  $\epsilon''$  is also known as the dielectric loss factor. The ratio  $\epsilon''/\epsilon' = \tan \delta$  is the dielectric loss tangent.<sup>8</sup>

If the dielectric relaxation can be described by a single relaxation time, then

$$\epsilon' = \epsilon_{\infty} + \frac{\epsilon_0 - \epsilon_{\infty}}{1 + \omega^2 \tau^2} \quad . . . . (5.6)$$

$$\epsilon'' = \frac{(\epsilon_0 - \epsilon_{\infty}) \omega \tau}{1 + \omega^2 \tau^2} \quad . . . . (5.7)$$

and  $\tan \delta = \frac{(\epsilon_0 - \epsilon_{\infty}) \tau}{\epsilon_0 + \epsilon_{\infty} \omega^2 \tau^2} \quad . . . . (5.8)$

where  $\epsilon_0$  is the dielectric constant at  $\omega = 0$  and  $\epsilon_{\infty}$  the dielectric constant at  $\omega = \infty$ .

The ac conductivity  $\sigma_{ac}$  may be expressed

$$\sigma_{ac} = \epsilon_0 \epsilon_r \omega \tan \delta \quad . . . . (5.9)$$

where  $\epsilon_0$  is the static dielectric constant,  $\epsilon_r$  the permittivity,  $\omega$  the angular frequency and  $\tan \delta$  the loss tangent.

The dielectric relaxation processes are labelled  $\alpha$ ,  $\beta$ ,  $\Gamma$  and so on, beginning at the high temperature end. Some polymers are wholly amorphous and there is only one phase present in the solid material. In such cases there is always a high temperature  $\alpha$ -relaxation associated with the micro-Brownian motion of the whole chains and, in addition, at least one low temperature ( $\beta$ ,  $\Gamma$ , etc.)

subsidiary relaxation. The relative strengths of the  $\alpha$  and  $\beta$ -dielectric relaxations depend on how much orientation of the dipolar groups can occur through the limited mobility allowed by the  $\beta$  process before the more difficult but more extensive mobility of the  $\alpha$  process comes into play: there is a partitioning of the total dipolar alignment amongst the molecular rearrangement process.

The transition from a glassy to a rubbery consistency is a characteristic of many polymeric solids, and depends upon the thermal energy of the molecules. At some stage as the temperature increases, the segmental mobility increases to the point where rubber like deformation under a small applied stress becomes possible. This segmental mobility depends on the nature of the interchain forces, and in the case of ionic polymers upon the degree of ionization and the presence of ionic bonds. The electrostatic forces between the bound ions in the polymer chain and the counter-ions reduce the segmental mobility and increase  $T_g$ . Above  $T_g$ , there is sufficient mobility, a sort of micro-Brownian motion which enables large-scale reorganisation of the chains to occur whereas below  $T_g$  the chains are frozen in position. In other words, an observed  $T_g$  is the temperature at which the time constant for a molecular rearrangement process becomes comparable with the time scale of the experiment used to measure it.

At the onset of  $T_g$ , permanent dipoles attached rigidly to the polymer backbone become free to orient in an electric field, and the glass transition is accompanied by a major dielectric dispersion.

### 5.3 ac Conductivity and Dielectric Relaxation in Nylon Polymers and Polycarboxylic Acids

Dielectric measurements have been used extensively to investigate molecular motion and relaxation behaviour in polymers.<sup>9</sup> Several distinct relaxation processes are usually present in a solid polymeric material. Thus multiplicity is manifested readily in a scan of dielectric loss as a function of temperature at constant frequency. As the temperature is raised, molecular mobilities of various types become successively energised with concomitant dipolar orientation. The same relaxation processes are generally responsible for dispersions in mechanical properties, although a particular molecular arrangement may produce a stronger dielectric response than a mechanical effect or vice versa.

Boyd has reported the dielectric loss in nylon 66 over a range of frequencies and temperatures.<sup>9</sup> He found that the principal dipolar orientation absorption is similar to that in amorphous polar polymers in that it involves long chain segment rearrangement in the amorphous

region. Studies on the dielectric relaxation behaviour of ethylene copolymers with carboxylic acid side groups have been reported.<sup>10-13</sup> The  $\alpha$  peak corresponds to a glass transition temperature associated with ionic clusters and  $\beta$  relaxation is due to the motion of hydrocarbon chains. A detailed study of the dielectric relaxation of polyethylene with phosphonic acid side groups was made by Phillips *et al.*<sup>10</sup> In this case the phosphonic acid groups do not dimerise as do carboxylic acids.

A study of the frequency and temperature dependence of the dielectric properties of nylon 666, nylon 666-g-maleic acid and nylon 666-PMA are reported here.

#### 5.4 Experimental

The preparation of nylon 666, N-PMA and N-g-MA samples are described in Section 2.1. All samples were dried in vacuum.

Hewlett Packard Impedance Analyzer Model 4192 A was used for the measurement of ac conductance  $\sigma_{ac}$ , and dielectric loss factor  $\tan \delta$ . In the lowest range of measurements the instrument gives a readability of 1 nS for  $\sigma_{ac}$  and 0.001 for  $\tan \delta$ . Using this instrument, measurements could be effected in the frequency range 10 kHz to 13 MHz. However, the upper limit of frequency was limited to 1 MHz since molecular processes in polymers



are sensitive only upto that frequency. All the measurements were carried out under dynamic vacuum so as to avoid the effect of adsorbed moisture.

## 5.5 Results and Discussion

The ac conductivity and the dielectric constant related property – dissipation factor ( $\tan \delta$ ) – are properties manifested by the release of charge carriers and a change in the molecular conformation giving rise to a change in the dipolar orientation. These properties of pristine nylon 666, N-g-MA and N-PMA have been evaluated in the temperature range from ambient to 200°C. The frequency range employed in the measurements varied from 100 kHz to 1 MHz. DSC thermograms are presented to corroborate the ergic phenomena detected in the electrical measurements.

### 5.5.1 DSC thermograms

The DSC thermograms of pristine nylon 666 and N-g-MA are presented in Figures 5.1 and 5.2. The broad endothermic transition occurring around 70°C is probably due to a solid-solid transition. Such broad transition have been reported in high molecular weight polymers.<sup>14</sup> The sharp endothermic at 170°C is due to melting.

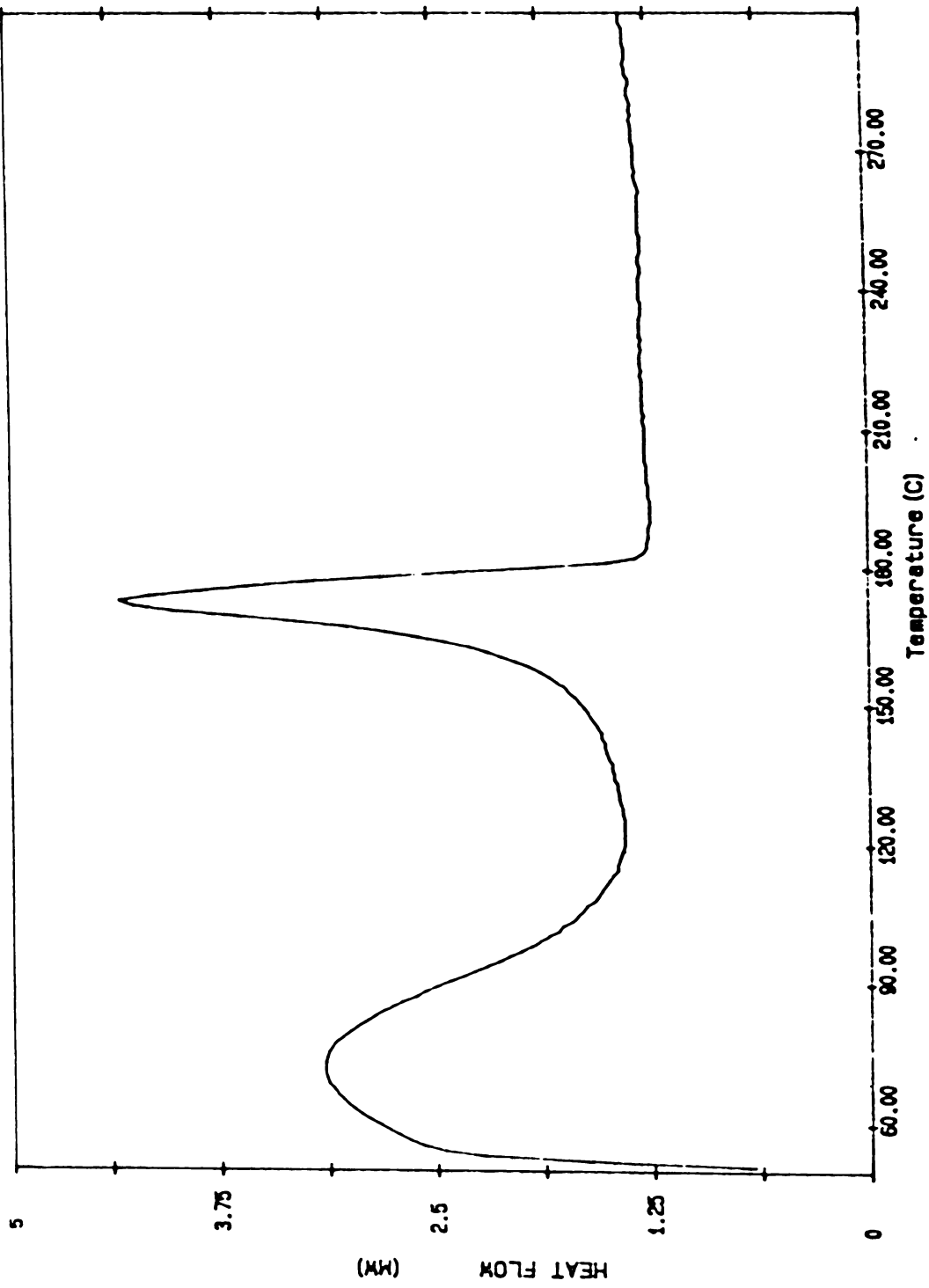


Figure 5.1 DSC thermogram of nylon 666.  
Atmosphere: nitrogen, Heating rate: 10.0 C/min.

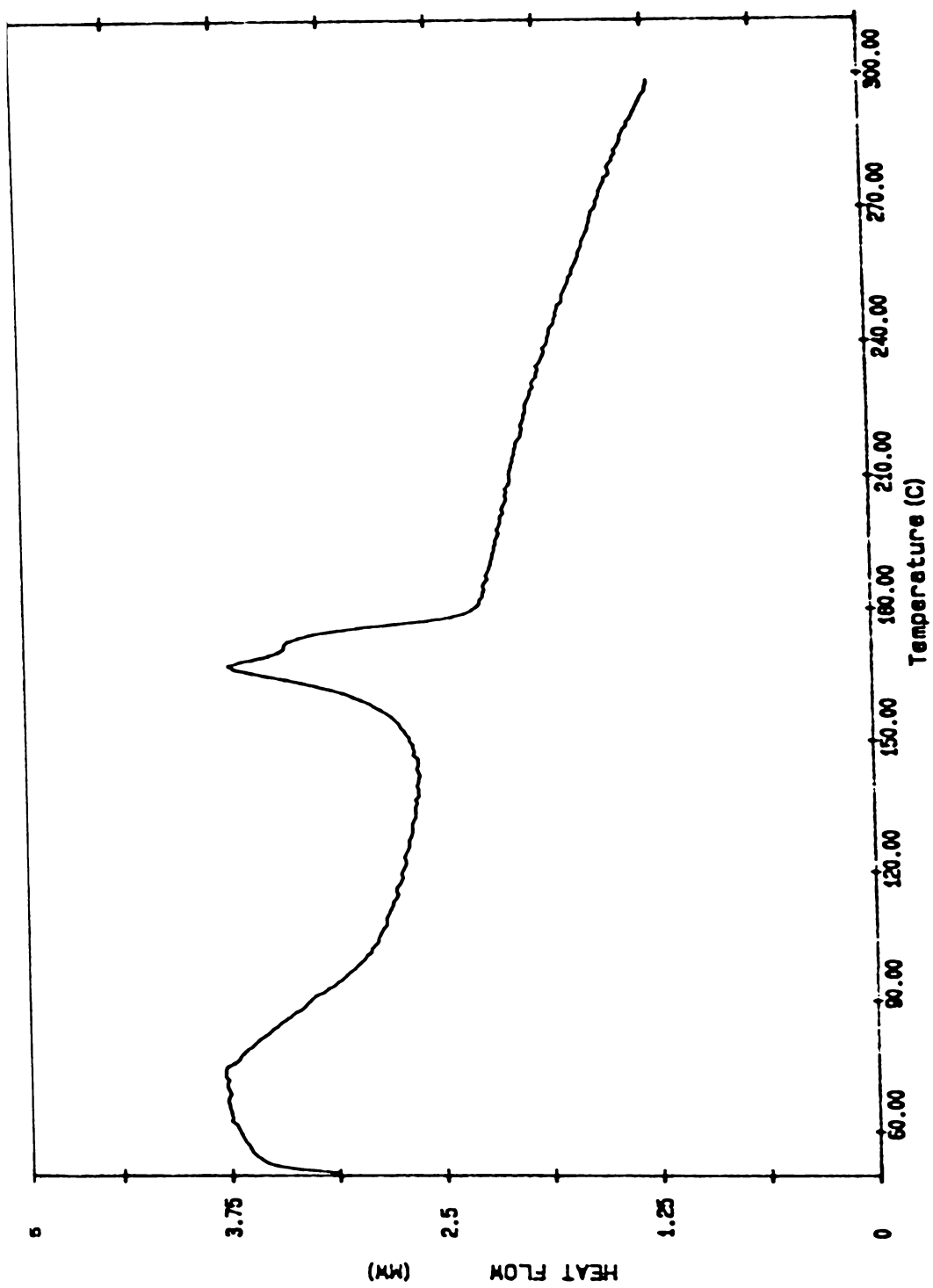


Figure 5.2 DSC thermogram of N-g-MA  
Atmosphere: nitrogen, Heating rate: 10.0 C/min.

### 5.5.2 ac Conductivity

The ac conductivity of pristine nylon 666 measured at 100 kHz and at 1 MHz as a function of temperature is presented in Figure 5.3. When this is compared with the results obtained for N-g-MA (Figure 5.4), it becomes evident that drastic changes have occurred to the molecular environment. Similar behaviour is observed at 1 MHz also (Figure 5.5). In the pristine polymer the charge carrier concentration is very low and probably conduction occurs through protons.<sup>15</sup> The relatively high ac conductivity is due to the contribution of capacitance which is susceptible to the temperature dependent relaxation phenomena and concomitant changes in dipolar orientation.<sup>7</sup>

Pristine nylon is a good insulator. At low temperature the activation energy for conduction is very high and the  $T_g$  is accompanied by a drop in activation energy. This may be due to the increasing mobility bestowed on the charge carrier. In nylon 666 the charge carrier is reported to be the amide proton.<sup>9</sup> Here also it is reasonable to assume that the amide proton is the charge carrier. Above the  $T_g$  the  $E_a$  has fallen to about 0.01 eV. The second factor which might have contributed to the increased conductivity is the release of more of the charge carriers by the polymer molecules, subsequent to a transition or relaxation.

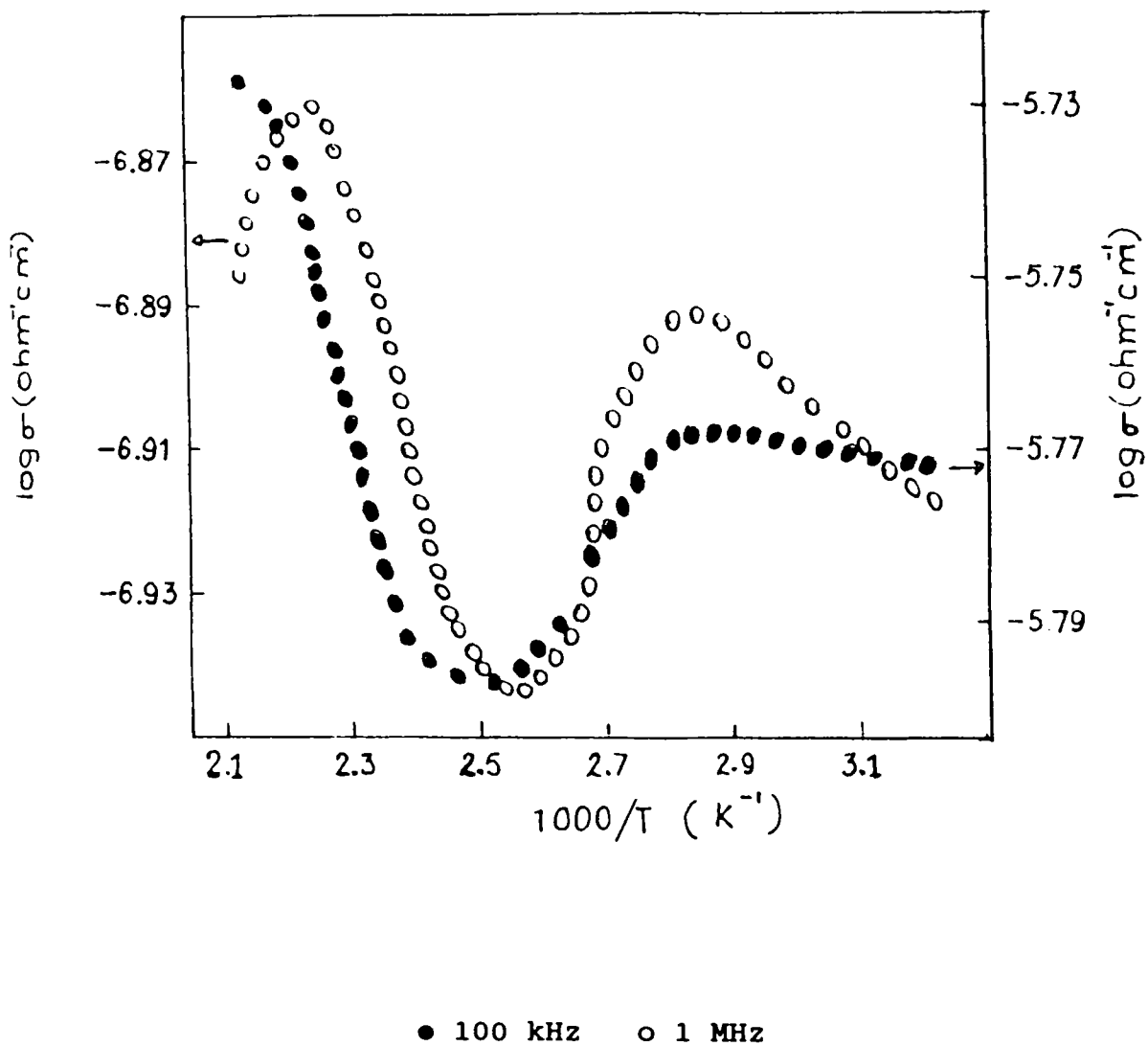


Figure 5.3 ac Conductivity of nylon 666 as a function of temperature at different frequencies.

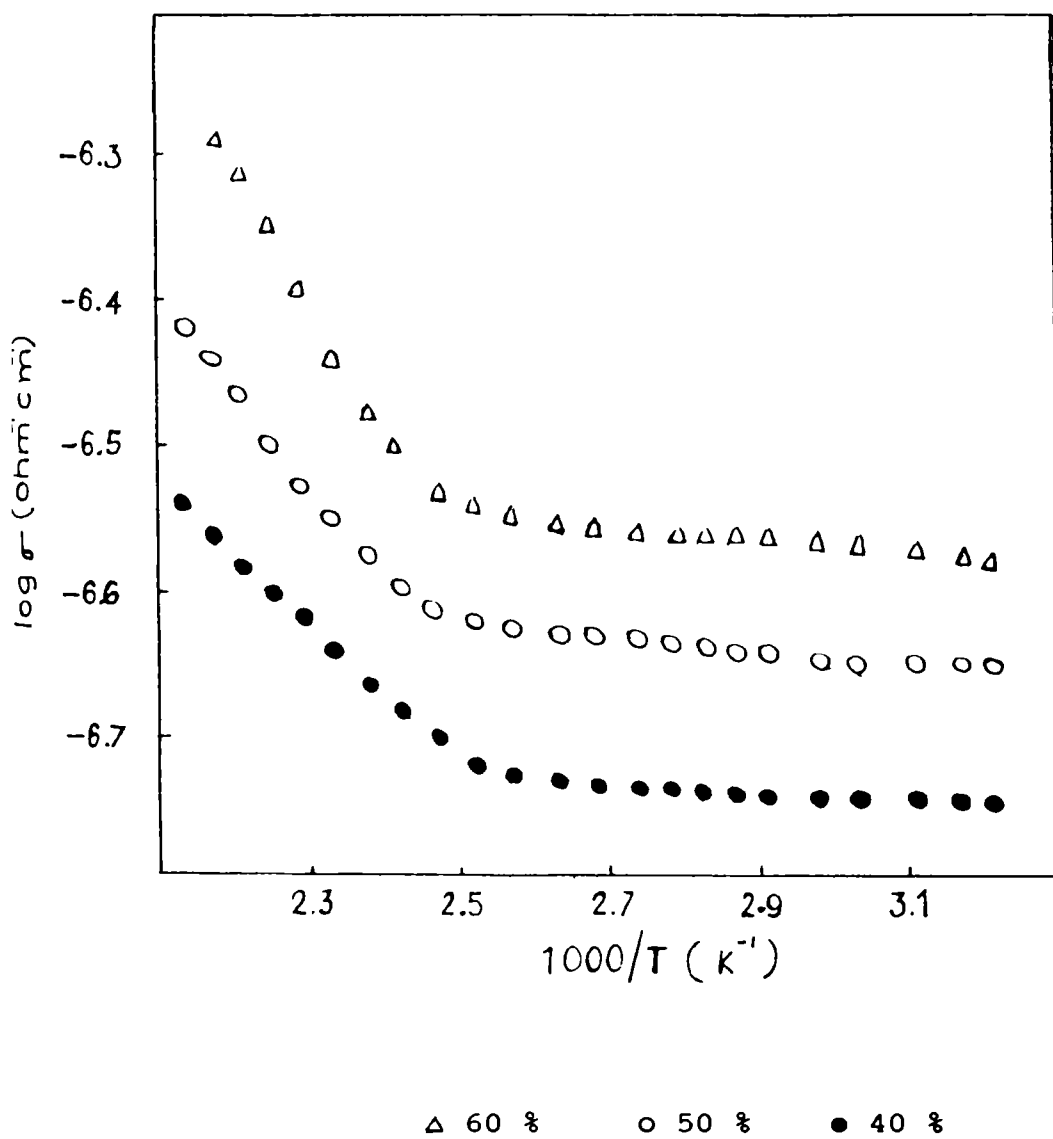


Figure 5.4 ac Conductivity of N-g-MA membranes as a function of temperature at 100 kHz, with different degree of grafting.

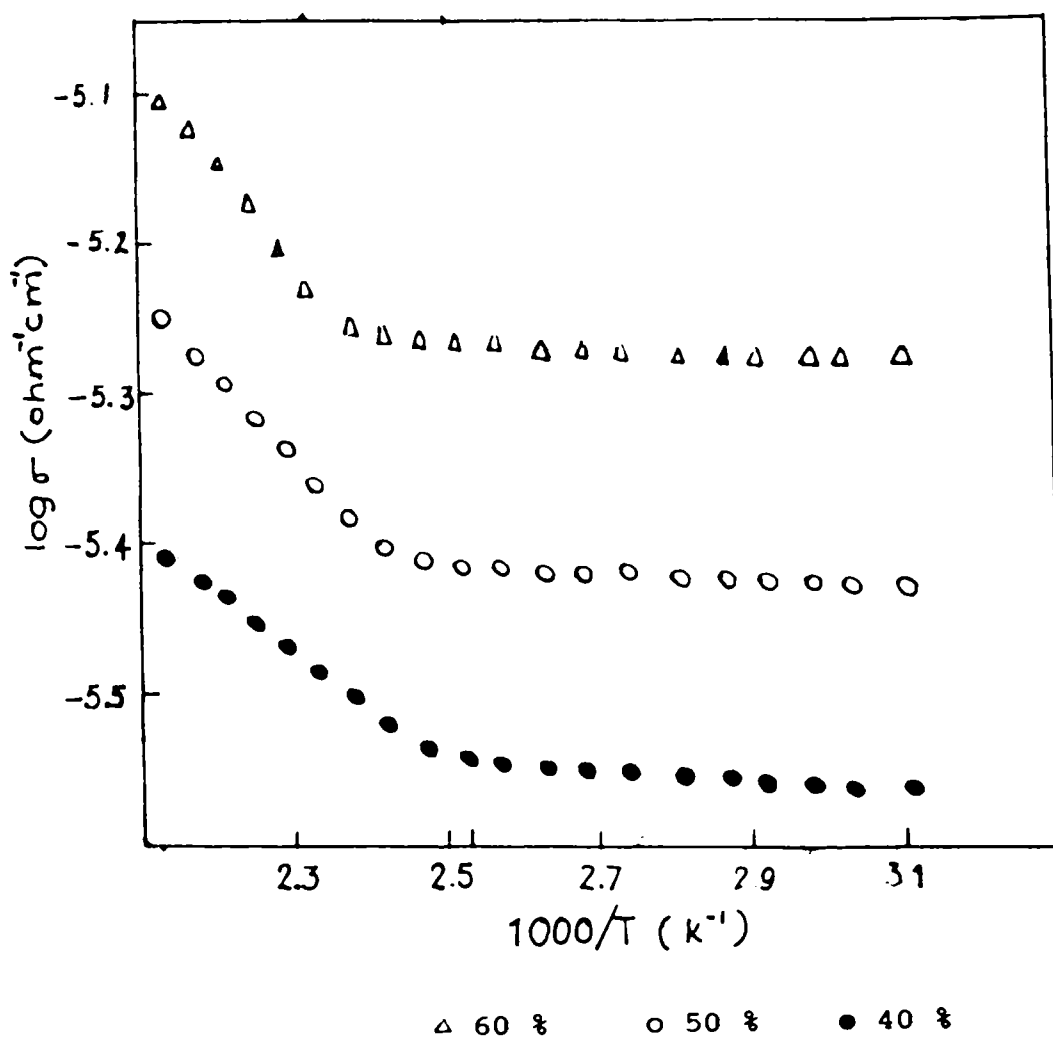


Figure 5.5 ac Conductivity of N-g-MA membranes as a function of temperature at 1 MHz, with different degree of grafting.

The maleic acid pendants grafted on the nylon backbone alters the dielectric property of the segment. Also the possible intermolecular hydrogen bonding through the carboxylic acid renders the macromolecular segment more rigid. This is very similar to the observation reported on ethylene copolymers with carboxylic acid functions. In the case of N-g-MA and N-PMA (Figures 5.4 to 5.7), the ac conductivity plots are concave down which indicates that the observed conductivity-temperature dependence is subject to a freezing in mechanism at the transition temperature.

Assuming the Arrhenius behaviour for conduction in the glassy and rubbery phases, the observed conductivity patterns can be described by the equations (5.1 and 5.2). In such a case  $E_r > E_g$  as can be seen from Table 5.1. This also indicates that even if weak it is ionic conduction that occurs in the pristine polymer.

The ac conductivity of N-PMA as a function of temperature is presented in Figures 5.6 to 5.7. The Arrhenius plots at the lower frequency (100 kHz) shows three regions characterized by distinct slopes. The corresponding activation energies are given in Table 5.2.



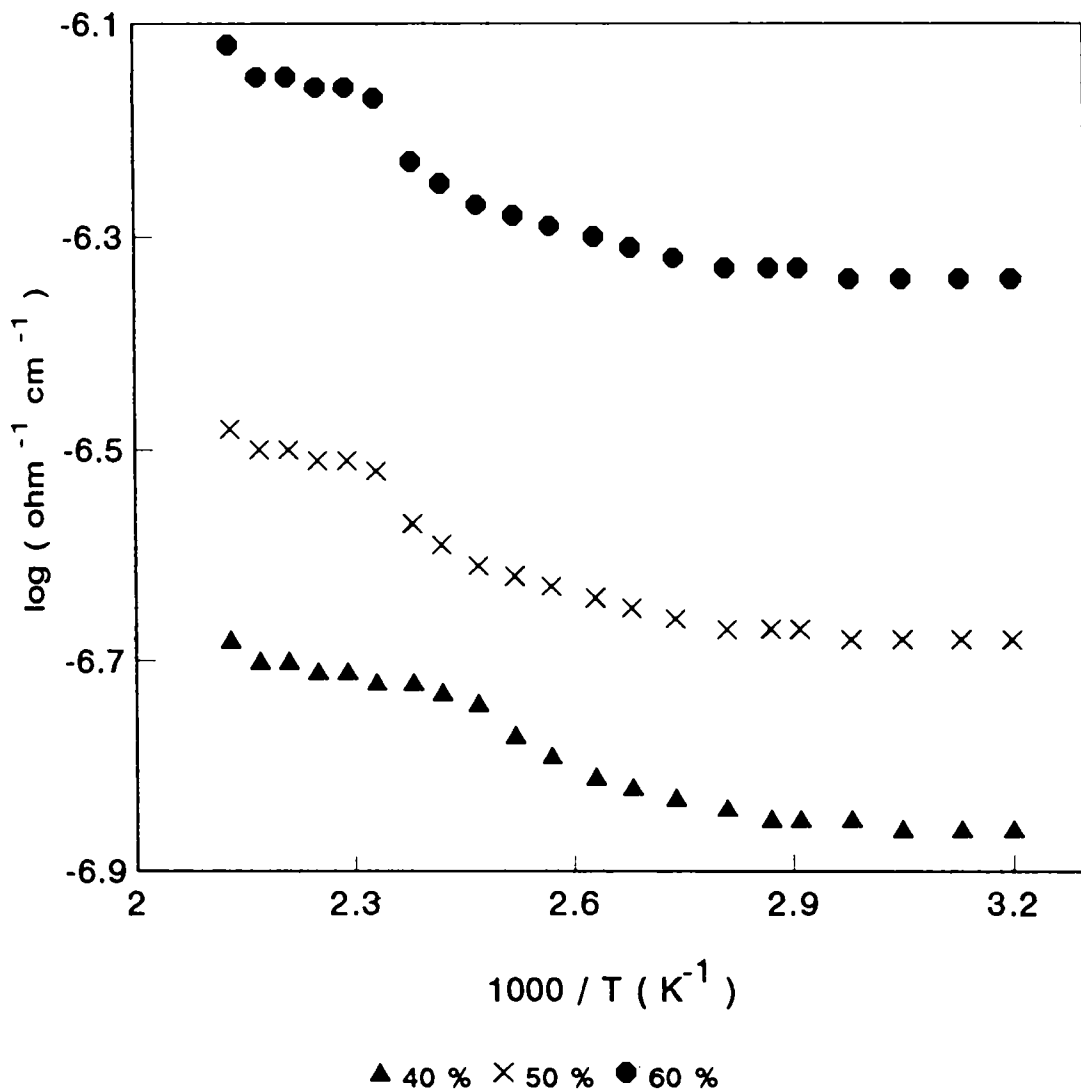


Figure 5.6 ac Conductivity of N-PMA membranes as a function of temperature at 100 kHz, with different composition.

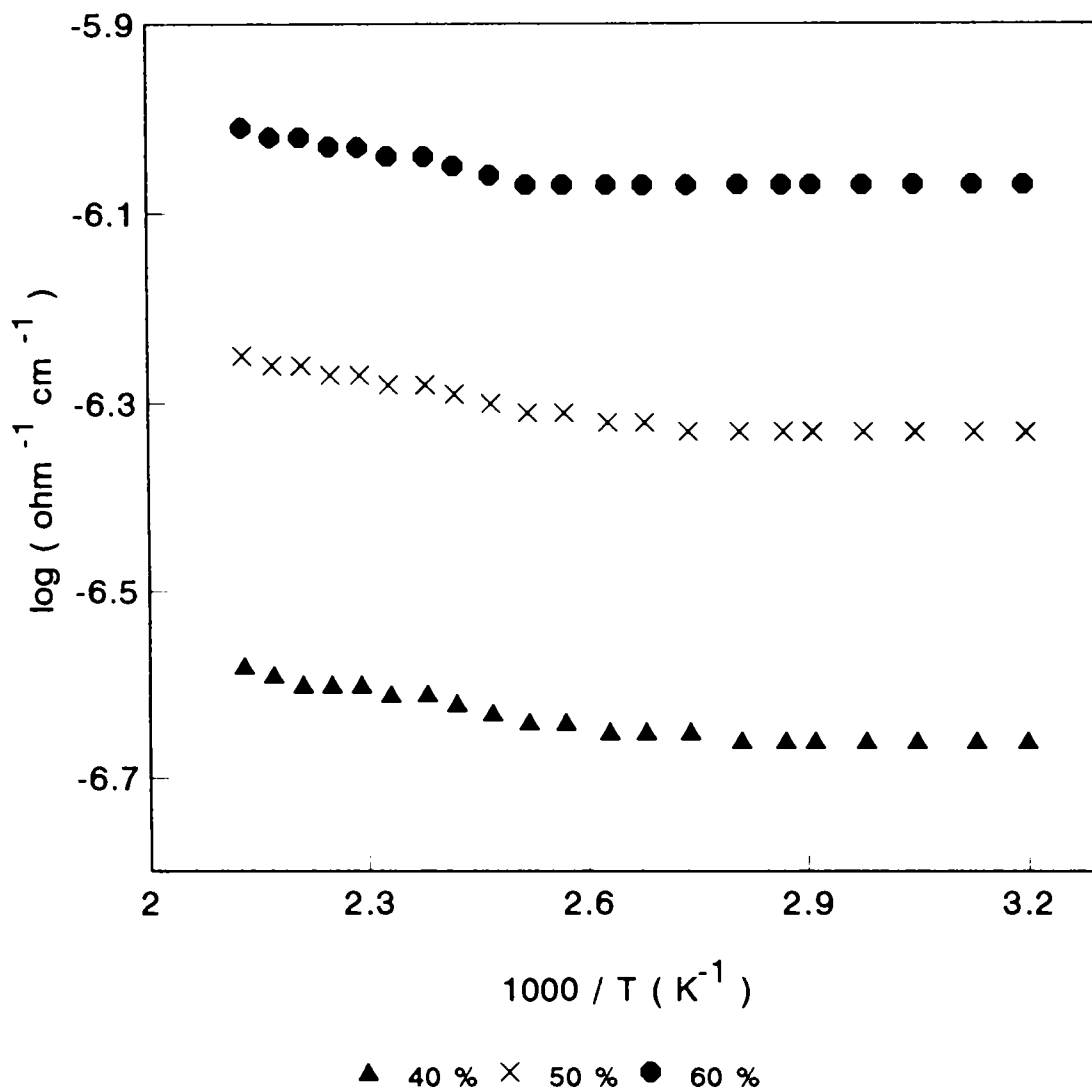


Figure 5.7 ac Conductivity of N-g-MA membranes as a function of temperature at 1 MHz, with different composition.

**Table 5.1 ac Conductivity data of N-g-MA membranes**

Sample	Temperature range (K)	Activation energy (eV) (100 kHz)
Nylon	310-360	3.50
	410-470	0.01
M1	320-420	0.06
	420-470	0.17
M2	320-410	0.04
	410-470	0.13
M3	320-400	0.04
	400-460	0.10

**Table 5.2 ac Conductivity data of N-PMA membranes**

Sample	Temperature range (k)	Activation energy (eV) (100 kHz)
I1	375-420	0.09
	420-470	0.03
I2	375-420	0.13
	420-470	0.03
I3	375-420	0.12
	420-470	0.04

(Activation energy( $E_g$ ) is not detectable in the region below  $T_g$ .)

The conductivity increases with increase in the proportion of ionomer in the interpolymer. Also the onset of an easily activated conduction mechanism occurs which is progressively shifted to higher temperatures with increasing ionomer content. The activation energy for this process varies from 0.02 to 0.12 eV which is typical for proton conduction in hydrogen bonded materials.<sup>15</sup> The ac conductivity pattern at 1 MHz is less sensitive to temperature. This also supports the fact that the conduction mechanism involves the transport of ionic species (proton) which are inherently less sensitive to higher frequencies.

### 5.5.3 Dielectric relaxation

The family of curves obtained for a plot of  $\tan \delta$  Vs temperature is given in Figure 5.8 for pristine nylon 666. At lower frequencies the relaxation peak becomes clearly defined. At higher frequencies  $\tan \delta$  decreases more rapidly around the transition temperature and assumes a nearly steady value which is characteristic of the rubbery state.

A plot of  $\log f_m$  Vs  $1/T$ , where  $f_m$  and  $T$  are the frequency and temperature at which the peak occurs in a  $\tan \delta$  plot is approximately linear for all cases over the temperature range studied. Activation energies were calculated from the slop of this plot. The activation

energy calculated for pristine nylon 666 is 0.02 eV (390-430 K) which is in good agreement with the value of  $E_a$  obtained from  $\sigma_{ac}$  measurements.

For N-g-MA no relaxation peak is observed (Figure 5.9) but a knee appears around 380 K. The disappearance of the peak is probably due to the rigidity imparted to the polymer segment by the carboxylic acid functions which can form strong hydrogen bonds either among themselves or with the amide functions. The possible inter and intramolecular hydrogen bondings are shown in Scheme 1. At temperatures above the knee there is enhanced conductivity. Such a change in conductivity and hence activation energy is associated with a change in the mechanism of conduction. Similar observations is also seen for N-PMA membrane (Figure 5.10).

Figure 5.11 presents the variation of capacitance with temperature for nylon 666. Capacitance refers to the ability of the material to store electrical energy which in turn, depends on the molecular level polarizability of the material. The temperature dependence of capacitance is low at lower temperatures. The capacitance variation with temperature shows a flat s-shaped inflection with onset at about 120°C which coincides with the  $\alpha$ -relaxation temperature indicating that  $\alpha$ -relaxation enhances the polarizability of the polymer segments.

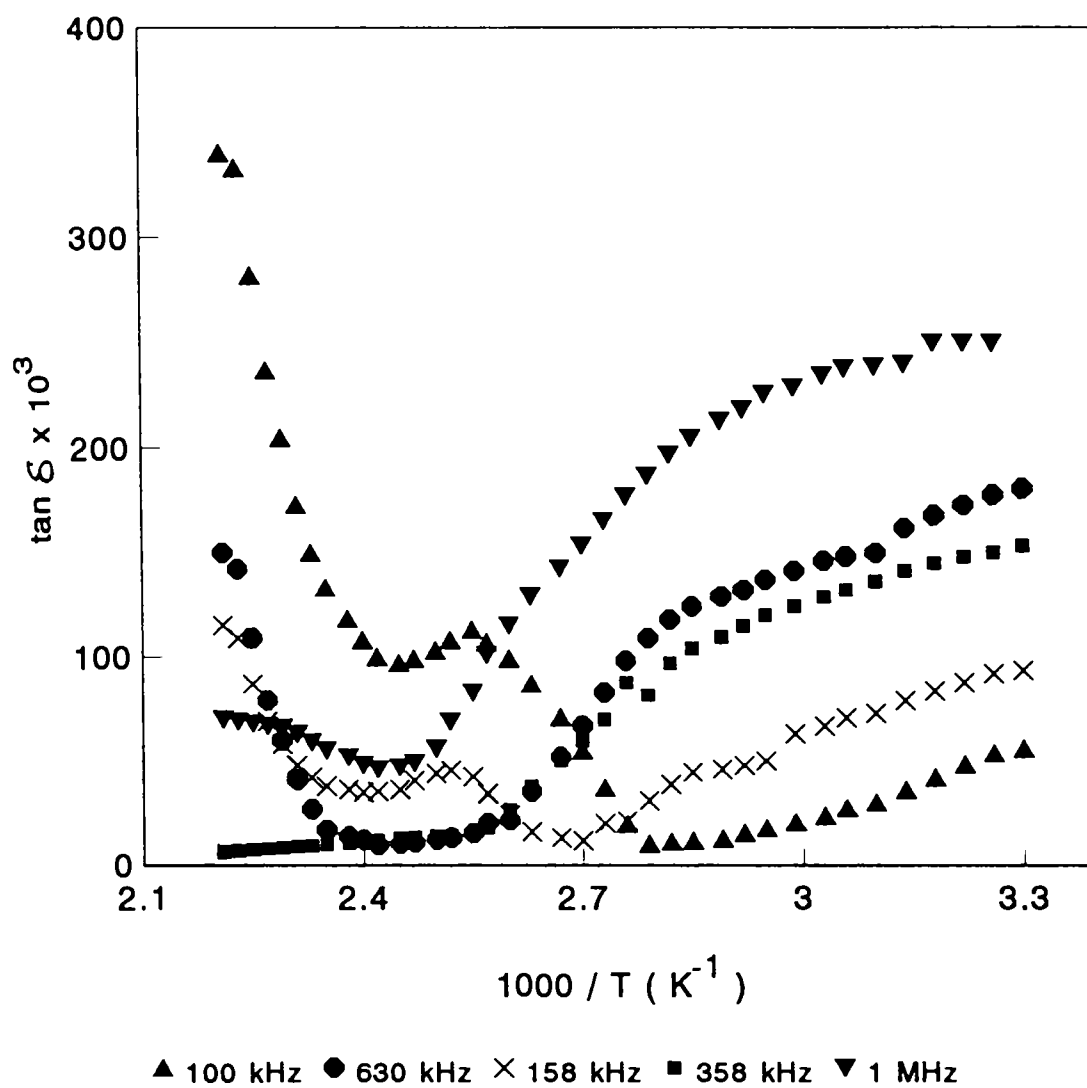


Figure 5.8 Dielectric loss factor of nylon 666 as a function of temperature at different frequencies.

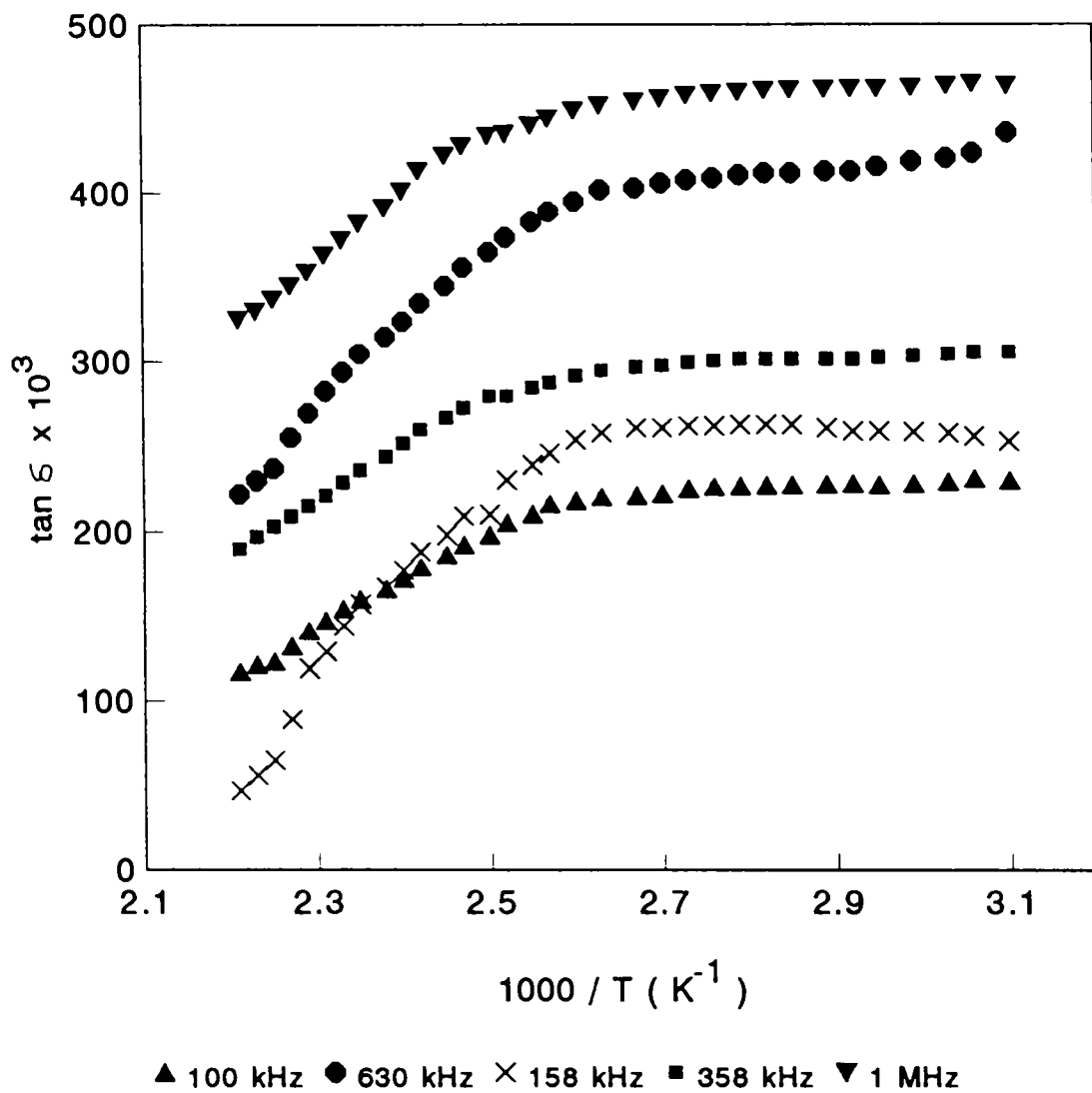


Figure 5.9 Dielectric loss factor of N-g-MA membrane as a function of temperature at different frequencies.

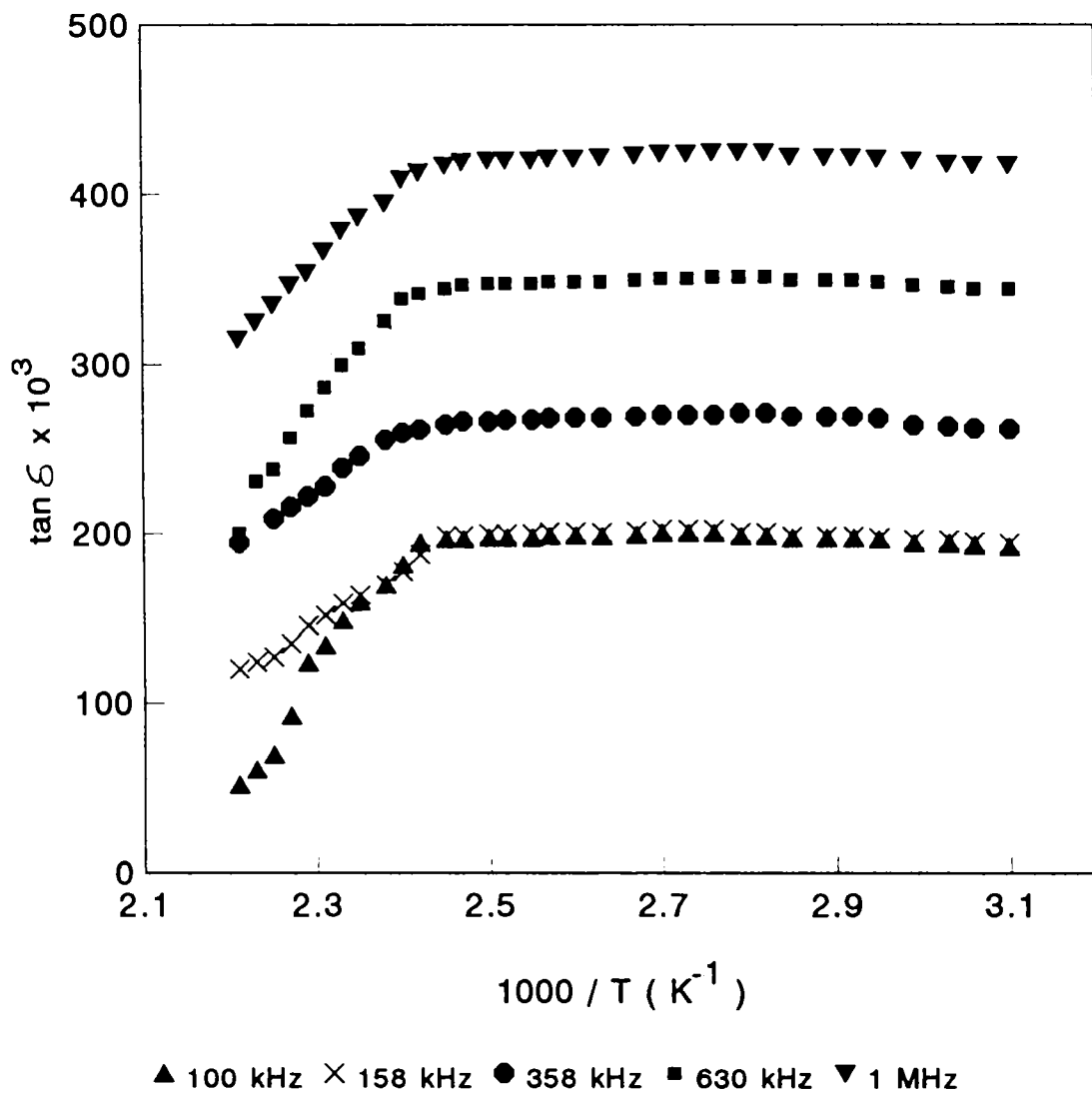


Figure 5.10 Dielectric loss factor of N-PMA membrane as function of temperature at different frequencies.



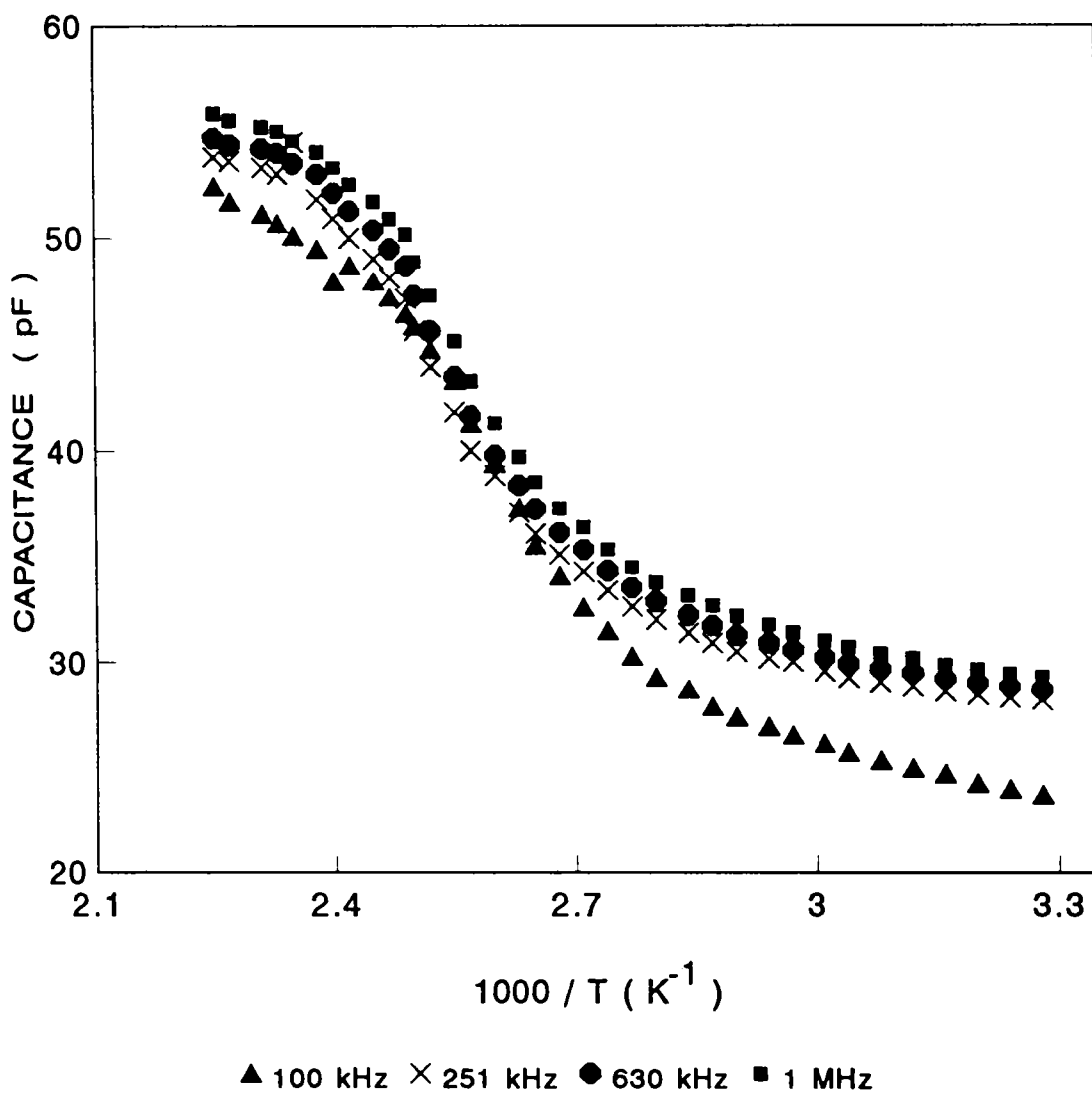


Figure 5.11 Capacitance of nylon 666 as a function of temperature at different frequencies.

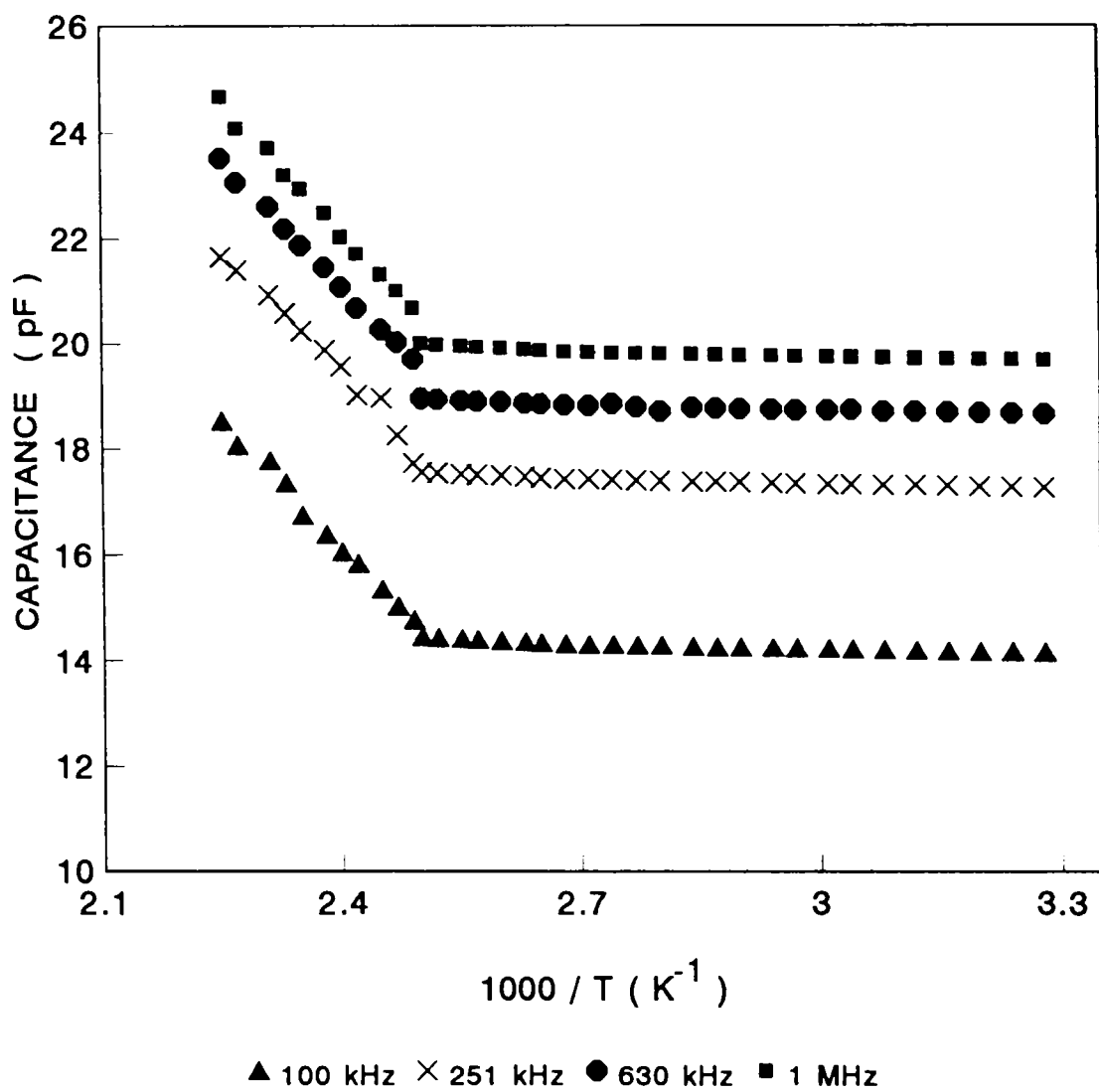


Figure 5.12 Capacitance of N-g-MA membrane as a function of temperature at different frequencies.

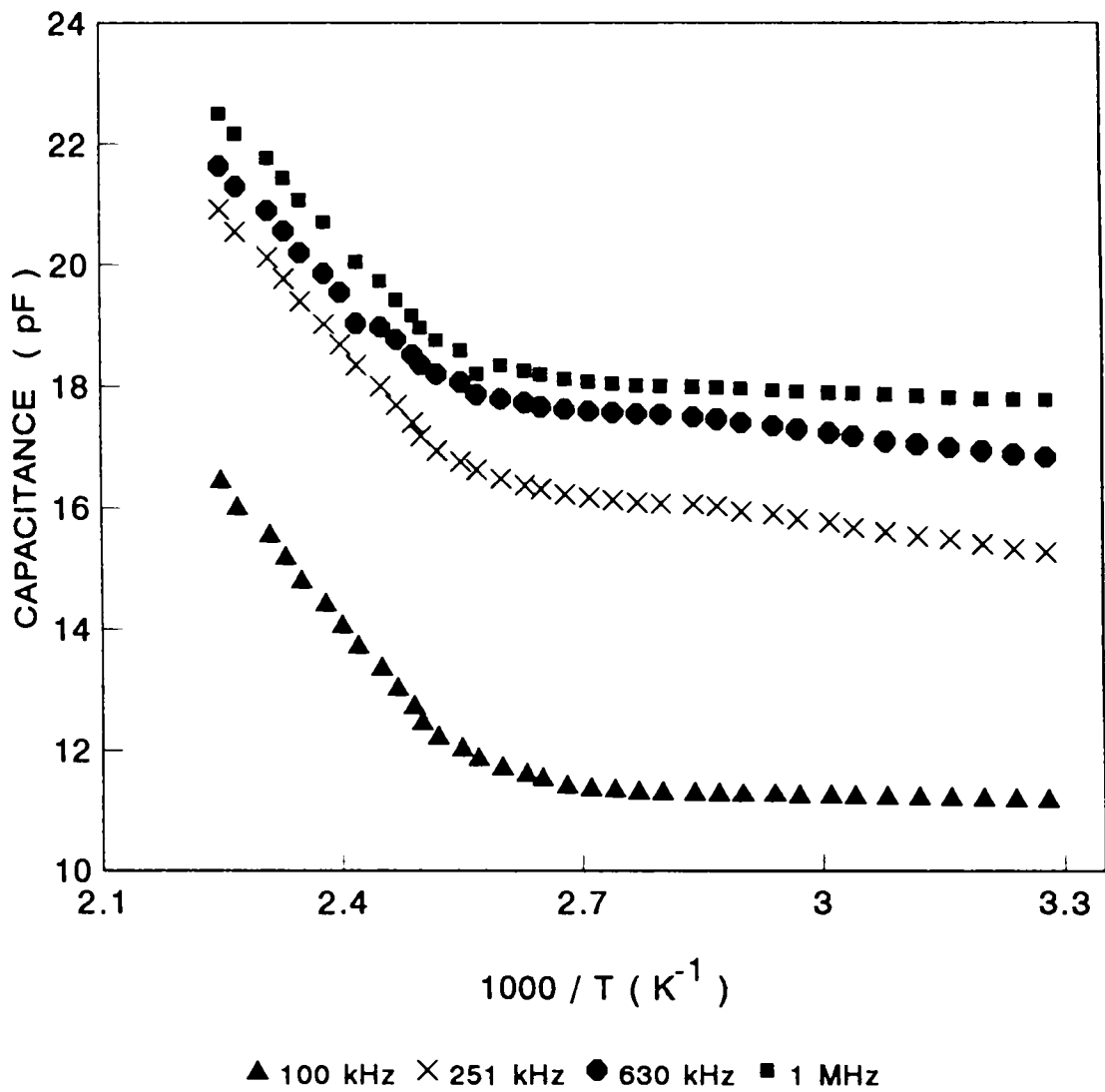
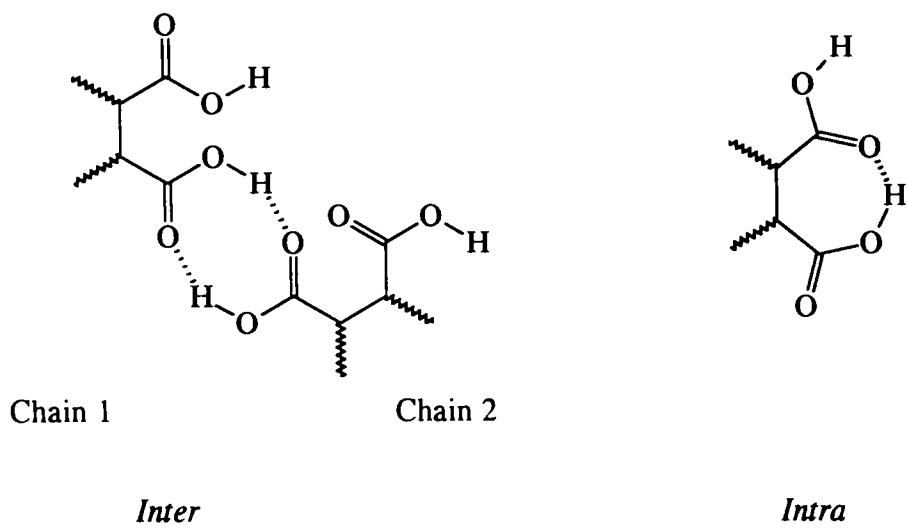
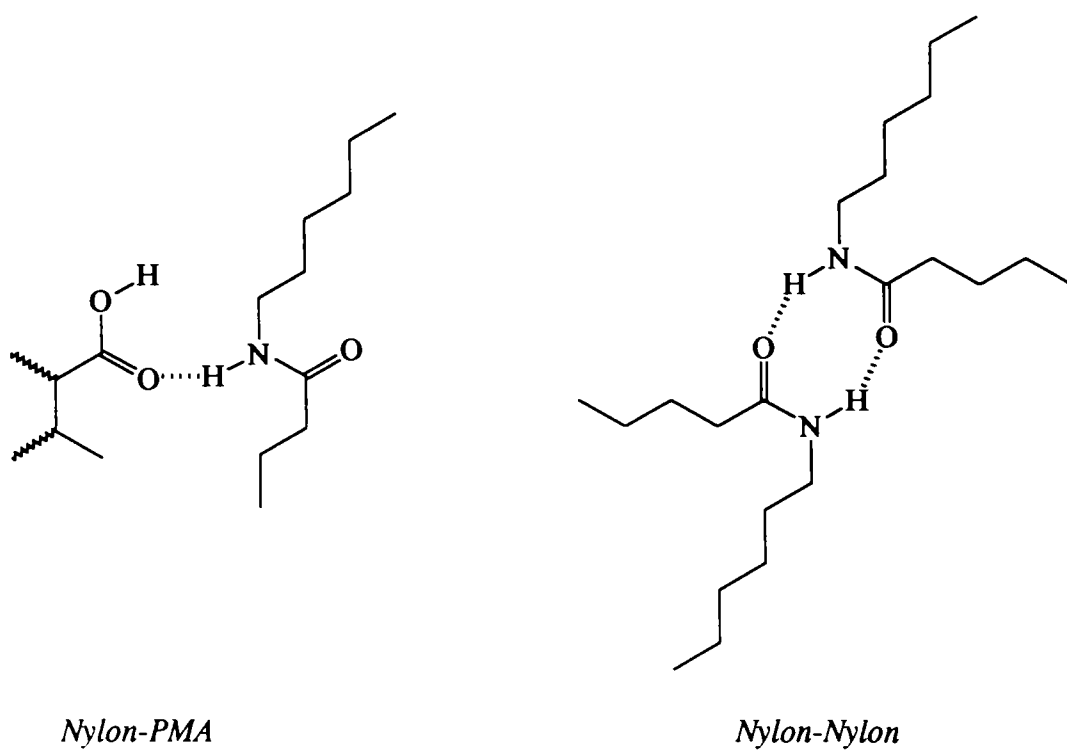


Figure 5.13 Capacitance of N-PMA membrane as a function of temperature at different frequencies.



**Scheme 1 a; Possibilities of hydrogen bonding in PMA**



**Scheme 1 b; Possibilities of hydrogen bonding in Nylon-PMA**

Figures 5.12 and 5.13 show the variation of capacitance with temperature for the N-g-MA and N-PMA interpolymer respectively. In the interpolymer and in N-g-MA the variation of capacitance increases sharply around 135°C. The involvement of the highly polar carboxylate function in the temperature dependence of capacitance is reflected in the same way.

The observations made above support the fact that grafting of a highly polar moiety onto nylon 666 backbone reduces its segmental mobility. This may be due to the strong hydrogen bond involving the carboxylic acid groups. The activation energies for conduction also support this view.

## References

1. McCrum, N. G.; Read, B. E.; Williams, G. "Elastic and Dielectric Effects in Polymer Solids", John Wiley & Sons, Inc.: New York, 1967.
2. Reich, S.; Michaeli, I. *J. Polym. Sci., Polym. Phys.* 1975, 13, 9.
3. Cohen, M. H.; Turnbull, D. *J. Chem. Phys.* 1959, 31, 1164.
4. Barker, R. E.; Thomas, C. R. *J. Appl. Phys.* 1964, 35, 87.
5. Miyamoto, T.; Shibayama, K. *J. Appl. Phys.* 1973, 44, 5372.
6. Kohan, M. I. "Nylon Plastics", Wiley-Interscience: New York, 1973, p. 313.
7. Blythe, A. R. "Electrical Properties of Polymers", Cambridge University Press: London, 1979, p. 17.
8. Debye, P. "Advances in Static Electricity", de Geest, W. Ed., 1970.
9. Boyd, H. R. *J. Chem. Phys.* 1959, 30, 1276.
10. Philips, P. J.; Emerson, F. A.; MacKnight, W. J. *Macromolecules* 1970, 3, 771.
11. Longworth, R.; Vaughan, D. J. *ACS Polym. rpt.*, 1968, 9, 525.
12. Read, B. E.; Carter, E. A.; Connor, T. M.; MacKnight, W. J. *Brit. Polym. J.* 1969, 1, 123.

13. Phillips, P. J.; MacKnight, W. J. *J. Polym. Sci. A2* 1970, 8, 727.
14. Rabek, J. F. "Experimental Methods in Polymer Chemistry", John Wiley & Sons: New York, 1980.
15. Glasser, L. *Chem. Rev.* 1975, 75, 21.

## CHAPTER 6

### SUMMARY AND CONCLUSIONS

Nylon 666-g-maleic acid (N-g-MA) with different degree of grafting, nylon 666-polymaleic acid interpolymer (N-PMA) with varying weight percentage of PMA and N-PMA-Ly with varying weight percentage of lysine were prepared and characterized by physico-chemical techniques. The ion-exchange membranes so formed were evaluated for their performance in dialysis and transport of metal ions under active conditions. The ac conductivity and dielectric properties of the membranes were studied by varying the frequency and temperature. The results obtained in this study leads to the following conclusions:

1. Dilute solution viscosity measurements of polymaleic acid in 0.05N NaCl solution confirms its polyelectrolyte nature. It is found that  $[\eta]$  of PMA increases with upto  $\alpha = 0.5$ , and the solution becomes turbid beyond this.
2. The ion-exchange capacity of N-g-MA membrane is neither directly proportional to the amount of maleic acid nor to the dosage  $\Gamma$  radiation given. The ion-exchange capacity of N-PMA membranes increases with increasing PMA content. Exchange capacity of N-PMA-Ly



depends on the external pH. Tensile strength of N-g-MA increases with decrease in the degree of grafting. In all three types of membranes studied, burst strength decreases rapidly with increasing capacity.

3. The membranes reported here possess good electrical properties. Electrical conductivity increases with external pH due to the dissociation of -COOH groups for N-g-MA and N-PMA membranes. N-PMA-Ly membrane behaves like a cation-exchange membrane at basic pH. Permselectivity values calculated from membrane potential data were found to decrease with increase in concentration as predicted by Donnan exclusion principle. The membrane potential data for N-PMA-Ly show that at intermediate pH the membrane is not permselective, it can exchange cations as well as anions.
4. N-g-MA and N-PMA membranes are permeable to KCl, NaOH, NaCl, Na<sub>2</sub>SO<sub>4</sub> and to a limited extent to urea and creatinine. The difference in permeability coefficients is due to the difference in the size of the hydrated ions, and electrical and geometrical effect of the membranes. Sodium hydroxide has the highest permeability coefficient due to its high counter-ion mobility. KCl moves faster than NaCl due to the difference in the size of the hydrated cation.

Sodium sulphate has comparatively low permeability coefficient value among salts due to the low mobility of  $\text{SO}_4^{2-}$  ions. Urea and creatinine have still lower permeability coefficient values which can be accounted for in terms of the permeation of neutral species through charged membranes.

5. The membranes exhibit active and selective transport of metal ions. In the active transport of metal ions,  $\text{H}^+$  controls the physical and chemical structure of the membrane and its concentration provides the driving force. In the selective transport of metal ions, the selectivity depends on both the size of the hydrated ions, and the interaction between the charge groups on the membrane and metal ion. The mean transport rate and transport fraction show maximum values at pH 1 in the right side.
  
6. For N-g-MA and N-PMA it is found that  $E_a, r > E_a, g$  which indicates that it is ionic conduction, even if weak, that occurs in the membranes. For nylon the relaxation peak becomes clearly evident at lower frequencies. For N-g-MA and N-PMA the  $\alpha$ -relaxation peak disappears. Grafting of a highly polar moiety onto nylon 666 backbone reduces its segmental mobility due to the strong hydrogen bonding involving the carboxyl groups.

**PART II**

---

**POLYMERS AS FLOCCULANTS  
AND CONTROLLED-RELEASE AGENTS**

## **CHAPTER 7**

### **CONTROLLED-RELEASE: AN OVERVIEW**

#### **Abstract**

This chapter gives a brief review of polymeric materials used in controlled-release, special mention is made of controlled-release molluscicides based on copper-release systems.

## **7.1 Introduction**

In a controlled-release system the active species is emitted from a reservoir in a dispenser or other device at a predetermined rate for a specified period of time.<sup>1</sup> A number of substances ranging from drugs to agricultural chemicals are often toxic or sometimes ineffective when administered by conventional means. Scientists have been turning to controlled-release technology to improve their product application mode.<sup>2</sup> Diffusion of active species through polymer membranes is an effective and reliable means for attaining the controlled-release of a variety of active agents.

## **7.2 Classification of Controlled-Release Systems**

According to the rate controlling mechanism, controlled-release systems can be classified based on the process involved namely diffusion, erosion, swelling and osmosis.<sup>3</sup> The classification of a device into any of these categories is determined by the nature of interaction between the polymer and the environmental fluid.

### **7.2.1 Diffusion controlled systems**

In diffusion controlled devices the diffusion of the active agent through any part of the device controls the

release rate. Matrix devices constitute a major category of diffusion controlled systems.<sup>4</sup> In this, the active agent is distributed in a polymer matrix. It can either be dispersed as a separate phase or be dissolved in the polymer. Release occurs by diffusion through the polymer. Moreover, the environmental fluid may leach the active agent out of the matrix if the polymer is permeable to the fluid. A dissolved active agent system may be obtained by soaking the polymer in a solution of the active agent and allowing it to equilibrate. Polymers used as the basis for this type of devices are mainly employed as reservoir devices such as polydimethylsiloxane, ethylcellulose and hydroxypropyl cellulose.<sup>5</sup>

#### **7.2.2 Erosion or chemical reaction controlled systems**

Here the polymer is an active participant in the release process. The active agent is physically immobilized in the polymer and is only released by erosion of the polymer. In chemical reaction controlled systems the active agent itself is chemically bound to the polymeric backbone. Release occurs by hydrolytic or enzymatic cleavage of this bond. Commonly used polymers in forming erodible devices are poly(vinyl pyrrolidone), and copolymers of methyl vinyl ether and maleic anhydride.<sup>6</sup>

### **7.2.3 Swelling controlled-release systems**

They are formed by dissolving or dispersing the active agent in a polymer matrix in which it is unable to diffuse to any significant extent. When the matrix is placed in an environmental fluid thermodynamically compatible with the polymer, the fluid is absorbed into the polymer causing it to swell. The active agent in the swollen part of the matrix can then diffuse out. A class of polymers called hydrogels, acrylamide and polyethylene glycols are considered suitable for such systems.<sup>7</sup>

### **7.2.4 Osmotic pumping systems**

In these systems osmotic pressure is the driving force. The osmotic pump consists of a core of water-soluble active agent, which is a solid.<sup>4</sup> The core is enclosed in a selectively water permeable but active agent-impermeable polymer membrane with a small orifice. In an aqueous environment water is transported into the core by permeation. Hydrostatic pressure is built up and the solution of the active agent and water is then pumped out through the orifice.

### **7.3 Advantages of controlled-release**

The advantages of controlled-release are many. The active agent is released at a controlled rate that

continuously maintains its concentration in the system within the optimum limits for a desired period. The principal advantage is that much less active ingredient is required for the same period of activity than is recommended in conventional method of application. In most instances the rate of degradation follows first order kinetics.<sup>8</sup> Thus if  $M_e$  is the minimum effective level,  $M_{\infty}$  the amount of agent applied initially, and  $k_r$  the rate constant for release, then  $t_c$ , the time during which an effective level of an active agent, e.g., pesticide is present after a single application would be

$$t_c = \frac{1}{k_r} \ln \frac{M_{\infty}}{M_e} \quad . . . . (7.1)$$

It follows from equation (7.1) that to increase the duration of effective action of a conventionally applied pesticide, the application of an exponentially greater quantity of the pesticide is required. If, however, the pesticide could be maintained at the minimum effective level by a continuous supply from a controlled-release system, then optimum performance of the active agent would be realized.

#### 7.4 Basic Components of Controlled-Release Devices

A controlled-release device consists of the active agent and a matrix that regulates its release.<sup>9-11</sup>



In selecting a polymer as the matrix, the following criteria should be considered.

- (a) Molecular weight, glass transition temperature and chemical functionality of the polymer must allow the proper diffusion and release of the active agent.
- (b) Polymer functional group must not react chemically with the active moiety.
- (c) The polymer and its degradation products must be nontoxic to the inhabitants other than the target life form.
- (d) The polymer must not decompose in storage or during the useful life of the device.
- (e) The polymer must be easily manufactured or fabricated into the desired product and should allow the incorporation of a large proportion of the active agent in the product without deteriorating its mechanical properties.
- (f) The loss of the polymer should not be excessive. Some of the polymers frequently used are nitrocellulose, starch, polyvinyl alcohol, polyamide and polybutadiene.

#### 7.5 Controlled-Release Molluscicides

Pests are organisms that compete with man for their food supply or damage his possession. Some specific pest

control agents are molluscicides and nematocides. By far the most serious injury that molluscs cause to human being is as alternate hosts or vectors of trematodes or flat worms. These trematodes or flukes live in the blood vessels of their human hosts and grow to a length of 10 to 25 mm. The eggs of the adult worm escape into the intestine or urinary bladder and, when they reach fresh water, they hatch into ciliated larvae. These enter the soft tissues of snail hosts and transform into sporocytes, eventually forming fork-tailed larve, which escape from the snail hosts and swim freely in freshwater until they contact human hosts. They penetrate the human hosts through the skin and eventually reach the mesentric vessels.

*Shistosoma Japanica* is endemic in Japan, China and other Asian countries, and is spread by snails. *Shistosoma mansonia* is common in North Africa and South America and is transmitted by snails. Swimmers itch occurs worldwide and is caused by snails. Schistomiasis is a major health problem of increasing severity, especially in the developing countries. The transmission cycle of schisomiasis can be interrupted by medical therapy, engineering sanitation practices and snail control.

### 7.5.1 Snail control techniques

Snail control techniques are of three categories: physical, biological and chemical. Chemicals such as copper salts cause distress and death of snails. Controlled release techniques are new means for fighting snails.<sup>12</sup> Molluscicides are widely used in much of the tropical world to control the snail hosts of shistosomiasis and other parasitic diseases. All commonly used molluscicides are nonpersistent. Rapid detoxification occurs through chemical interaction with dissolved minerals and gases, organic absorption, and absorption by suspended matter and bottom soil; biodegradation through bacterial, algae and fungal attack.

Controlled-release molluscicides based upon trialkylorganotin and copper sulfate incorporated in an elastomeric or plastic base were developed by Cardarelli et al.<sup>13</sup> Copper sulfate pentahydrate and niclosamide as controlled-release agent were also developed. Copper sulfate, cuprobam and copper dimethyldithiocarbamate are effective against most aquatic snails at 3.5 ppm in water. Snail mortality is not directly dependent on agent concentration, but rather the interval from treatment time to mortality is proportional to concentration. The vital factor is the exposure time.

Snail mortality occurs through a chronic intoxication syndrome at 1 ppb and higher. The dosage rate is not controlling with respect to mortality. The end result is the same whether a given population is exposed to 1 or 100 ppb, only the time to a given degree of mortality differs. Death occurs through proteolysis, the destruction of the cell walls within specific connective tissue followed by massive internal hemorrhage. Since specific peptide linkages appear to be involved, as well as possible interruption of amino acid coordination sites, it is unlikely that tolerance can be developed.

Copper sulphate is easily soluble in water and its release can be controlled only through a physical barrier like a porous binder through which diffusion become the controlling process. Cuprobam and copper dimethyldithiocarbamate are very sensitive to pH and light and the transformation of the dispensed species poses a problem. A releasing agent tolerant to the pH range of water in active natural habitat, insensitive to light and nonallergic to the human will be a preferred candidate for application in controlled-release system.

## References

1. Helaly, F. M. "Slow Toxic Rubber Formulation for Pest and Parasitic Plant Control", Ph.D Thesis, Manosura University, Egypt, 1982.
2. Baken, J. A. "Theory of Controlled Delivery Systems", Goulding, R. L. Ed.; Proc. Int. Controlled-Release Pesticide Symp., Wright State University, Dayton, 1975, 76.
3. Baker, R. W. "Controlled-Release of Biologically Active Agents", John Wiley & Sons: New York, 1987, 1-83.
4. Fan, L. T., Singh, S. K. "Controlled-Release a Quantitative Treatment", Springer Verlag: Berlin Heidberg, 1989, 1-27.
5. Langer, R. "Polymeric Delivery Systems for Controlled Drug Release", *Chem. Eng. Commun.* 1980, 6, 1-48.
6. Brunt, V. "Perfecting Polymers to Release Drugs", *Biotechnology* 1986, 4, 756.
7. Roorda, W. E., Bodde, H. E. "Synthetic Hydrogds as Drug Delivery Systems", Scientific edition: 1986, 8, 165.
8. Fanger, G. O. "General Background and History of Controlled-Release", Cardarelli, N. F. Ed.; Proc. Int. Controlled-Release Pesticide Symp., University of Akson, Akson, 1974, 18.

9. Scher, H. B. "Microencapsulated Pesticides", Scher, H. B., Ed.; ACS Symp. Ser., 53. Am. Chem. Soc.: Washington DC, 1977, 27.
10. Robinson, J. R. "Controlled-Release Pharmaceutical Systems", Long, F. H., Neil, W. P., Stewart, R. D. Eds.; Chemical Marketing and Economical Reprints: Am. Chem. Soc.: San Francisco, CA, 1976, 212.
11. Lewis, D. H.; Coswar, D.R. "Principles of Controlled-Release Pesticides", Scher, H. B. Ed.; ACS Symp. Ser. 53: Am. Chem. Soc.: Washington DC, 1977, 30.
12. Faust, E. C.; Russel, R. F. "Graig and Faust's Clinical Parasitology", Kimpton: London, 1946.
13. Cardarelli, N. F. "Controlled-Release Pesticides Formulations", CRC Press: Cleveland, 1976, 7-30.

## CHAPTER 8

### SALICYLIC ACID-FORMALDEHYDE CONDENSATE

#### Abstract

Poly(methylene salicylic acid) (PMS) was prepared and characterized by IR,  $^1\text{H}$  NMR,  $^{13}\text{C}$  NMR, mass spectra and TLC. The controlled-release of copper by the copper salt of PMS was investigated to assess its viability as a controlled-release molluscicide. The mass spectra showed unusual multiplicity in peaks. TLC runs on silica gel using acetic acid showed three constituents. FAB-MS indicated the presence of dimer, trimer and tetramer. The release rate of copper showed it to be an effective matrix for the controlled-release of copper.

## 8.1 Introduction

Several synthetic resins derived from substituted phenols and formaldehyde have been reported in the literature.<sup>1-3</sup> In recent years, resins prepared by the condensation of substituted benzoic acid with formaldehyde have attracted the attention since they exhibit ion-exchange character, fungicidal activity and favourable properties for photographic and powder coating applications. Reprographic coatings of greater stability and copies of superior fastness to moisture and light than clay and other phenolic resin coatings are obtained with condensation products of formaldehyde, with 2- or 4-hydroxy or 2,6-dihydroxybenzoic acid combined with a metal.<sup>4</sup>

Condensation of salicylic acid with formaldehyde has been reported by many workers.<sup>5,6</sup> Giuseppe *et al.*<sup>7</sup> reported the molecular weight of the condensate as 800 and equivalent weight 164.9. The ion-exchange capacity is found to be 4.6 meq/g. The adsorption of several heavy metal ions on these weakly acidic ion-exchange resin, the distribution coefficient of several heavy metal ions in HCl solution and their elution behaviour have been discussed.<sup>8</sup> All these workers have reported the condensate as a polymer without detailed characterization.



We have synthesized PMS by the reported method.<sup>2</sup> The spectral, thermal and chromatographic characterization of PMS are reported here.

Salicylic acid is a well-known drug and is well-tolerated in biological systems. Controlled release of metals for biological control is a problem faced by the paint and water care industries. Copper is an established agent for the control of fungus as well as parasite vectors in the aquatic environment. Controlled-release formulation using PMS as the matrix to release copper as the active agent is also studied.

## 8.2 Experimental

### 8.2.1 Synthesis of the polycondensate

PMS was synthesized according to the method reported earlier.<sup>6</sup> Salicylic acid (0.1 mol), 37% formaldehyde (10 mol), catalyst (conc. sulphuric acid) were taken in a flask and heated on a water bath for 6 h. The lower viscous layer of the reaction mixture was washed with distilled water and dried. The product obtained was purified by precipitation from methanol by diluting with water.

### 8.2.2 Preparation of copper-PMS (Cu-PMS) complex for controlled-release formulation

The complex was prepared by mixing copper sulphate pentahydrate (0.6 g) in 50 ml water and PMS (2 g) in 50 ml water neutralized with NaOH to pH 6. The precipitate was filtered and washed several times with distilled water and dried in an oven at 110°C.

### 8.2.3 Leaching studies

The dried Cu-PMS complex was powdered and sized. The fraction passing through 100-200 mesh (150  $\mu$ ) was used. 1 g of powdered sample was kept in 2.5 l distilled water contained in a stoppered glass bottle. The system was shaken occasionally and allowed to settle. Aliquots were withdrawn at regular intervals. The copper concentration in the leachate was measured using ICP/AAS.

### 8.2.4 Instruments

FTIR spectra were recorded using Shimadzu 220A FTIR spectrophotometer in the region 400-4000  $\text{cm}^{-1}$ . CHN analysis was done using Heraeus-CHN-rapid analyzer.  $^{13}\text{C}$  and  $^1\text{H}$  nmr spectra were recorded using JEOL GSX 400 NMR spectrometer. FAB-MS was recorded using JEOL SX-102 (FAB) mass spectrometer in glycerol matrix with the matrix peaks at 75, 93 and 185. TGA-DSC curves were recorded in dynamic

nitrogen atmosphere using Perkin Elmer Delta series thermal analyzer. The mass of the samples used were in the range of 10-13 mg. The heating rate given was 10°C/min.

### 8.3 Results and Discussion

#### 8.3.1 Spectral studies

The results of CHN analysis are reported in Table 8.1. The frequencies of the important absorption bands for PMS and Cu-PMS are given in Table 8.2. The vibrations due to the phenyl group were observed in the region 1550 to 1610  $\text{cm}^{-1}$ .<sup>9</sup> The bands in the region 1350 to 1500  $\text{cm}^{-1}$  were caused by methylene bending which denotes the existence of methylene bridges. A considerable decrease for carbonyl stretching frequency from 1650 in PMS to 1550  $\text{cm}^{-1}$  is observed in the case of Cu-PMS indicating coordination through the oxygen atom of the carbonyl group. The broad band at 3450  $\text{cm}^{-1}$  for Cu-PMS is due to the O-H stretching frequency. The compound has considerable amount of bound water, which cannot be driven out by the drying method employed. The thermal study of this compound also indicates weight loss below 100°C due to the slow loss of bound water. The band at 3050  $\text{cm}^{-1}$  for PMS indicates the presence of bounded O-H, which could be phenolic. COOH is hydrogen bonded. C-O $\nu$  phenol

and C-O $\nu$  primary alcohol are present (1200, 1080  $\text{cm}^{-1}$ ).<sup>10</sup> The band at 1280  $\text{cm}^{-1}$  might be due to dimeric COOH. All these observations indicate the presence of an oligomeric compound.


Table 8.1 CHN analysis value of PMS and Cu-PMS

Compound	% of C	% of H	% of N
PMS	60.82	4.51	-
Cu-PMS	47.90	4.05	-

Table 8.2 IR absorption bands ( $\text{cm}^{-1}$ ) of PMS and Cu-PMS

PMS	Cu-PMS	Assignment of relevant bands
3050	3450	$\nu$ O-H stretching and bound water
1650	-	C-O stretching
1600	1610	Phenyl vibration
-	1550	C-O stretching
1437	1450	Symmetric $\text{COO}^-$
1280	1378	$\text{CH}_2$ twisting
1200	1230	CH plane

An X-ray diffraction diagram shows that PMS (Figure 8.1) is crystalline. It was found that Cu-PMS is amorphous since there were no peaks in the X-ray diffraction pattern.

$^1\text{H}$  nmr studies show that (Figure 8.2)  $\text{CH}_2\text{OH}:\text{CH}_2:\text{ArH}$  is present in the ratio 4:2:4, at  $\delta$  4.9,  $\delta$  3.9 b and at  $\delta$  6.8-7.8.<sup>11</sup>  $^{13}\text{C}$  nmr shows 14 signals and 14 carbons were located.  $\delta$  118, 128, 130, 135 and 139 are due to aryl carbons.<sup>12</sup>  $\delta$  35 is probably due to impurity,  $\delta$  40 corresponds to  $\text{ArCH}_2\text{Ar}$  and  $\delta$  56 to  $\text{ArCH}_2\text{OH}$ .  $\delta$  158, 160 are due to phenolic carbons and  $\delta$  172, 174 due to -COOH, but both these indicate two carbons. Hence it is reasonable to conclude that two COOH groups are in different environments.

The optical spectral data for the material do not indicate the presence of heterogeneity in the compound. However, the mass spectra showed unusual multiplicity in peaks. FAB-MS (Figure 8.3) shows  $m/z$  value of 601, indicating molecular weight of PMS to be 600. Peaks at 451, 301 and 151 correspond to trimer, dimer and monomer respectively. Hence, effort was made to resolve the material into the probable constituents present. TLC runs on silica gel using a solution of PMS in drops of acetic acid and water showed three constituents as shown in Figure 8.4.

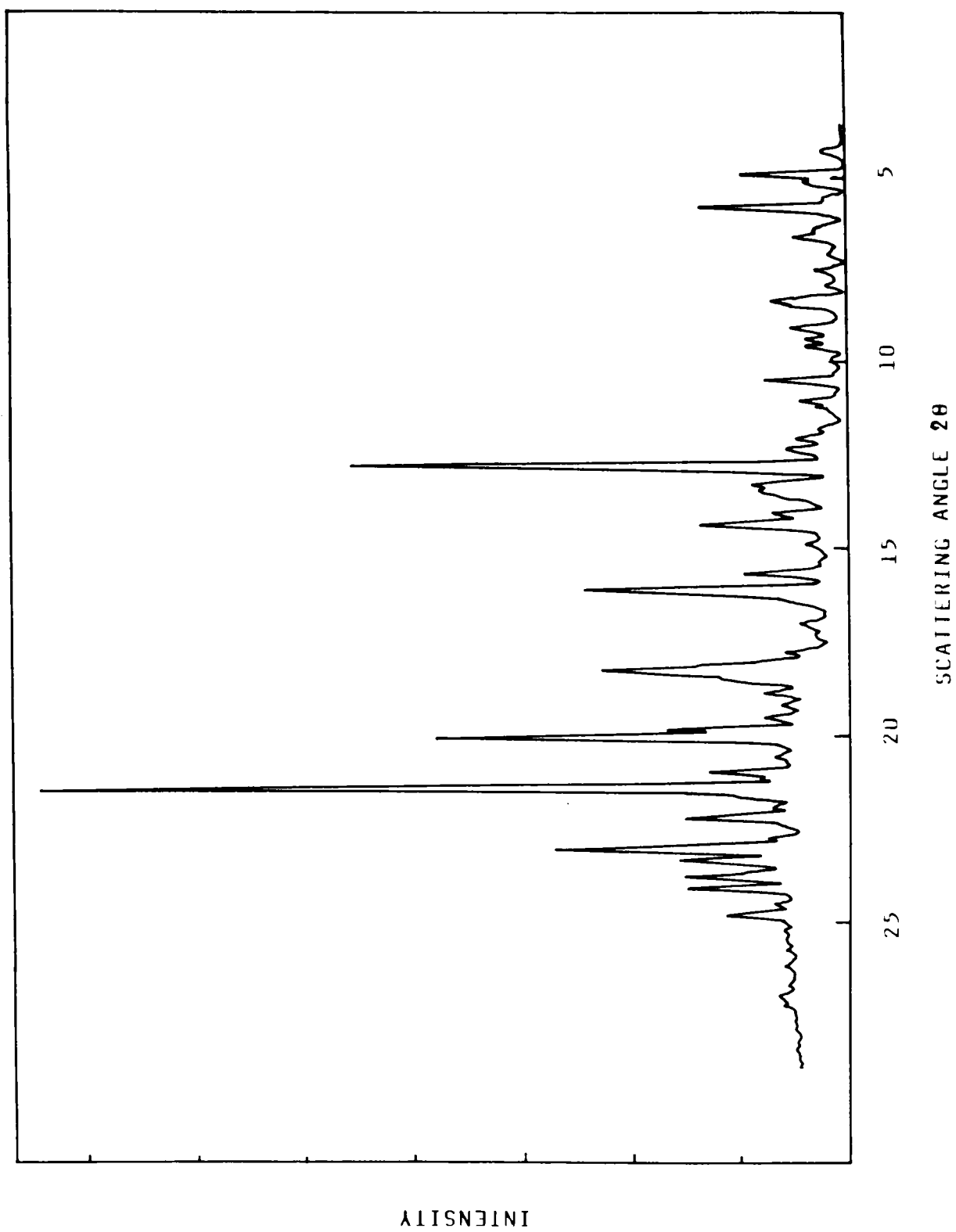


Figure 8.1 XRD pattern of PMS

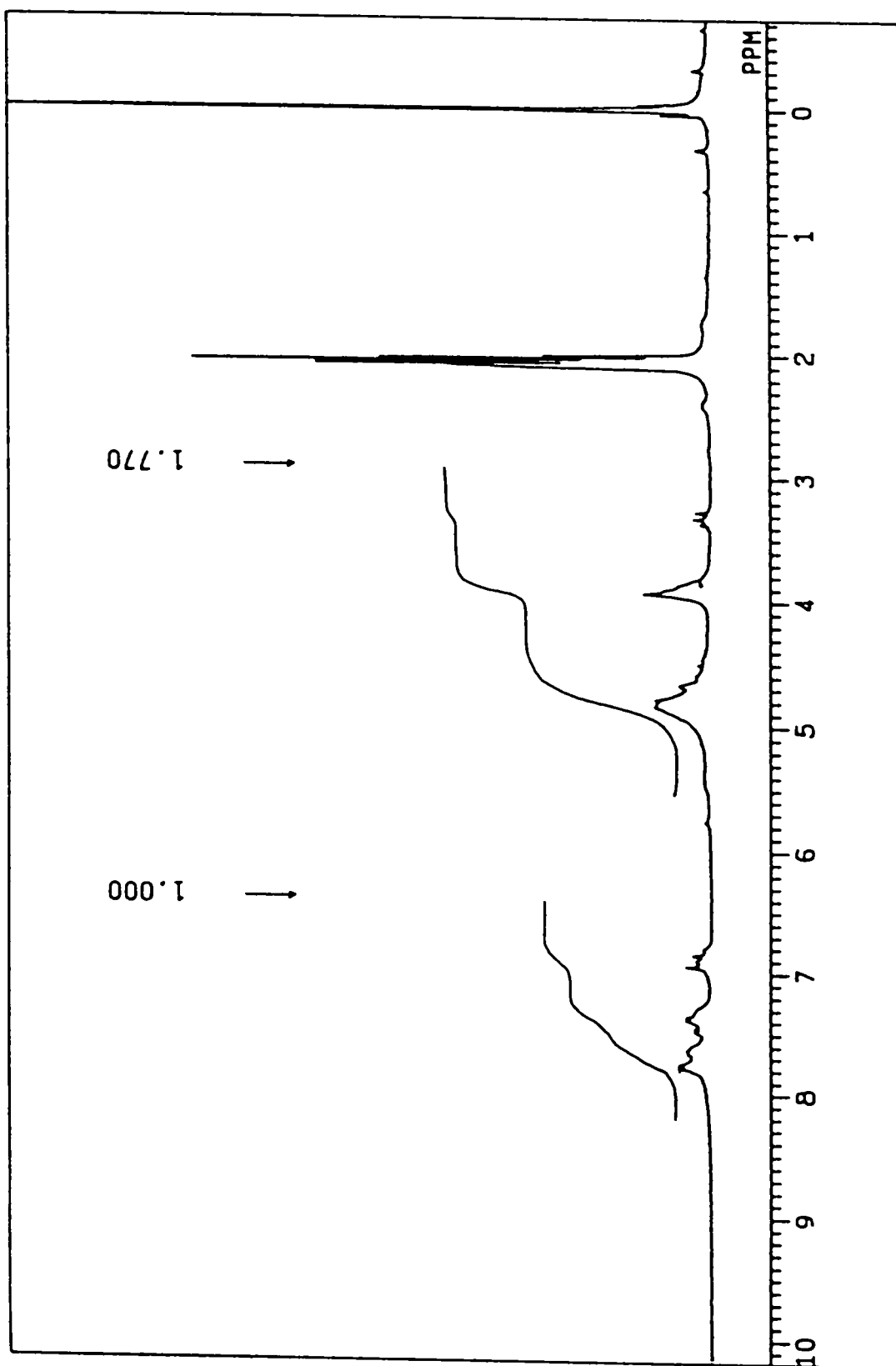


Figure 8.2  $^1\text{H}$  NMR of PMS, solvent: acetone

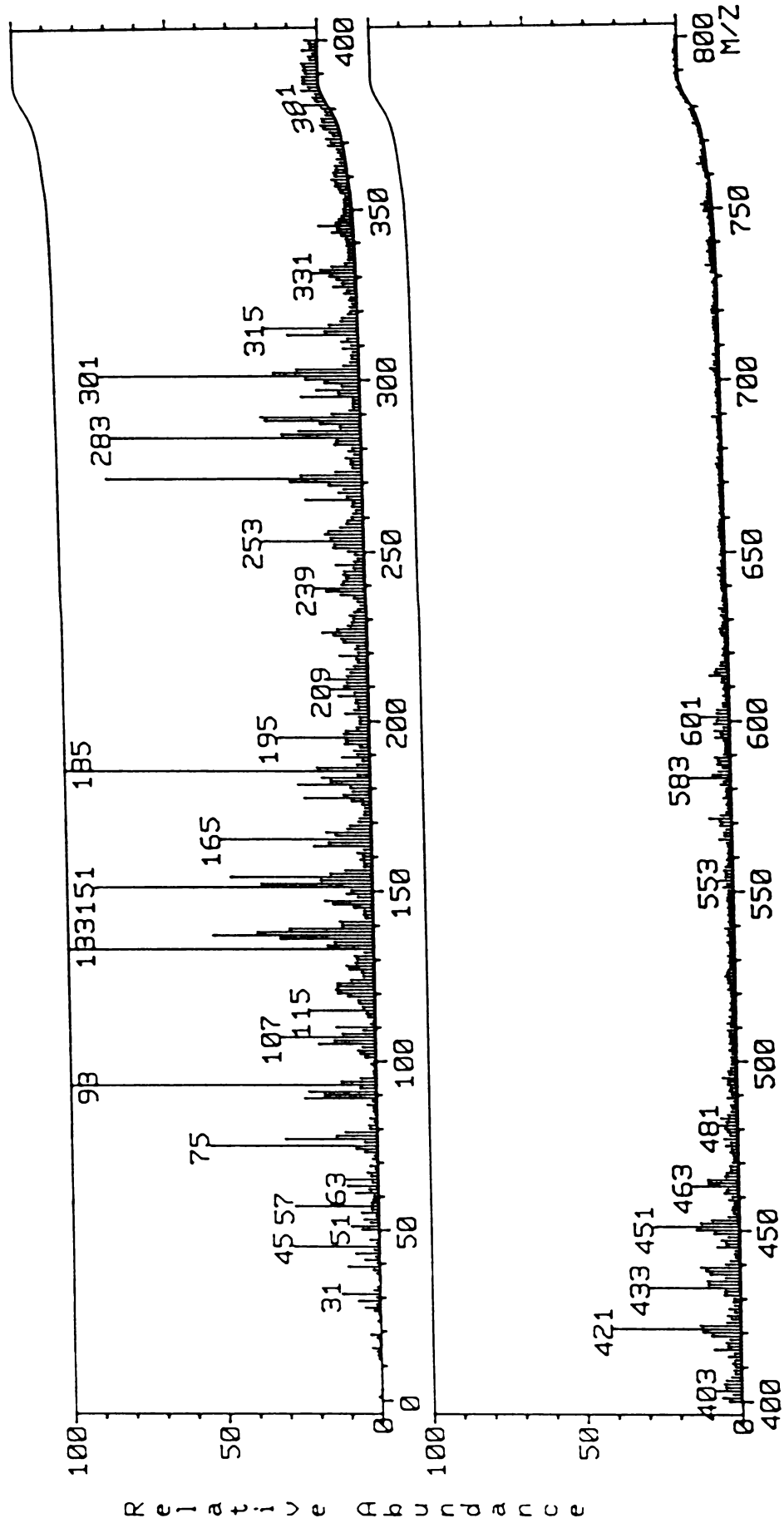


Figure 8.3 FAB-MS of PMS matrix - glycerol



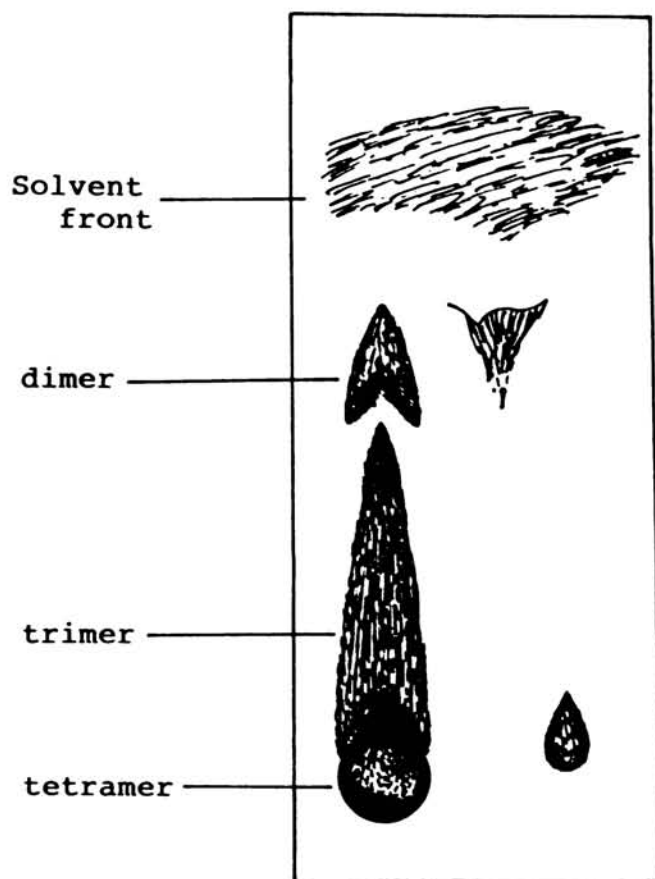


Figure 8.4 TLC runs of PMS

### 8.3.2 Thermal studies

TG-DSC curves for PMS and Cu-PMS compounds are shown in Figures 8.5 and 8.6. It is seen that there are two stages of decomposition. The mass loss in the first stage might be due to the removal of bound water for Cu-PMS as is also evidenced by the ir spectra. The weight loss for PMS indicates that it might be due to the removal of one carboxyl group. The second stage of decomposition might be either due to the decomposition involving the functional groups or due to the degradation of the oligomer backbone. It is seen from the figure that the final decomposition stage is shifted from 525°C for PMS to 350-380°C in Cu-PMS. This might be due to the catalytic effect of the metal ions on the decomposition of PMS.

The kinetic parameters for the different stages of decomposition were calculated using Coats-Redfern equation.<sup>13</sup> The final form of Coats-Redfern equation is

$$\log g(\alpha)/T^2 = \log \frac{AR}{\phi Ea} - \frac{Ea}{2.303 RT} \quad . . . . (8.1)$$

where  $\alpha$  is the degree of conversion,  $\phi$  the heating rate, A the pre-exponential factor, Ea the activation energy, T the temperature in Kelvin, R the gas constant and g is the function  $\alpha$ ,

where

$$g(\alpha) = 1 - (1-\alpha)^{1-n}/1-n$$

when

$$n \neq 1 \text{ and}$$

$$g(\alpha) = -\ln(1-\alpha)$$

when

$$n = 1$$

A plot of  $\log g(\alpha)/T^2$  against  $1/T$  is linear and the value of  $E_a$  is obtained from the slope and the intercept gives  $A$ . The entropy of activation  $\Delta S$  is calculated using the relation  $A = kT/h e^{\Delta S/R}$  where  $k$  is the Boltzmann constant, and  $h$  is the Planck's constant. The results are presented in Table 8.3. The correlation coefficients are in the range of 0.9983 to 0.9390. A comparison of  $E_a$  values for the second stage of decomposition shows that the  $E_a$  value decreases in the case of Cu-PMS indicating faster rate of decomposition probably due to the catalytic activity of the metal. This is indicated by a similar trend in entropy of the activated states. The  $\Delta S$  value for PMS is negative indicating a highly ordered activated state.

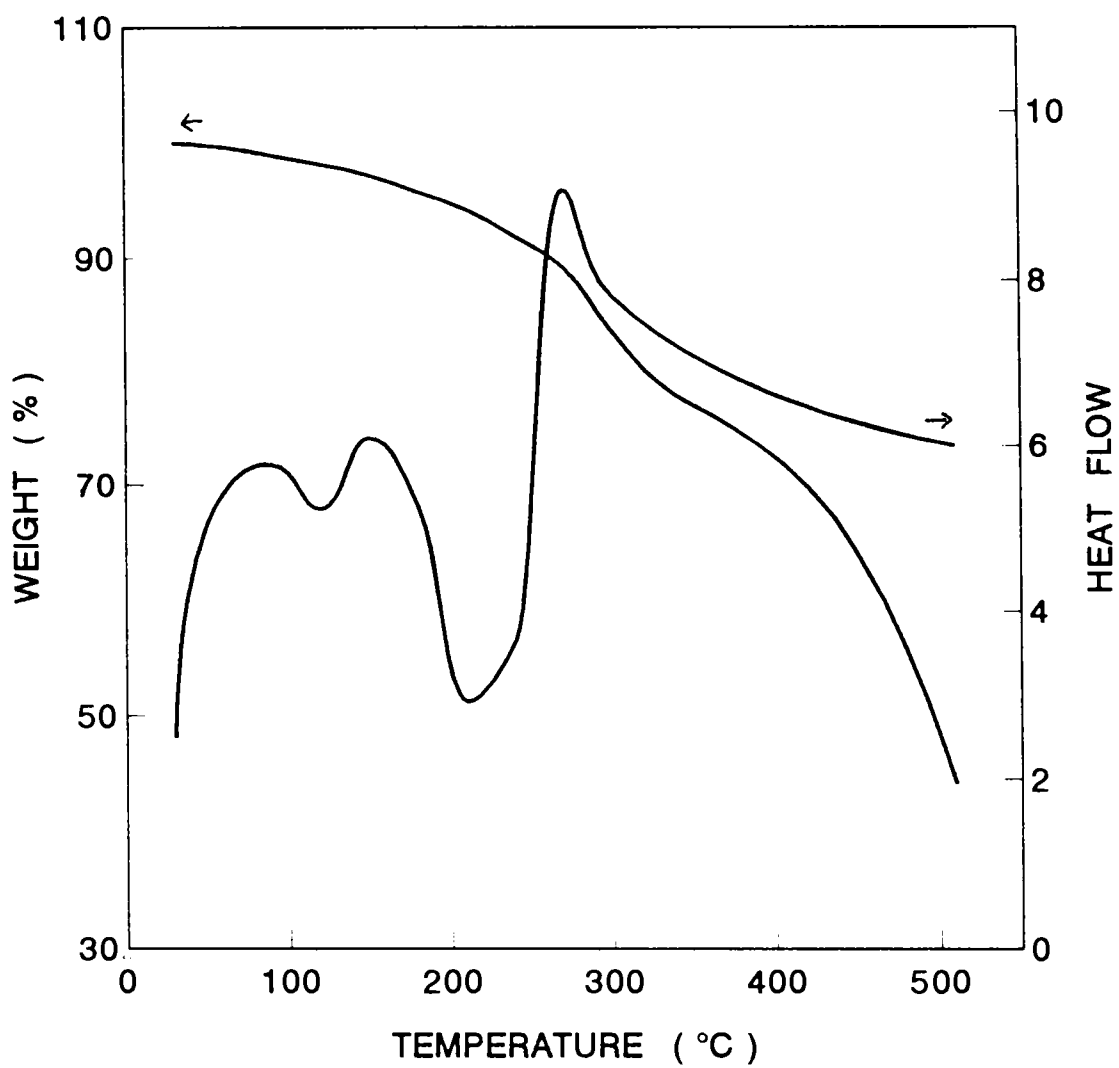


Figure 8.5 TG-DSC of PMS, atmosphere: nitrogen. Scanning rate: 10°C/min.

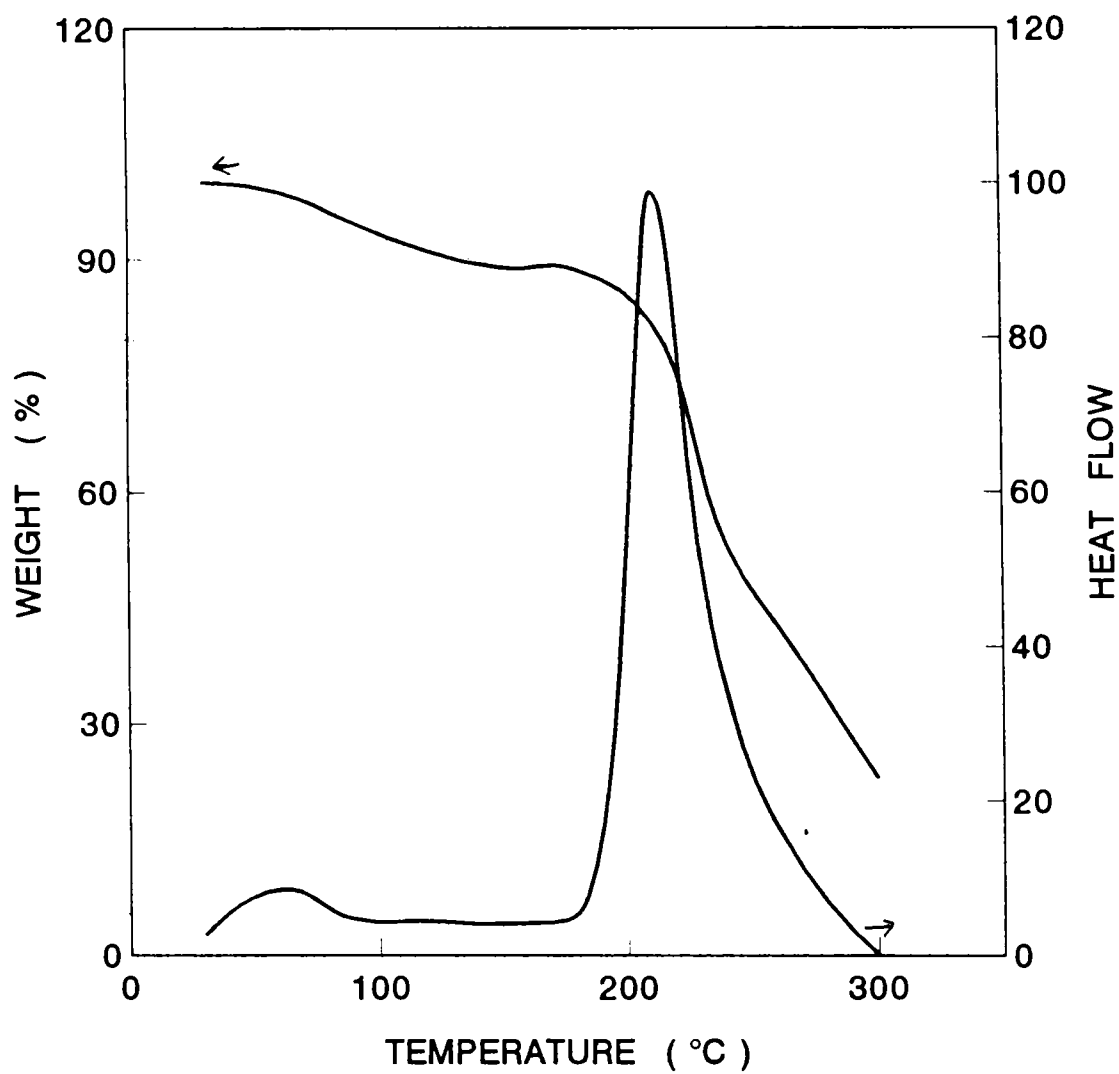


Figure 8.6 TG-DSC of Cu-PMS, atmosphere: nitrogen.  
Scanning rate: 10°C/min.

Table 8.3 Kinetic parameters for the thermal decomposition of PMS and Cu-PMS

Compound	Stage of decomposition	Order (n)	Ea (kJ mol <sup>-1</sup> )	A (S <sup>-1</sup> )	S (kJ mol <sup>-1</sup> K <sup>-1</sup> )	r
PMS	I	1.04	121.78	398560.10	-142.7	0.9684
	II	1.60	27.16	19.08	-228.6	0.9900
Cu-PMS	I	1.46	101.19	292127.00	-102.9	0.9390
	II	1.19	14.66	0.16	-264.1	0.9983

For the second stage of Cu-PMS  $\Delta S$  has become more negative which might be due to the chemisorption of the decomposition products.<sup>14</sup>

### 8.3.3 Leaching behaviour of copper ions

Table 8.4 shows the release rate of copper ions over a long period of time. The release rate of copper ions from the PMS matrix during the first few months are much higher than that in the steady state. The rate becomes steady in the range 7.68 to 7.13  $\mu\text{g/l}$ . From these results it can be concluded that PMS can be used as binding matrix for bioactive materials for gradual release over long period of time.

**Table 8.4 Leaching rate of Cu**

Time in months	Concentration of Cu ( $\mu\text{g/l}$ )
1	13.20
2	12.00
3	10.50
4	9.35
5	9.25
6	9.15
7	8.89
8	7.68
9	7.49
10	7.32
11	7.21
12	7.13

#### **8.4 Conclusion**

The optical spectral data of PMS did not indicate the presence of heterogeneity in the compound. The FAB-MS showed multiplicity in peaks. The peaks corresponding to tetramer, trimer and dimer were obtained. The runs on silica gel could also separate three constituents. X-ray pattern revealed that the compound is crystalline. Leaching studies of Cu-PMS indicates that PMS can be used as binding matrix for bioactive materials release over long period of time.

## References

1. Chatterjee, S. K. *J. Polym. Sci.* 1970, 8(5), 1299.
2. Nasser, J. G. *Chem. Abstr.* 1966, 64, 8394c.
3. Giuseppe, C.; Grieco; Civo. *Chem. Abstr.* 1969, 70, 80813a.
4. Hayashi; Takao; Kato; Hajime. *Chem. Abstr.* 1973, 78, 10212.
5. Marvin, J. M. *Acc. Chem. Res.* 1993, 26, 241.
6. DeGeiso, R. C.; Donaruma, L. G.; Tomic, E. A. *Anal. Chem.* 1962, 34, 845.
7. Giuseppe, C.; Egidio, M. *Chem. Abstr.* 1967, 67, 72340s.
8. Kim, D. W.; Kim, K. S. *Chem. Abstr.* 1985, 103, 38255v.
9. Das, A. P.; Nayak, P. L.; Lenka, S. *J. Appl. Polym. Sci.* 1987, 34, 2151.
10. Dyer, G.; Hartley, J. G.; Venanzi, L. M. *J. Chem. Soc.* 1965, 1293.
11. Silverstein, R. M.; Bassler, G. C.; Morrill, T. C. "Proton Magnetic Resonance Spectrometry", John Wiley & Sons: New York, 1980.
12. Yamamoto, Y.; Toyota, E.; Shimokawa, S. *Bull. Chem. Soc. Jpn.* 1989, 62, 2717.
13. Coats, A. W.; Redfern, J. P. *Nature* 1964, 68, 201.
14. Madhusudanan, P. M.; Yusuff, K. K. M.; Nair, C. G. R. *J. Therm. Anal.* 1975, 8, 31.



## CHAPTER 9

### SEPARATION OF EUROPIUM FROM RARE EARTH CHLORIDE

#### Abstract

An amphiphilic flocculant (PAA) was prepared by Hofmann degradation of polyacrylamide. The optimum pH range for the flocculation of Eu(II) sulphate using PAA was 3 to 3.5. The purity of  $\text{Eu(II)SO}_4$  precipitated using PAA is much higher than that obtained by coprecipitation with barium sulphate.

## 9.1 Introduction

Europium (Eu, atomic number 63) is one of the least abundant of the rare earths. In the earth's crust as a whole, its average concentration is estimated to be 0.5 ppm as compared to 150 ppm for the entire rare earth group including yttrium.<sup>1</sup> Europium constitutes 0.3% of the rare earth group. Rare earth oxide obtained from bastnasite, one of the most important sources of rare earths, contains approximately 0.1%  $\text{Eu}_2\text{O}_3$ . Europium content of the oxides obtained from monazite (including xenotime) varies with the source of ore from about 0.03 to 0.12%.<sup>2,3</sup>

Europium is one of the most valuable rare earths. The range of its applications include luminophores, hardware, nonmetallic ferromagnetics and the list continues to grow.<sup>4</sup> The fluorescent characteristics of europium are of considerable interest in connection with electronic energy transfer processes and their use in laser systems. The annual production of europium in the country in 1989 is in the range of 2000-2800 Kg the cost is \$ 50/g.<sup>5</sup> Of the quantity recovered more than 95% is used for the production of red phosphors for use in colour television tubes.<sup>6</sup> In India the process for the separation of Eu is still in the developing stage.

Europium has the effect of dispersing the absorption peaks for certain types of compounds over a wide frequency range. This dispersion will frequently separate otherwise overlapping peaks. Generally, complexes of europium are used to bring about this effect.<sup>7</sup> Minor amounts of europium are used together with lithium iodide in scintillation detectors, as a component of control rods and as a burnable poison in nuclear reactors.<sup>6</sup>

Three lanthanides (samarium, europium and ytterbium) have divalent states that are capable of being exploited, but only  $\text{Eu}^{2+}$  has any appreciable stability in aqueous solutions. Europium has traditionally been separated from other lanthanides by chemical reduction and coprecipitation with barium sulphate.<sup>8-11</sup>

The only producer of europium in the country is the Indian Rare Earth Ltd., Udyogamandal. Currently, the process employed for the separation of europium from gadolinium concentrate (about 1% europium) involves:

- (a) Reduction of  $\text{Eu(III)}$  to  $\text{Eu(II)}$  using zinc in weak acid medium.
- (b) Coprecipitation of  $\text{Eu(II)}$  with barium sulphate.
- (c) Oxidation and release of coprecipitated europium.
- (d) Repetition of the process for further purification.

The method has a number of disadvantages:

- (a) The operations are discrete.
- (b) Requires the addition of  $\text{BaSO}_4$  for coprecipitation.
- (c) The enrichment factor is only moderate.

This chapter describes the recovery of europium from gadolinium concentrate using polyamino acrylic acid (PAA) as flocculant. Polyelectrolytes can act as primary coagulant in neutralizing the double layer directly and allowing the aggregation to take place. It can also bring about flocculation through a bridging mechanism.<sup>12</sup> La Mer and coworkers<sup>13-15</sup> have contributed in developing an acceptable model which explains the ability of polymers to flocculate suspensions. The theory assumes that a colloidal particle may attach to one or more absorption sites on the long polymer chain with the remainder of the chain extending out into the bulk of the solution. Other particles may also become attached to the chain at other sites, and hence the polymer molecule serves as a bridge. The particles thus become bound to flocs and grow in size. The removal of suspended metal species at low concentrations from water is an important step in the clarification of industrial effluents and in the recovery of metal values. Common separation processes become ineffective here because of small particle size.

## 9.2 Experimental

### 9.2.1 Materials

Samples of gadolinium concentrate as oxide was obtained from Indian Rare Earths Ltd., Udyogamandal. The oxide was dissolved in concentrated HCl, the solution was evaporated to dryness to remove excess of HCl, and was dissolved in distilled water.

### 9.2.2 Methods

Polymerization of acrylamide was carried out in aqueous medium in presence of sodium hydroxide and potassium persulphate as catalyst. The hydroxide-acrylamide ratio was kept at 0.25:1 and temperature at 80°C under an atmosphere of nitrogen. Reaction time was 1 h. The polymer obtained was subjected Hofmann degradation and the product was precipitated at pH 4.0, pH being adjusted with conc. HCl. The precipitate was purified by dissolving in water and reprecipitating with conc. HCl. The precipitate was dried in vacuum. Nitrogen was determined by the micro-Kjeldhal method.<sup>16</sup>

#### (a) Reduction of Eu(III) to Eu(II)

Reduction of Eu(III) to Eu(II) was achieved by passing through a Jones reductor.<sup>16</sup> This consists of a

column of amalgamated zinc packed in a long glass tube provided with a stopcock, through which the solution to be reduced may be drawn. Gadolinium concentrate solution was reduced using zinc in weak acid medium under an atmosphere of nitrogen. pH was adjusted to 3.0 using dilute HCl.

**(b) Floc growth measurement**

Measured volumes of Eu(II) solution in a special cuvette was mixed with different amounts of sulphate and flocculant. The cell was gently inverted twenty times and mounted on the holder for optical measurement. Optical absorbance was measured at different time intervals. Experiments were repeated for different concentrations of sulphate, HCl and amount of flocculant.

**(c) Sedimentation studies**

The visual observation of the settling of the flocs is rather difficult. Hence sedimentation time, the time required for the complete settling was obtained from absorbance Vs time plot. Sedimentation time was taken as the time after which no change in absorbance was observed. The rate of subsidence of the solid phase was observed by recording the volume of the solution containing the solid phase as a function of time, in a graduated cylinder filled to the mark with suspension under examination.

#### **(d) Particle size measurement**

Particle size were measured in aqueous solutions, saturated with flocculated Eu(II) sulphate avoiding any dissolution. Following homogenization of the suspension, it was left to sediment undisturbed in the cuvette and recording the transmittance at 420 nm for different time intervals. Europium concentration was measured using ICP/AAS.

#### **(e) Thermal analysis**

Thermal stability of polyelectrolyte was studied using TGA in dynamic nitrogen atmosphere using Perkin-Elmer Delta Series Thermal Analyzer. The heating rate given was 10°C/min.

### **9.3 Results and Discussion**

#### **9.3.1 Characterization of polyampholite**

The nitrogen content of the polyampholite was found to be 6.1%. Amine group content was 1.20 meq/g and carboxyl group content 0.4 meq/g. The intrinsic viscosity was found to be 14.2.

#### **9.3.2 Effect of pH on reduction medium**

The pH of the reduction medium was adjusted in the range 3 to 3.5. Lower pH lead to the evolution of

hydrogen in the reductor. At high pH, the major rare earth constituents were hydrolyzed to give insoluble hydroxides. In the pH range 3 to 3.5, samarium which is the major constituent in the test solution gave least contamination.

### 9.3.3 Effect of sulphate concentration

Sulphate was added so as to avoid reoxidation of Eu(II) to Eu(III). Concentration ratio of Eu(II):  $\text{SO}_4^{2-}$  was varied from 20 to 30 times the weight of europium present in the stock solution. It was observed that below this ratio of sulphate the formation of  $\text{EuSO}_4$  was very slow. When the concentration exceeded this range, the coprecipitation of other rare earth(III) sulphate was significant.

### 9.3.4 Flocculation studies

Flocculation experiments were carried out by mixing the polyelectrolyte solution with the Eu(II) sulphate solution. The effect of polyelectrolyte on the rate of sedimentation of Eu(II) sulphate is presented in Figure 9.1. The sedimentation of Eu(II) sulphate becomes considerably faster due to the addition of polyelectrolyte. The europium oxide was recovered by the direct calcination of the sedimented Eu(II) sulphate, at



1600°C. The interference of the polyelectrolyte at this temperature is unlikely due to the fact that it cannot withstand temperature above 250°C as observed from the thermal decomposition studies given in Figure 9.2. The concentration of europium thus recovered was found to be 70%.

#### 9.3.5 Sedimentation experiments

Figure 9.3 shows the time depended change in sediment volume after flocculation. This represents "phase settling" type flocs, where settling occurs when a suspension of the flocculated particles reach a concentration that causes them to contact each other obstructing the free settling paths of individual particles.<sup>17</sup> The result is that the solid phase as a whole assumes a common settling rate. It was observed from the figure that the settling rate increased with increasing concentration of flocculant. For a dose of 100 mg/l the settling takes around 50 minutes.

#### 9.3.6 Particle size analysis

Assuming the suspension to be homogeneous the concentration of particles in the light beam will be the same as that at any point in the suspension. During sedimentation, the number of particles leaving the beam is balanced by other particles entering from above.

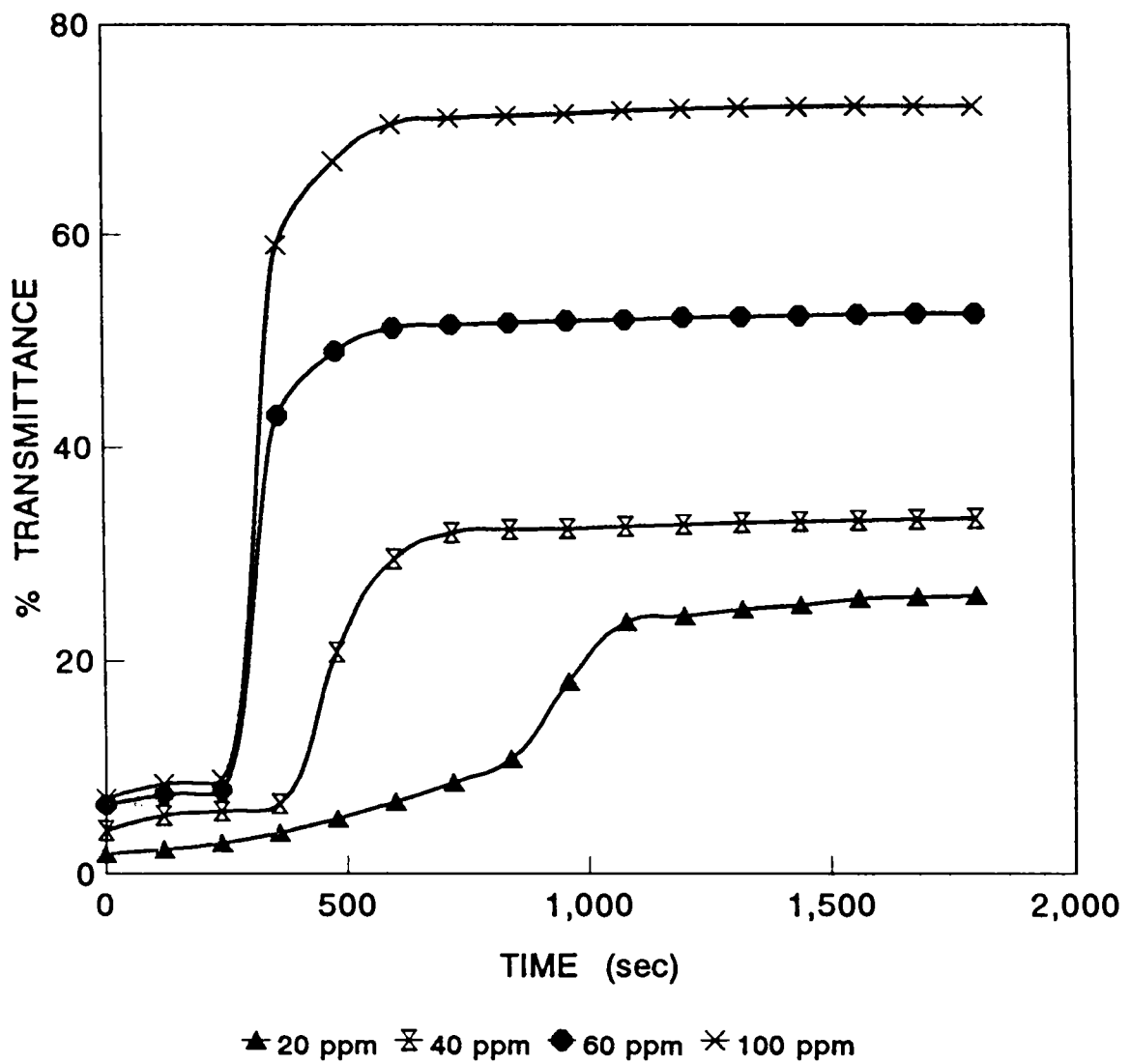


Figure 9.1 Sedimentation of Eu(II) sulphate with polyelectrolyte, concentration of sulphate 0.045 mole/litre.

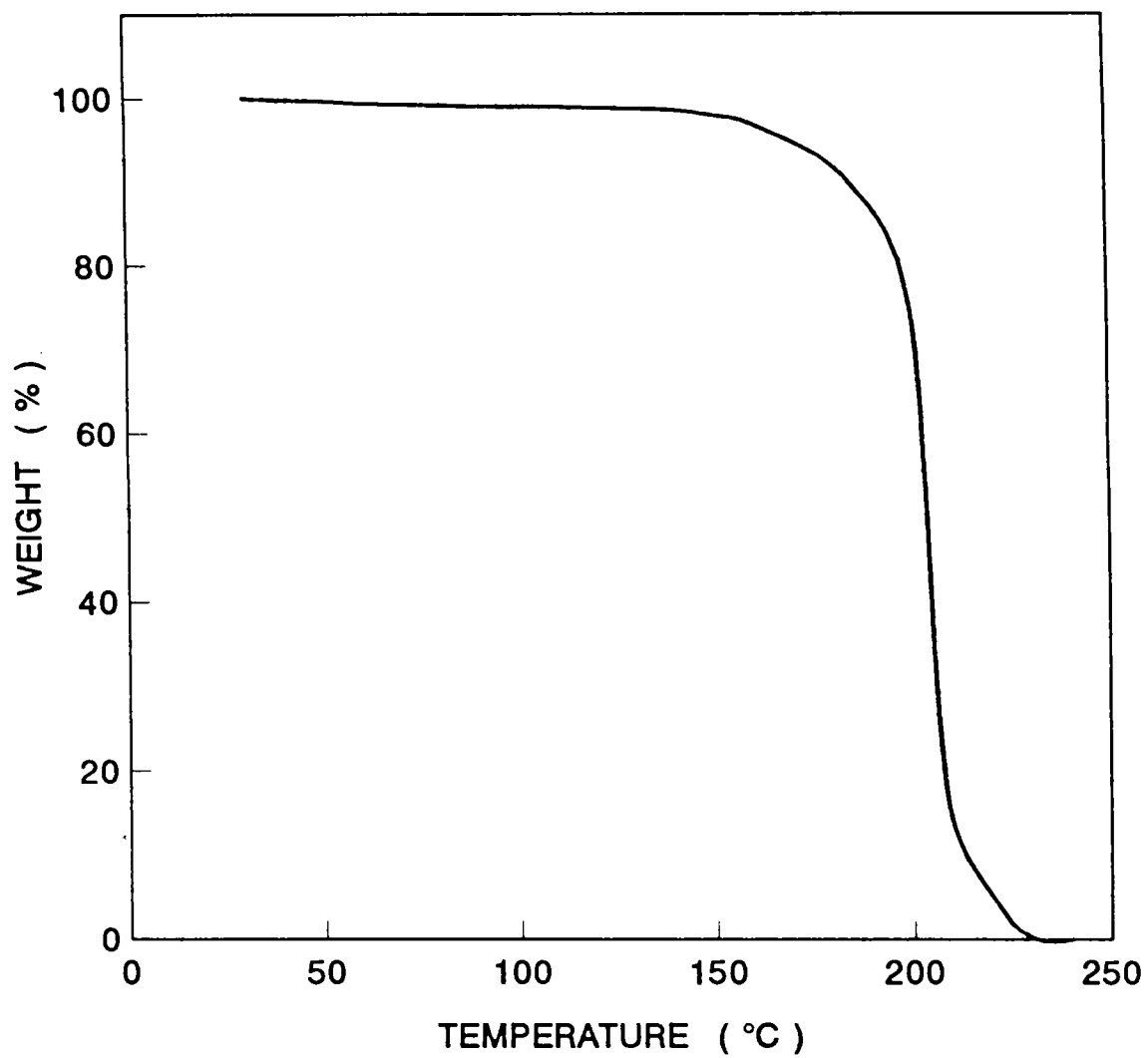


Figure 9.2 Thermal decomposition of polyelectrolyte, atmosphere: nitrogen. Scanning rate: 10°C/min.

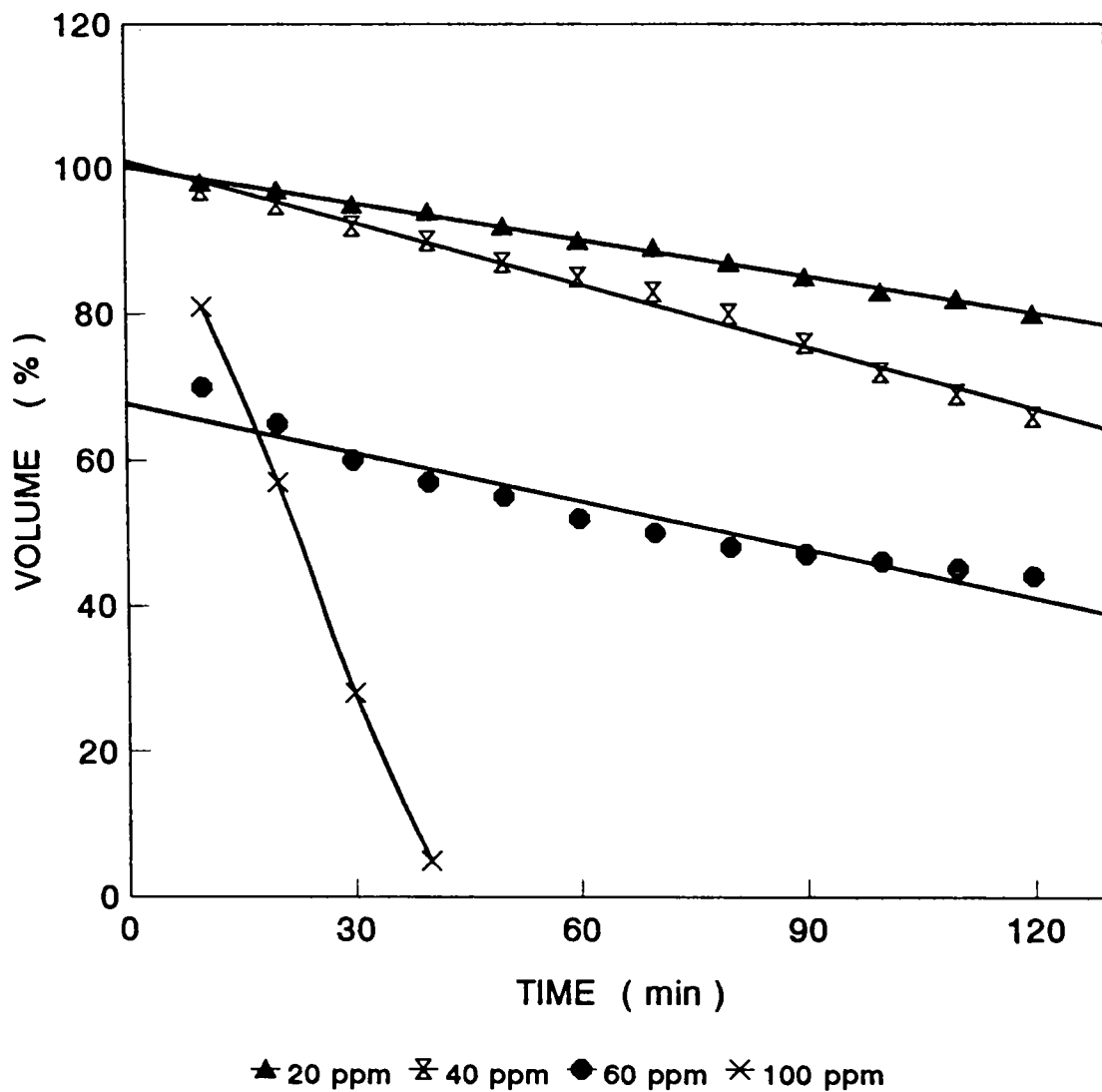


Figure 9.3 Volume percentage of solid as a function of time at different concentration of polyelectrolyte.

Following the fall of largest particles in the suspension from the liquid front to the level of the light beam, there will be no more particles of this size to enter the path of the light beam. Therefore, the concentration of the particles in the light beam at time 't' will be the concentration of particles with the diameter smaller than the diameter 'd<sub>st</sub>' given by the Stokes equation. The Stokes diameter d<sub>st</sub> is proportional to the square root of the sedimentation velocity 'u', which is defined as

$$u = l/t \quad . . . . (9.1)$$

where l is the sedimentation distance.

$$l = kF \quad . . . . (9.2)$$

where k is a constant and F is the percentage of the total optical density measured due to the sedimental particle so that

$$u = kF/t \quad . . . . (9.3)$$

The particle size is thus defined by the slope b of the graph F as a function of t.<sup>18-20</sup>

$$F = bt \quad . . . . (9.4)$$

The relative particle size of the suspended material calculated from a plot of transmittance Vs time plot is given in Table 9.1. It is clear that the particle size of

the flocculated Eu(II) sulphate have improved considerably with the use of flocculant, thus ensuring faster sedimentation.

Table 9.1 Particle size growth for Eu(II)SO<sub>4</sub> in presence of SO<sub>4</sub><sup>2-</sup> ions and polyelectrolyte: Eu(II) concentration 0.016 g/l

Sulphate concentration (moles/l)	Relative particle size (arbitrary unit)			
	Sulphate	Polyelectrolyte		
		20 ppm	40 ppm	100 ppm
0.027	0.00105	0.021	0.026	0.034
0.031	0.00195	0.035	0.039	0.046
0.038	0.00220	0.040	0.043	0.052
0.045	0.00230	0.050	0.057	0.070

#### 9.4 Conclusion

This study reveals that amphiphilic polyelectrolyte based on polyacrylic acid can accelerate particle growth of Eu(II) sulphate. A controlled excess of sulphate ions also aids particle growth thus helping faster sedimentation. This points to the possibility of developing a reduction-flocculation-sedimentation sequence as a viable alternative to coprecipitation method for the recovery of europium from rare earth concentrate.

## References

1. Sinha, S. P. "Europium", Springer-Verlag, Inc.: New York, 1967.
2. Harris, R. E.; Woyski, M. M. "Treatise on Analytical Chemistry", McGraw-Hill: London, 1963, 8, 1-146.
3. Vickery, R. J. "Analytical Chemistry of Rare Earths", Springer-Verlag, Inc.: New York, 1961.
4. Selin, D. L.; Tarasova, N. P.; Malkov, A. V.; Poskrbyshev, G. A. *React. Kinet. Catal. Lett.*, 1989, 39, 273.
5. Solomon, S.; Lee, A. *J. Chem. Edn.*, 1994, 71, 247.
6. Othmer, K. "Encyclopaedia of Chemical Technology", Vol. 14.
7. Silverstein, R. M.; Bassler, G. C.; Morrill, T. C. "Proton Magnetic Resonance Spectrometry", Wiley: New York, 1980.
8. McCoy, H. N. *J. Amer. Chem. Soc.*, 1935, 57, 1736.
9. Marsh, J. K. *Inorganic Synthesis*, 1957, 5, 32.
10. Hulet, E. K.; Bode, D. D. "Separation Chemistry of Lanthanides and Transplutonium Actinides", MTP International Review of Science: Butterworths, London, 1972, 7, 1-45.
11. Onstott, E. I. *J. Amer. Chem. Soc.*, 1955, 77, 2129.
12. Stuster, W. W.; Wang, L. K. *Separation and Purification Methods* 1977, 6, 153.

13. La Mer, V. K. *J. Colloid. Sci.*, 1964, 19, 291.14. La Mer, V. K.; Healy, T. W. *Rev. Pure and Appl. Chem.*, 1963, 13, 112.
15. Michaels, A. S. *Ind. Eng. Chem.*, 1954, 46, 1485.
16. Vogel, A. I. "A Textbook of Quantitative Inorganic Analysis", Longman Group Ltd., England, 4th edn., 1978, p. 143.
17. Schwoyer, W. L. K. "Polyelectrolytes for Water and Wastewater Treatment", CRC Press, Inc.: Florida, 1981.
18. Jellinek, Z. K. "Particle Size Analysis", Ellis Horwood: Chichester, 1974, p. 70.
19. Adamson, A. W. "Physical Chemistry of Surfaces", Wiley Interscience: New York, 4th edn., 1978, p. 485.
20. Dalas, E.; Koutsoukos, P. G. *Journal of Education*, 1990, 67, 356.



A part of the contents of this thesis has been published/communicated for publication in the following forms:

1. Preparation, Characterization and Alkali Metal Ion Permeation Through Nylon 666-g-Maleic Acid Membranes. K. Usha and V. N. Sivasankara Pillai, *Polymer International* (In Press).
2. Studies on Metal Complexes of SMH Resin. Rita Mendez, K. Usha, K. K. Mohammed Yusuff and V. N. Sivasankara Pillai, *European Polymer Journal* (In Press).
3. Preparation, Characterization and Alkali Metal Ion Permeation Through Nylon 666-PMA Interpolymer Membranes. K. Usha and V. N. Sivasankara Pillai (Communicated to *European Polymer Journal*).
4. AC Conductivity and Dielectric Relaxation in N-g-MA and N-PMA. K. Usha and V. N. Sivasankara Pillai (Communicated to *Polymer Science: Polymer Physics Edn.*).
5. AC Conductivity and Dielectric Relaxation in N-g-MA Polyelectrolyte. K. Usha and V. N. Sivasankara Pillai, 10th International Conference on Solid State Ionics, 3-8 December 1995.
6. Studies on Metal Complexes of SMPH Resin. Rita Mendez, K. Usha, K. K. Mohammed Yusuff and V. N. Sivasankara Pillai, National Symposium on Current Trends in Coordination Chemistry, CUSAT, March 23-25, 1995, p.48.

